POLITECNICO DI TORINO

Collegio di Ingegneria per l'Ambiente e il Territorio

Corso di laurea Magistrale in **Ingegneria per l'Ambiente e il Territorio**

Tesi di Laurea Magistrale

Use of multispectral images with high resolution frequency for the recognition of crops and practices relating to the CAP (Community Agricultural Policy)

Relatori:

Prof. Piero Boccardo

Candidato:

Sean De Costanzo

Dicembre 2024

ABSTRACT

Generally, it is difficult to inspect directly all EU agricultural soils since it demands a very high number of means and people to work on site and the territory is continuously under the variation of seasons and changing weather. That often hinders soil inspection aimed at preventively checking the compliance of the soil postponing The Common Agricultural Policy (CAP) payments in favors of the farmer. Furthermore, a not efficient analysis of the land would imply not completely right data about it. That is why it is necessary to develop new techniques that can enhance the area, the effectiveness and the objectivity of CAP controls, and to decrease the dependency on conventional monitoring technique.

Whereas global population continues to increase at a rate of about 100 million per year and is expected to reach around 10 billion by 2050, cropland areas are not increasing and have stagnated around 1.5 billion hectares globally (*Prasad S. Thenkabail , 2010)* . Indeed, cropland areas have even begun to decrease in some countries with important food contribution (e.g., USA) due to increasing demand of fertile arable lands for alternative uses such as biofuels, encroachment from urbanization, and industrialization. Since the number of cultivated areas have decreased, the extension of forests and pastures has increased. With the beginning of the Industrial Revolution man has started damaging the environment by incessantly exploitation natural resources in addition to the abuse of pesticides and herbicides in the last 50 years, the drastic extraction of aquifers, and the salinization of fertile soil due to the excessive irrigation (*Prasad S. Thenkabail, 2010)*. During the 90s the productivity per unit of land increased and came through a series of factors such as high-yielding varieties, fast growing varieties, irrigation, supplemental irrigation, crop intensification, and farm management (e.g., application of nutrients, herbicides, pesticides, and drainage) leading to action by CAP for recovery plans **(Fig.1)**. In order to create sustainable ways of using water and to reduce the exploitation of cultivated lands aimed at intensive food production, a new system has been set up, namely Geospatial Information System (GSAA). It is globally developed and requires information like crop types, precise location of crops, cropping intensities, cropping calendar, crop health, watering methods (e.g., irrigated, supplemental irrigated, rainfed), flood and drought information, water use assessment and yield or productivity (expressed per unit of land and\or unit of water).

CHAPTER 1

1. Introduction

1.1 Objectives of the study

The project was addressed to calibrate deductions from remote sensing to fit the specific local agricultural context, the aim of this work is to classify different cultures with the Planetscope satellite based on multitemporal images taking in consideration to make it possible to have better control addresses on the ground. Copernicus is the EU's Earth Observation (EO) program aimed at monitoring the Earth and its environment. It is extremely difficult to determine the cultures present in a certain study area because of the presence of a high number of particles that are acquired. It is crucial to lower that number by calibrating data so as to determine the reliability of the datum for a certain number of cultures: a value of accuracy in which a culture is effectively present in the interested area is assigned. Furthermore, it can be analyzed the probability of giving a certain recognition value to the selected culture through the spectral signatures in which the frequency spectrum of every interested culture can be compared. If the spectrum is common to the others is difficult to carry out the classification. Another instrument that can be used is the error matrix meant for recognizing a class over another. It follows from *(Jonas Schmedtmann, Manuel L. Campagnolo, 2015)* that if the accuracy is high, the number of samples extracted from the study area that can be studied becomes smaller given that the datum is clearer. For example, in *(Filippo Sarvia, Samuele De Petris, 2022),* in the separation between winter and summer crops by using a multi-temporal Normalized Difference Vegetation Index (NDVI) profile. It is important the agronomic knowledge about crop development in such periods allows for defining a proper temporal window in order to focus the analysis on vegetation active phases. Without that information there may be classification errors. Despite the improvement in such differentiation, similar NDVI temporal behavior could occur. For example, in Italy, soya and rice were poorly separable while working with NDVI temporal profile. Therefore, appropriate data calibration and maximum spectral separation are required classifying the region of interest of different cultures.

1.2 CAP introduction

The Common Agricultural Policy (CAP) was launched in 1962 and is a partnership between society and agriculture that ensures a stable supply of food, safeguards farmers' income, protects the environment and keeps rural areas vibrant with the objectives of providing affordable food for EU citizens and a fair standard of living for farmers. The AGEA (Agency for Agriculture Gants) represents the national agency for CAP application in Italy and deals with satellite monitoring particularly in the agricultural sector following the project Reg. (EU) 18 May 2018, n. 746.

The CAP is a common policy for all EU countries. It is managed and funded at European level from the resources of the EU's budget. In Italy, funded with a total of 41.5 billion euros in the 2014–2020 CAP, several regional payment agencies (PA) exist and refer to the national one the AGEA. According to Art. 17 of Reg. (EU) n. 809/2014 application for CAP subsidies must be presented by the farmer to the competent PA through the Geo-Spatial Aid Application (GSAA). GSAA contains information about managed fields (land use, location, and size) for which CAP contribution is requested. Additionally, it allows the unique identification of agricultural parcels populating databases useful for systematic checks. GSAA data are managed by farmers through a GIS (Geographic Information System) based system. payment agencies (PA) verify application

compliance with requirements through the Integrated Management and Control System (IACS), relying on administrative (AC) and spot controls (SC). AC is automatically carried out by IACS for all the applications (100%) with the aim of verifying their compliance: with eligibility criteria and maintenance of long-term commitments, with due deadlines and with required documentation. Moreover, IACS verifies that no other EU grant is financing the same field. As far as SCs are concerned, they are performed on a sample subset of GSAAs corresponding to 5% of the total. SCs are intended for: (i) checking the truthfulness of declared areas; (ii) verifying compliance of the application with the eligibility criteria; (iii) testing commitments and obligations from farmers according to the declared crop. Field selection by SCs is managed for 80% according to risk-based criteria and for the 20% randomly. SCs are presently performed by photo interpretation of high-resolution satellite/aerial images and/or, in specific and rare cases, by direct ground controls (GC) *(Filippo Sarvia, Samuele De Petris, 2022).*

While being cost-effective, farmers should work in a sustainable and environmentally friendly manner so as to maintain our soils and biodiversity. The responsibility for supervising and allocating the CAP funding rests with each EU Member State, which must set up its own paying agencies. This process includes verifying the eligibility of applicants, ensuring compliance with CAP regulations, and assessing the information provided within farmers' applications. It is necessary to treat all applications submitted by the farmers and the rural development project managers to receive CAP contributions. In addition, administrative checks and on-the-spot controls ensure that beneficiaries meet the necessary conditions to receive payments.

After these verification and compliance checks, the paying agencies proceed with the payments.

1.3 New reform of the CAP in the agricultural sector

The European Parliament, the Council of the EU and the European Commission agree on further reform of the Common Agricultural Policy (CAP). This provisional political agreement paves the way for the formal approval of the necessary legislation by the European Parliament and the Council in Autumn 2021.

With the new legislation there are strengthened requirements that must be respected (concerning the CAP strategic plan) by 6.7 million beneficiaries who receive direct payments for cultivation and livestock farming in a more sustainable way aimed at safeguarding the environment, the agricultural landscape, the actions on climate change, and rural community. *(https://agriculture.ec.europa.eu/)*

The CAP is financed through two funds as part of the EU budget *(Robert Ackrill, Adrian Kay, 2008):*

- The European agricultural guarantee fund (EAGF) provides direct support and funds market measures, F is associated with the Common Market Organization (CMO), which provides direct payments to farmers as compensation for their efforts to ensure market stability, boost agricultural productivity, and preserve the environment.
- The European agricultural fund for rural development (EAFRD) finances rural development focused on climate change adaptation by ensuring sustainable management of natural resources, building rural economies and communities, and supporting agricultural competitiveness and sustainable rural development.

In the context of the major COVID health crisis that demonstrated the resilience of the EU's food sector, and against a backdrop of growing challenges in relation to climate change, biodiversity loss and management of natural resources, much is expected from the new CAP over the period 2023-2027. The approved Plans are designed to make a significant contribution to the ambitions of work strategy and Biodiversity strategy of the European Grean Deal. At the same time, more

than ever, the CAP must target better and address the specific needs of the farm sector and rural areas.

Fig.1 Common Agricultural Policy (CAP) for recovery plan

1.4 Standard requirements and EU support

Farmers must comply with a set of basic standards in order to receive EU income support. The interaction between compliance and the support provided to farmers is called cross-compliance. Through cross-compliance, farmers are encouraged to meet high EU standards for public, plant and animal health and welfare. The standards that farmers must respect include: (i) statutory management requirements, that apply to all farmers, whether or not they receive support under the Common Agricultural Policy (CAP); (ii) good agricultural and environmental conditions, that apply only to farmers receiving support under the CAP. Farmers who breach EU law on the environment, public and animal health, animal welfare or land management will have their EU support reduced and could incur additional sanctions. Within the 2014-2020 CAP, a significant part of the budget was allocated to 'greening' practices such as crop diversification, maintenance of permanent grassland, and designation of ecological focus areas (EFA) *(Filippo Sarvia, Samuele De Petris, 2022).*

The objectives of CAP concern climate change, management of natural resources, and biodiversity *(sportello dell'agricoltura, 2019).* Taken as a whole, the CAP's objectives will cover the three dimensions of sustainability (environmental, economic and social).

With the Grean Deal Plan *(sportello dell'agricoltura, 2019)* and new agrarian reforms new aims are developed: i) support farmers and improve agricultural productivity, ensuring a stable supply of affordable food; ii) safeguard European Union farmers to make a reasonable living; iii) help tackle climate change and the sustainable management of natural resources; iv)maintain rural areas and landscapes across the EU; v) keep the rural economy alive by promoting jobs in farming, agri-food industries and associated sectors.

1.5 The Grean Deal Plan

When assessing Member States' draft Common Agricultural Policy Strategic Plans according to the specific objectives of CAP (Common Agricultural Policy), the Commission will do so in the light of Green Deal targets for 2030 as set out in the Farm to Fork Strategy and the EU Biodiversity Strategy for 2030 **(Fig.2)**.

Fig.2 Green deal plan for the evaluation of the strategic plan of the Common Agricultural Policy (CAP)

With CAP Strategic Plans Member states must be changing the legislation on climate change, energy, water, air, biodiversity and pesticides. They will have to update their plan, if necessary, in order to align them to changes to the relevant legislation. Member States will demand higher standards regarding the CAP focusing on the environment as well as on the climate compared to the previous (current) policy period.

New requirements will fill gaps in the current rules – for example:

1. A new obligation to protect wetlands and peatlands - which are major carbon sinks – as of 2025 at the latest.
2. Inclusion of relevant elements of the Water Framework Directive and the Directive on the Sustainable Use of Pesticides.
3. Increasing the sustainability:

To improve long-term soil health, farmers will be required to carry out beneficial crop rotations. Crop "diversification" (the current obligation) will be permitted as an alternative although it does not have the same benefit for soil health as crop rotation. If a CAP Strategic Plan contains that option, a Member State will have to demonstrate that crop diversification clearly helps to preserve soil potential. There will also be exemptions for smaller holdings (i.e., with no more than 10 hectares of arable land) and for farms with a large proportion of permanent grassland. Organic farmers will automatically be considered as meeting the obligation. With exemptions taken into account, the obligation of crop rotation or diversification will apply to an estimated 86% of the EU's arable land **(Fig.3)**.

Fig.3 Crop rotation technique

Farmers will also increase their contribution to biodiversity by in principle devoting at least 4% of their arable land to non-productive features and areas, including fallow land is possible add 3% for non-productive areas by farmers. The option of using catch crops and nitrogen fixing crops provides a limited value for biodiversity, that means that it will be possible farming no more than 10 hectares of arable land. When that exemption is accounted for, the obligation of devoting a proportion of land to non-productive features will apply to an estimated 85% of the EU's arable land *(sportello dell'agricoltura, 2019).*

1.6 Operation of agricultural monitoring from Satellite

Commonly, the images are captured in vertical stripes by satellites orbiting in space over a period of 5 days covering the entire surface of the earth. The images are available on the Copernicus platform and can be used freely. A pilot project was experienced in Italy in 2018; AGEA (Agency for Agriculture Gants) proceeded to verify Common Agricultural Policy (CAP) applications for the Titles III and V of EU Regulation no. 1307/2013 (Basic Payment and Small Farmers Scheme) based on markers derived from satellite data in the province of Foggia (SE-Italy). Specifically, AGEA's markers allow checking for each parcel the presence of: plowing, crop development, mowing of meadow, and checking the existence of vegetation and crop harvest. Afterward, they are used to establish different control phases, such as financial Agronomy 2022, 3 of 20 impact analysis of the farmer's application or a parcel-specific assessment carried out by a qualified operator with other data sources (orthophotos, geotagged images). Other provinces enter the same project in the following years.

The monitoring procedure is based on three key points:

1. Starting the detection process with the monitoring system.

2. Communication of the results of the application of the monitoring system and request for consequent actions.

3. Closing the detection process with the monitoring system.

They are evaluated using satellite evaluation indices if the images of the land captured by satellite present certain characteristics: plowing, mowing, vegetation growth, activity, harvest, abandonment, uprooting. For each plot examined, the satellite data evaluation processes produce

the following color classifications from white (less impactful) to red (non-compliant plot) *(Agriculture Desk, 2019).*

For surfaces of 2000 m2 the evaluation is carried out based on the type of macro-use of the land whether used for pasture or arable use. In the case of a surface area less than or equal to 2,000 m2, in the absence of values on satellite indices and for all other macro-uses, checks are carried out on the consistency of the data on the Geographic Information System (GIS).

For the companies present in the Graphic Company File, AGEA initiates control activities with the monitoring system so that the farmer, by communicating the data of his plot to the AGEA monitoring program, can receive the status of his plot *(sportello dell' agricoltura, 2019).*

CHAPTER 2

2. CAP agricultural monitoring with remote sensing technique and Sentinel-2 data satellite

2.1 Remote sensing definition

Remote sensing (RS) is the art, science, and technology of observing an object, scene, or phenomenon by instrument-based techniques. 'Remote' because observation is done at a distance without physical contact with the object of interest *(Klaus Tempfli, Norman Kerle, 2001)*. The energy can be light or another form of electromagnetic radiation, Remote sensing force fields, or acoustic energy, an example of a remote sensor is a camera. Today most remote sensors are electronic devices. The data recorded by such sensors, for example, a scanner detecting thermal emission (heat), used to be converted to images for visual interpretation. The "remote sensing" technique consists in the recording produced by an electronic sensor that will be converted into a "Remote sensing" picture **(Fig.14)**. RS defined as above is applied in many fields, including architecture, archeology, medicine, industrial quality control and robotics.

2.2 Electromagnetic energy

Light has two oscillating components: electrical energy and magnetic energy **(Fig.4)**. Therefore, electromagnetic energy (EM).

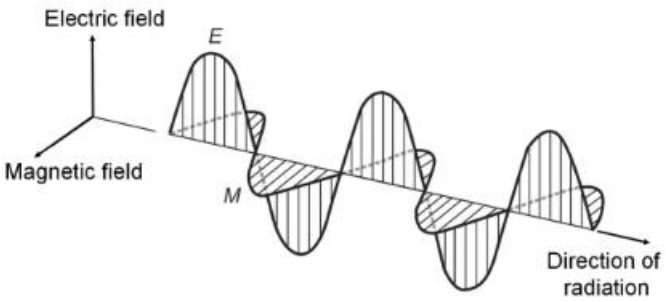

Fig.4 Electrical energy and magnetic energy

All EM energy travels at the speed of light, which is approximately 300,000 km/s. It seems to be fast, but the distances in space are astronomical. The equation of the electromagnetic energy wave (E) is:

$$E = \alpha \sin\left(\frac{2\pi}{\lambda}x + \varphi\right)$$

Where **(Fig.5)**:

- $'\alpha\ '$is the amplitude, the peak value of the wave.
- $'\lambda'$ is the length of one cycle of the oscillation. It is usually measured in micrometers (µm = 10−6 m).
- $'x'$ is the travel distance on x axis.
- $'\varphi'\ is\ the\ angle\ from\ 0\ to\ 2\pi.$

The amount of time needed by an EM wave to complete one cycle is the period (T) of the wave, while the frequency is the number of cycles of the wave that occur in one second. The measure unite is the Hertz (1Hz=1 cycle per second).

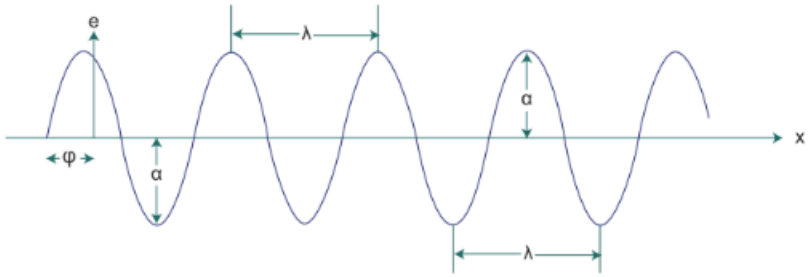

Fig.5 Characteristics of an electric wave *(Klaus Tempfli, Norman Kerle, 2001)*.

Based on Einstein's famous energy formula: c= $\lambda * v$ (the letter c is commonly used as a symbol for the speed of light; v is the frequency), short wavelength implies high frequency, while long wavelength is equivalent to low frequency. Blue light is of higher frequency than red light **(Fig.6)**. According to the equation of Max Planck, the amount of energy held by the energy of a photon relating to a specific wavelength is:

$$Q = h \times \nu = h \times \frac{c}{\lambda}$$

Where Q is the energy of a photon measured in Joule and h is Planck's constant ($6.6262*10^{-34}\ Js$). The energy carried by a single photon of light is sufficient to excite a single molecule of a photosensitive cell of the human eye, thus contributing to vision. From the equation of Max Planck long wavelength radiation has a low energy level while short wavelength radiation is of high energy. According to the theory, blue light is more energetic than red light. In **Fig.6** EM radiation beyond violet light is very dangerous for body with increasing frequency. UV radiation can already be harmful to eyes. Overall, it is more difficult to detect radiant energy of longer wavelengths than energy of shorter wavelengths.

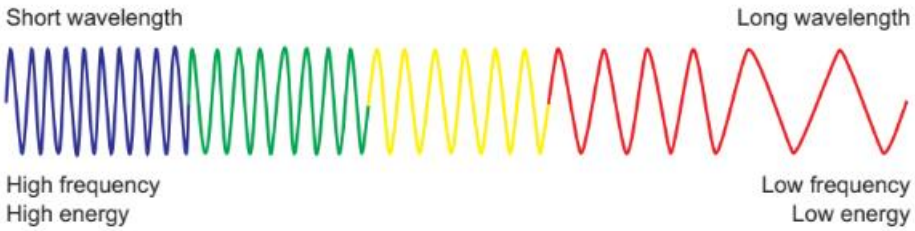

Fig.6 Relationship between wavelengths, the frequency and energy

The Sun is an approximate black body. A black body has the maximum emissivity of 1 equal to radiation adsorbed and not reflected any. A black body can have different temperatures, black bodies emit predominantly infrared energy. When heating up a black body beyond 127 K (1000 ◦C) the emission of light becomes dominant, from red, through orange, yellow, and white (at 6000 K) before ending up at blue, beyond which the emission includes increasing amounts of ultraviolet

radiation. ‘White’ is not a color but a perfect mixture of color. At 6000 K a black body emits radiant energy of all visible wavelengths equally. Higher temperature corresponds to a greater contribution of radiation with shorter wavelengths **(Fig.7)**.

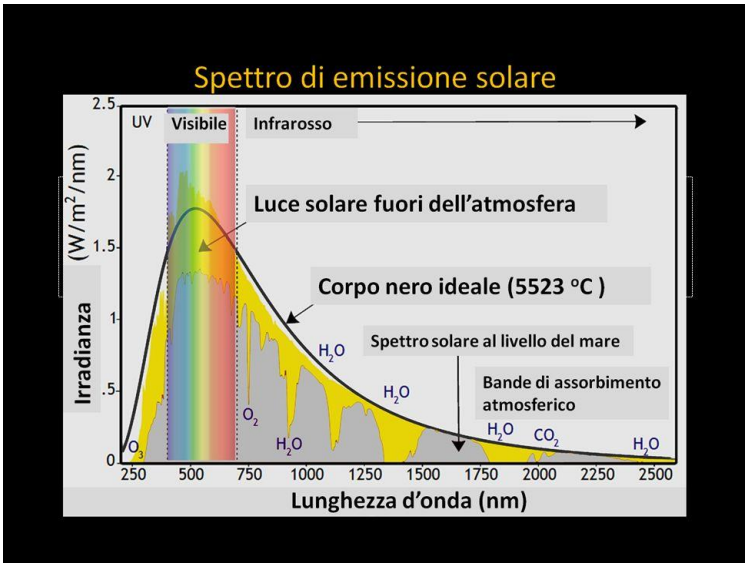

Fig.7 Black body radiation curves with temperature in Kelvin

The most important quantities of remote sensing spectra are:

Radiant emittance is the power emitted from a surface; it is measured in watt per square meter Radiometric units (Wm−2). The spectral radiant emittance characterizes the radiant emittance per wavelength (Wm−2*µm−1).

Radiance is the radiometric measure, which describes the amount of energy being emitted or reflected from a particular area per unit solid angle and per unit time. Radiance is the observed intensity (Wm−2*sr−1).

Irradiance is the amount of incident energy on a surface per unit area and per unit time (W*m^−2).

2.3 Electromagnetic spectra

The range of wavelengths of EM radiation is called EM spectrum. The **Fig.8** shows the total spectrum of EM radiation. The spectrum is divided: gamma rays, X-rays, UV radiation, visible radiation (light), infrared radiation, microwaves, and radio waves. Every named portion represents a range of wavelengths, not one specific wavelength. The EM spectrum is continuous. In the visible electromagnetic spectra **(Fig.9)**, blue light is a wavelength of around 0.45 µm. Red light has a wavelength of around 0.65 µm while green light has a wavelength of 0.54 µm. Electromagnetic radiation outside the range 0.38 to 0.76 µm is not visible to the human eye.

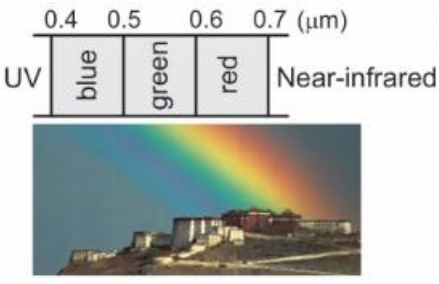

Fig.8 the spectrum of light

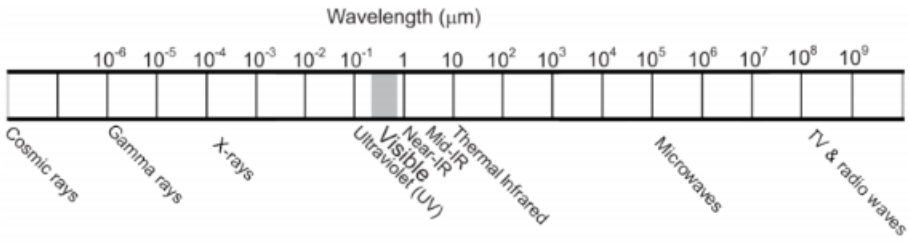

Fig.9 The total spectrum of EM radiation

The radiation beyond red light towards larger wavelengths in the spectrum is referred to infrared (IR). It is possible to discriminate vegetation types and the stress state of plants by analyzing "near-infrared" (and "mid-infrared') radiations. Healthy vegetation has a high reflectance in the NIR range. Mid-IR is also referred to short-wave infrared (SWIR). SWIR sensors are used to monitor surface features at night. Infrared radiation with a wavelength longer than 3 μm is termed thermal infrared (TIR), because it causes the sensation of 'heat'. Thermal emission of the surface of the Earth at (300 K) has a peak wavelength of 10 μm **(Fig.7)**. The body of man emits "heat energy", with a maximum at $\lambda \approx 10$ μm. Surface temperature is needed for studying a variety of environmental problems and for analyzing the mineral composition of rocks, the condition of vegetation, etc. *(Klaus Tempfli, Norman Kerle, 2001)*.

2.4 Atmospheric Scattering

Atmospheric scattering **(Fig.10)** occurs when the particles or gaseous molecules present in the atmosphere cause the EM radiation to be redirected from its original path. The amount of scattering depends on several factors including the wavelength of the radiation, particles, gases, and the distance that the radiant energy travels through the atmosphere. On a clear day the colors are bright, the 95% of the sunlight detected by our eyes (comparable with remote sensor) is energy reflected from objects, instead, 5% is light scattered in the atmosphere. On cloudy or hazy day colors, most of the energy hitting our eyes is scattered light. In the atmosphere, there are three types of scattering according to the size of particles:

1. Rayleigh scattering dominates where electromagnetic radiation interacts with particles that are smaller than the wavelengths of light (O2, N2, dust). Shorter wavelengths (blue) are scattered more than longer wavelengths light (red), because the electromagnetic wave pass above the particle. Rayleigh scattering causes us to perceive a blue-sky during daytime and a red sky at sunset.
2. Mie scattering occur when the wavelength of the EM energy is similar in size to the atmospheric particles. The aerosol (gases, water vapor and dust) are particles responsible for this effect. Generally, it is restricted to the lower atmosphere where larger particles are

more abundant and it dominates under overcast cloud conditions. It has a greater effect on radiation of longer wavelengths than Rayleigh scattering.

3. Non-selective scattering occurs when the particle size is much larger than the radiation wavelength. Typical particles responsible for that effect are water droplets and larger dust particles (e.g., clouds like white bodies).

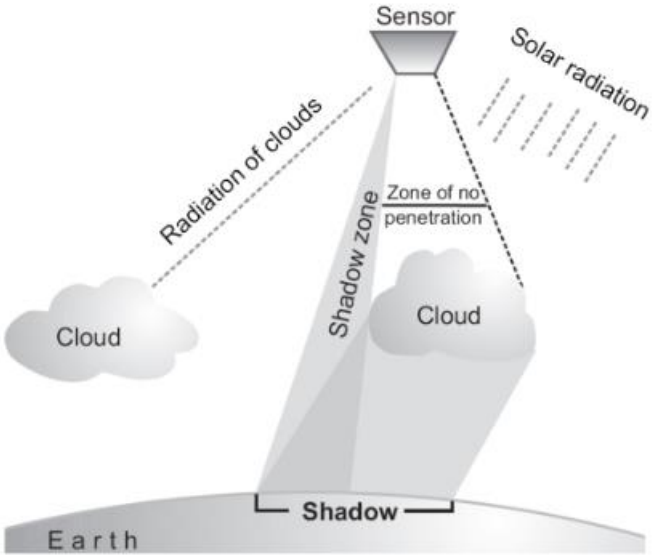

Fig.10 Clouds effects in Remote Sensing

2.5 Reflectance curves

A spectral band or wavelength band is an interval of the EM spectrum for which Spectral band the average radiance is measured. Sensors like a panchromatic camera, a radar sensor, or a laser scanner only measure in one specific band while a multispectral scanner or a digital camera's measure in several spectral bands at the same time. It is possible to have a reflectance curve for each material type of interest. Such a curve shows the portion of the incident energy that is reflected as a function of wavelength, measurements can be carried out in a laboratory or in the field using a field spectrometer.

1. Vegetation

The reflectance characteristics of vegetation depend on the properties of the leaves, including the orientation and the structure of the leaf canopy. The amount of energy reflected for a particular wavelength depends on leaf pigmentation, leaf thickness and composition (cell structure), and on the amount of water in the leaf tissue *(Klaus Tempfli, Norman Kerle, 2001).* The **Fig.11** shows an ideal reflectance curve of healthy vegetation. Due to the presence of chlorophyll in plants there is a peak in the green light band **(Fig.11)**.

Visible band:

In the visible portion of the spectrum, the reflection of blue and red components of incident light is comparatively low because these portions are absorbed by the plant (mainly by chlorophyll) for photosynthesis.

NIR band:

The reflectance in the NIR range is the highest, but the amount depends on the leaf development and on the cell structure.

SWIR band:

In the SWIR range, the reflectance is mainly determined by the free water in the leaf tissue. The wavelength ranges around 1.45 and 1.95 µm are called water absorption bands. When leaves and plants dry, they become yellow, so the process of photosynthesis doesn't predominate and the reflectance is higher in the red color band 0.6 and 0,7 µm.

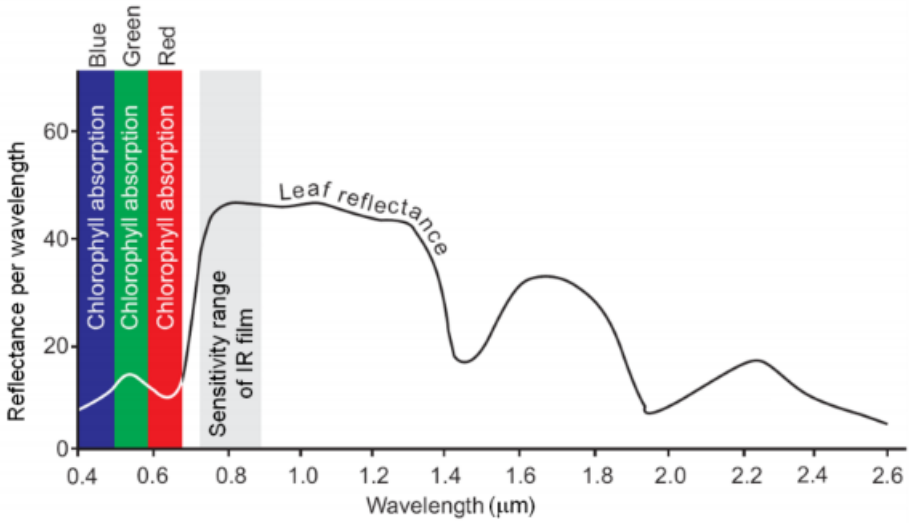

Fig.11 Spectral reflectance curve of healthy vegetation *(Klaus Tempfli, Norman Kerle, 2001).*

2. Soil

The main factors influencing the reflectance are soil color, moisture content, the presence of carbonates, and iron oxide content. It is remarkable in **Fig.12** the typical shapes of most of the curves, which show a convex shape in the range 0.5 to 1.3 µm and dips at 1.45 µm and 1.95 µm. At these dips water absorption bands can be identified again, they are caused by the presence of soil moisture. The iron-dominated soil **(Fig.12-e)** has quite a different reflectance curve, which can be explained by the iron absorption dominating at longer wavelengths.

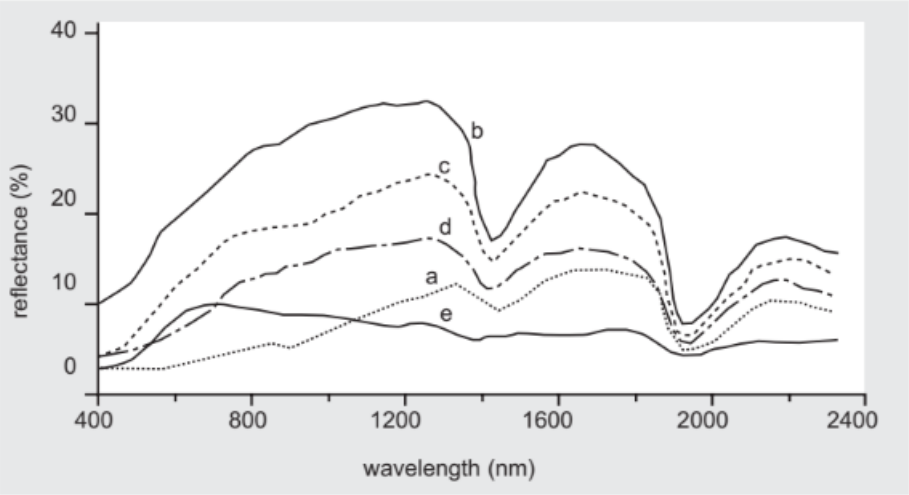

Fig.12 Spectral reflectance for five mineral soils: (a) organic, (b) minimally altered, (c) iron altered, (d) organic affected, (e) iron dominated *(Klaus Tempfli, Norman Kerle, 2001)*.

3. Water

Compared to vegetation and soils, water has a lower reflectance. Vegetation may reflect up to 50%, soils up to 30–40%, while water reflects at most 10% of the incident energy. Water reflects EM energy in the visible range and a little in the NIR. Water containing plants has a pronounced reflectance peak for green light because of the chlorophyll of the plants.

Up to what has been analyzed, the behavior of sunlight reflected on the surfaces in the ecosystems of soil, water, and vegetation can be overall summarized in **Fig.13**.

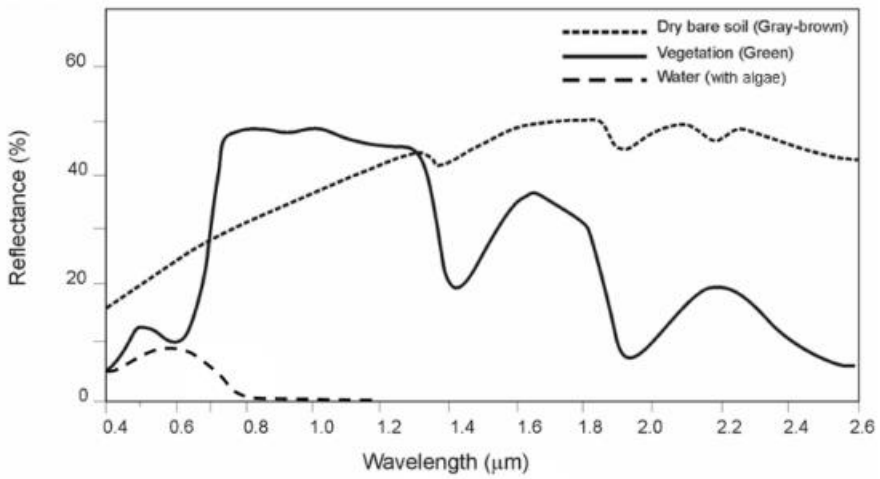

Fig.13 Spectral reflectance curve for the ecosystems of soil, the vegetation and water in different spectral bands

The scene classification layer (SCL) is useful to detect and remove bad observations (mainly clouds and shadows) from images while composing time series. Technical features and the code value assignment of the Sentinel-2 multi-spectral sensor (multi-spectral instrument, MSI) and SCL encoding are reported in **Table.1**.

Table.1 Sentinel-2 MSI technical features and SCL classification *(Filippo Sarvia, Samuele De Petris, 2022)*

Table 1. Sentinel-2 MSI technical features and SCL code pixel assignment.

MSI Technical Features			SCL Codes	
Geometric Resolution (m)	Bands	Wavelength (nm)	Code	Description
10	b2	458–523	0	No data
	b3	543–578	1	Saturated or defective
	b4	650–680	2	Dark area pixels
	b8	785–900	3	Cloud shadows
20	b5	698–713	4	Vegetation
	b6	733–748	5	Not vegetated
	b7	773–793	6	Water
	b8a	855–875	7	Unclassified
	b11	1565–1655	8	Cloud medium probability
	b12	2100–2280	9	Cloud high probability
60	b1	433–453	10	Thin cirrus
	b9	935–955	11	Snow
	b10	1360–1390	-	-

2.6 Geospatial Data Acquisition

Limiting the spatial interest of RS to objects that can be located on the surface of the Earth, using a geodetically defined coordinate system, Geospatial Data Acquisition (GDA) is the term used. The outcome of GDA is not simply an image as obtained by converting sensor recordings, but the processing/interpretation and validating require knowledge about the sensing process and yields data readily suited for analysis, for example in a Geographic Information System (GIS). Typical products derived from geospatial data are orthophoto maps, “satellite image maps”, topographic maps, thematic maps such as land use maps. Over the years, the technique of photogrammetry has evolved offering an extension from the traditional ground-based methods to a large extent observing directly in the field and then by measuring terrain features indirectly on a remote screen. Geospatial Data Acquisition is important to the science of remote sensing for navigating and planning, mapping, monitoring, modeling, and decision making.

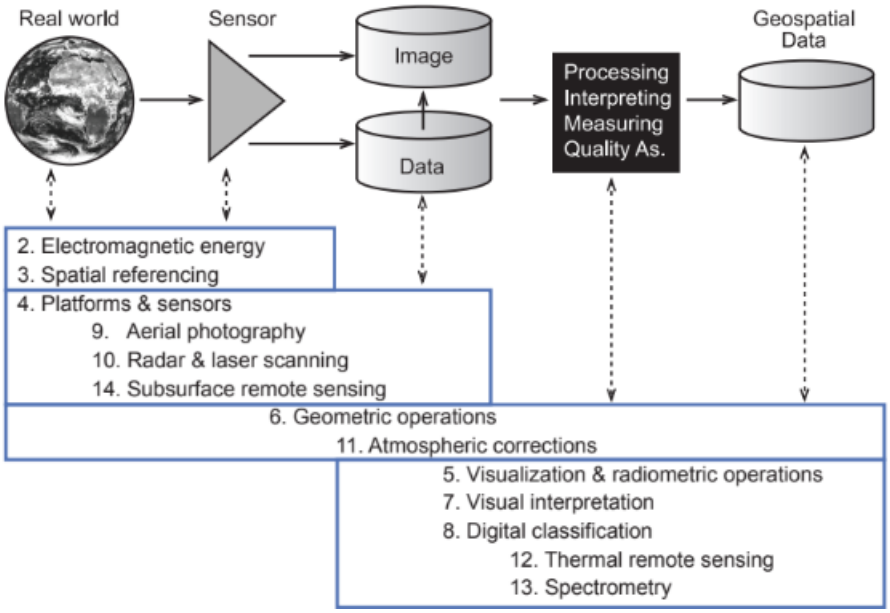

Fig.14 Remote sensing process (*Klaus Tempfli, Norman Kerle, 2001*)

In this context, the data derived from Earth observation play a key role. Specifically, among the various satellite missions available, the data derived from the Sentinel-2 mission allow to obtain satellite images with excellent geometric, temporal and spectral resolution. Sentinel-2 satellites, thanks to the Multispectral Instrument (MSI), acquire data in 13 spectral bands. These bands have been selected to cover a wide range of wavelengths, from the visible to the short-wave infrared spectrum. The Sentinel-2 bands are provided at different geometric resolutions. Precisely, the visible and near-infrared bands are provided at 10 meters of resolution, near-infrared and shortwave infrared bands at 20 meters, while the aerosol, water vapor and cirrus bands at 60 meters of resolutions (*Gascon et al., 2014).*

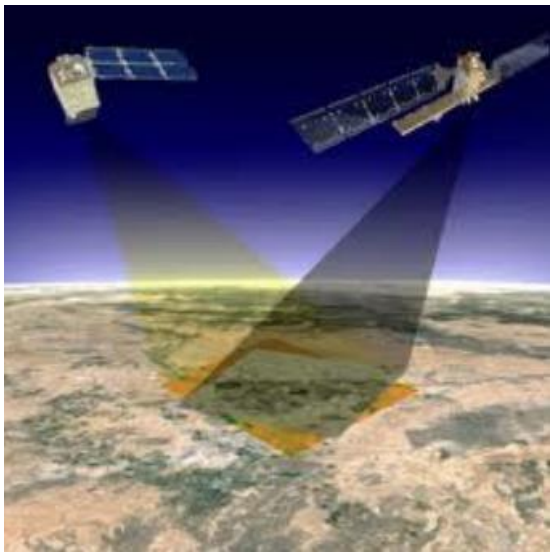

Fig.15 Satellite data acquisition (*sportello dell'agricoltura, 2019)*

The versatility of Sentinel-2 data, combined with the EU's promotion of the integration of satellite data within the Common Agricultural Policy (CAP) monitoring, sets the basis for a transformation of CAP controls management, there is still work to adapt the high resolution images coming from the satellite Sentinel-2 at the CAP techniques in the agricultural field with a detail of up to 10 m on the ground and a horizon on the ground of 250 km (*sportello dell'agricoltura, 2019)*. Through these methods and by reducing the operation in situ, it is possible to accurate information about the territory plants and cultures. The vegetation index (the Normalized Difference Vegetation Index, NDVI) is an example to determine the presence of plants or forest from water, crops or buildings **(Fig.16)**. Referring to vegetation, these vegetation spectral indices generally combine the reflected signal in the red band (580-750 nm), which can be correlated with the absorption operated by chlorophyll to support photosynthetic function, instead the features depend on the leaf structure and canopy reflected in the near-infrared band (750- 1100 nm). Multi-time series analysis of vegetation index maps allows to describe the behavior of natural or crop vegetation over the years *(Kurbanov and Zakharova, 2020; Xue and Su, 2017).*

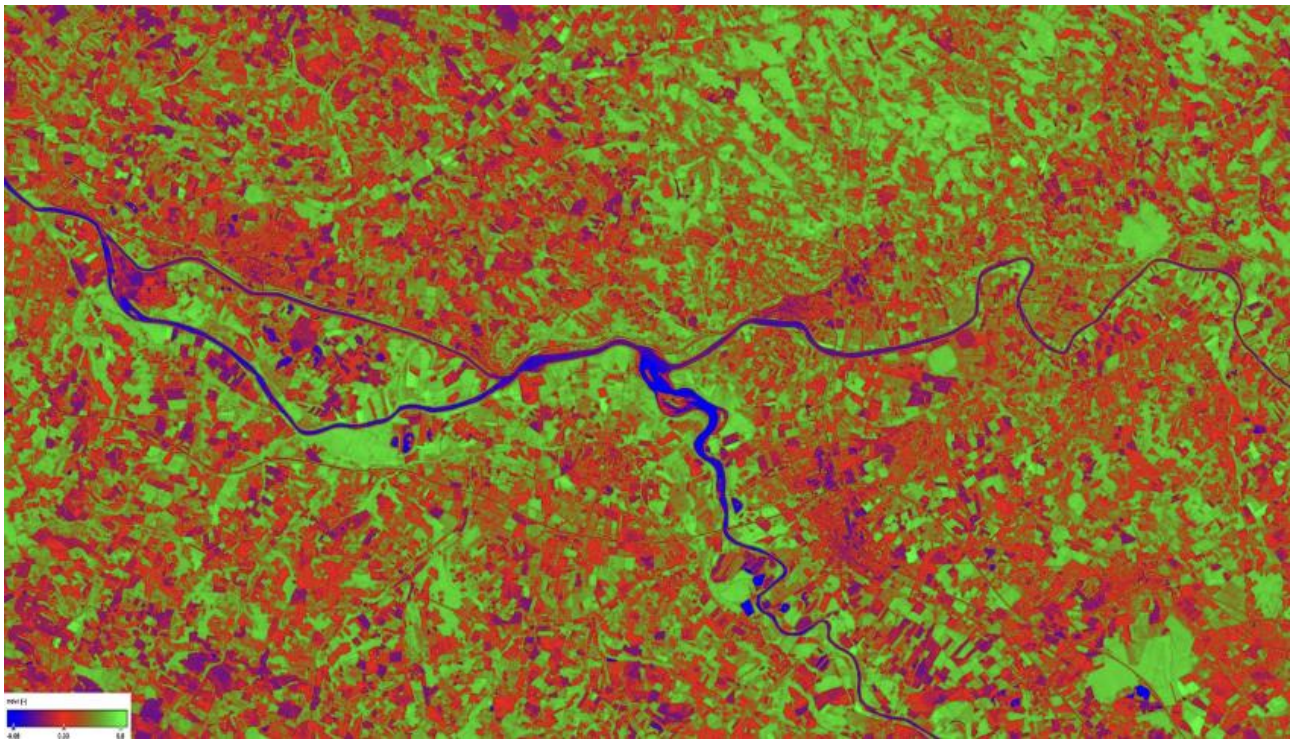

Fig.16 NDVI index used to distinguished plants or forest from water, crops or buildings (*sportello dell'agricoltura, 2019)*

2.7 Crop classification technique

Minimum Distance (MD) and Random Forest (RF) algorithms are largely used in agriculture for supervised crop classification. In particular, MD consents a complete control of results and a more reasonable tuning of the few parameters that it requires. According to a crop classification approach based on NDVI temporal profile, MD is in charge of comparing the Euclidean distance from each cell and the class centroids. Otherwise, Random Forest (RF) classification is based on the arbitrary choice of an indefinite number of decisions previously taken. It requires more parameters for the elaboration of data and the results are more complex to interpret.

2.7.1 SI: Separability index and NDVI Index

A separability analysis, based on statistical concerns, was therefore performed in order to detect the most suitable moment and bands useful in the classification of cultures. The average and the standard deviation are calculated for all bands and the images of the respective periods are select through Sentinel-2 images. In the classification are taken into account: band wavelength, class i-esima e class j-esima (e.g., rice and soya). Than, the separability index SI is calculated. Separability is statistically possible when SI > 1 and it depends from mean values of lambda spectral bands and variances of lambda spectral bands in time domain field. Once the best spectral bands are individualized, a new Minimum Distance (MD) is carried out. Again, Otsu's Method (OM) applied on the DL image histogram was used to locate a proper threshold to separate soya and rice from other summer crop. Following *(Filippo Sarvia, Samuele De Petris, 2022*) study, through remote sensing techniques for the vegetation index NDVI for meadow detection it has low values of NDVI standard deviation (σNDVI). Differently, others crops of interest (CoI), as corn, wheat, and soya are characterized by a greater NDVI variability along the year; they present the typical phenological behavior where NDVI starts to grow after plow, reaches the maturity plateau and finally decreases after the harvest. That generates higher values of σNDVI.

2.7.2 Cultures classification and wheat detection

In accordance with the Title III of Reg. (EU) 1307/2013) of Common Agricultural Policy (CAP) 2020, ARPEA (Piedmont Regional Agency for Agricultural Payments) indicated the crops of interest (CoI), namely soya, corn, wheat, rice, and meadow. Local agronomic calendars were taken into consideration to support the recognition of the phenological development of CoI. Crop development can greatly differ around the world. In particular, it can vary in terms of length, strength, and period of the year **(Fig.17)**. Agronomic calendars have a key role in classification processes and cannot be neglected.

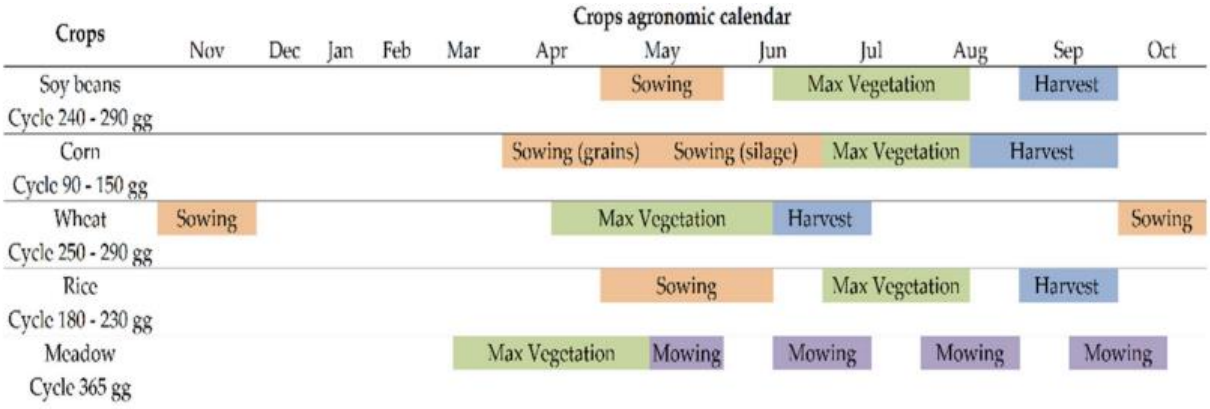

Fig.17 Crops of interest (COI) like soya, corn, wheat, rice, and meadow and periods of growing *(Filippo Sarvia, Samuele De Petris, 2022)*

The calendar in **Fig.17** considers the summer and the winter period of growth of the cultures mainly relying on crops local phenological behaviors *(Filippo Sarvia, Samuele De Petris, 2022)*. The Distance Layer (DL) is generated during Minimum Distance (MD) classification method and DL image histogram was analyzed by Otsu's method (OM) **(Fig.18)**, searching for an automatic and objective threshold, for example, able to separate the wheat from other winter crops. OM is a

nonparametric and unsupervised thresholding approach that locates the threshold where the separability of image pixels is maximum.

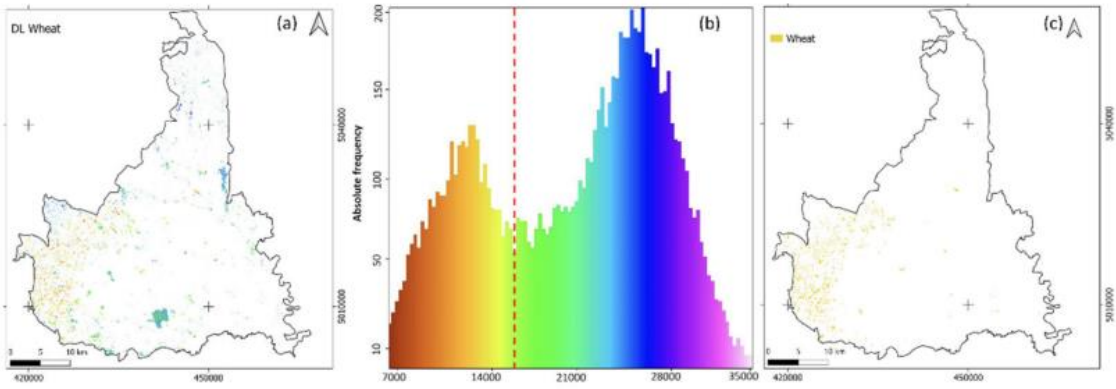

Fig.18 a) DL map of wheat. (b) Wheat DL map frequency histogram (units are NDVI × 10,000). Red line is threshold found by OM. (c) Fields classified as wheat (reference system is WGS84/UTM 32N, EPSG: 32632), *(Filippo Sarvia, Samuele De Petris, 2022*)

2.7.3 Spectral signatures of corn culture

Corn detection in the DL image histogram **(Fig.19b)** shows two peaks. The first, centered around DL low values (about 2000), is probably related to corn fields. The second, centered around DL high values (about 12,000), is probably related to other summer crops. It is worth noticing that the DL map **(Fig.19a)** alone is already able to provide a preliminary overview of the spatial distribution of corn (red) and other summer crops (green). The **Fig.19c** shows the map of corn fields as classified by the proposed method.

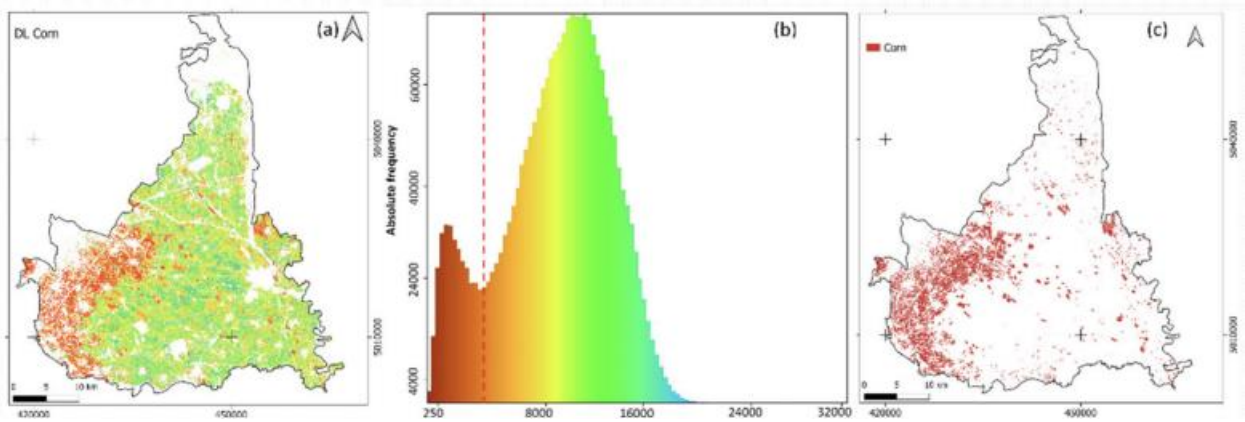

Fig.19 (a) DL map of corn. (b) Corn DL map frequency histogram. Red line is threshold found by OM. (c) Fields classified as corn (reference system is WGS84/UTM 32N, EPSG: 32632)

2.7.4 Spectral signatures of soya and rice cultures

The spectral profile **Fig.20** of soya and rice was analyzed by visual interpretation. It is clear that: (i) visible bands show low separability; (ii) NIR and MIR bands show high separability values; (iii) NIR and MIR related separability is generally lower in June ($S \approx 1$) than in July and August ($S > 2$). From an agronomical point of view, that can be interpreted as probably due to the similar earlier development stage that the two analyzed crops present in June month.

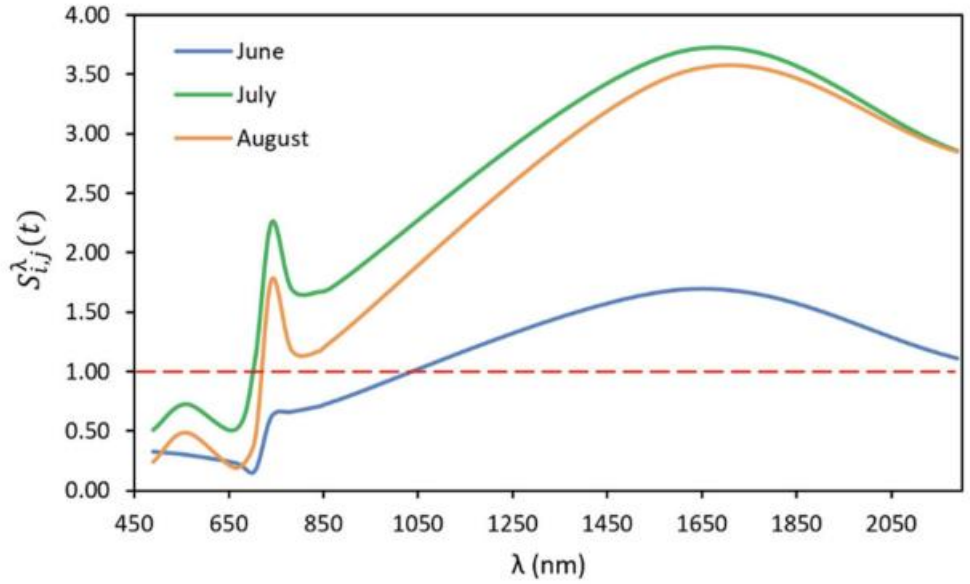

Fig.20 Spectral signatures of rice and soya in June, July and August months and their separability index SI. SI =1 is threshold value *(Filippo Sarvia, Samuele De Petris, 2022*)

In July the spectral response of the two crops appears to maximize their separability. In that period of the year, soya and rice are showing two different phenological stages. In fact, in July, soya is experiencing its node development and bloom; rice is approaching panicle formation while exiting its tillering phase. With reference to the selected band subset (b5-b8a, b11, and b12) from the July acquisition, Minimum Distance (MD) was run trained with 132 soya and 140 rice fields from GCs *(Filippo Sarvia, Samuele De Petris, 2022*). OM was used to locate a proper threshold in the correspondent DL image histogram **Fig.21b** to separate these two classes from the remaining ones. DL image histogram shows a drastic fall just after the OM threshold (2500). **Fig.21c** shows the final map of soya and rice fields.

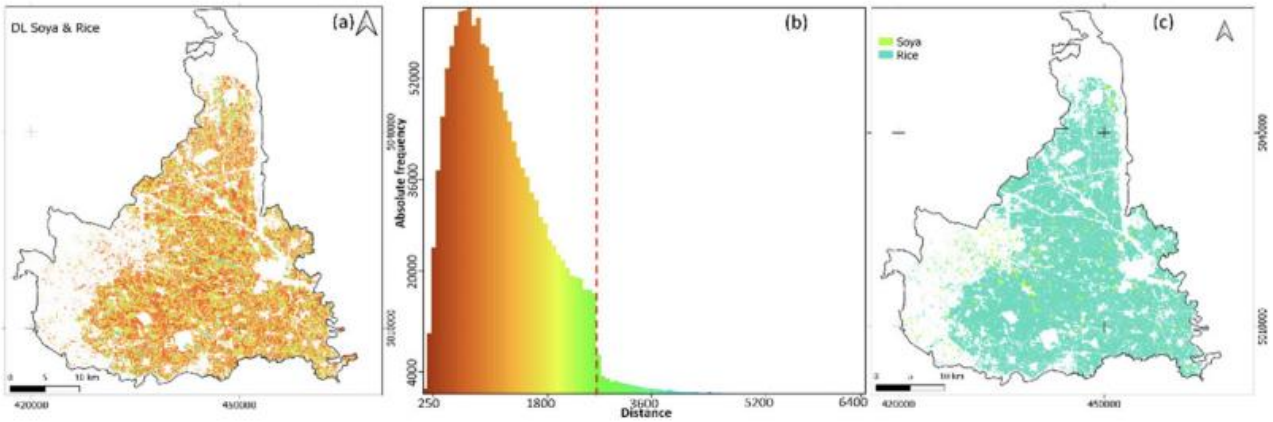

Fig.21 (a) DL map of soya and rice. (b) Soya and rice DL map frequency histogram. Red line is threshold found by OM. (c) Fields classified as soya and rice (reference system is WGS84/UTM 32N, EPSG: 32632), *(Filippo Sarvia, Samuele De Petris, 2022*)

CHAPTER 3

3. Study Area

3.1 Study area description

The study area (*https://it.wikipedia.org/wiki/Norcia*) **(Fig.23)**, is located at an altitude of 600 meters above sea level (m s.l.m.), in the province of Perugia and it covers an area of about 100 km^2 and borders with Appennino Umbro-Marchigiano and Lazio and Marche in the north, limited by Altopiano di Santa Scolastica which has tectonic origin, and it is part of Monti Sibillini National Park Area. Three main floors cover a surface of 15 km² which define the interested territory: Pian Grande, Pian Piccolo (province of Perugia), and Pian Perduto (province of Macerata). Particularly, Pian Grande is situated at few kilometers from the center of Norcia, and it is territorially bounded to the north-east by Monte Vettore (2.476 m), to the south-east by Monte Guaidone (1.647 m), to the north-west by Monte Veletta (1.614 m), and to the south-west by Monte Ventosola (1.718 m).

From the geographic point of view, the area of interest is in the meeting place of two different landscape: Valnerina and Monti Sibillini. Mountainous area of tectonic origin with grassy slopes or covered with beech forests, rounded by glacial and aeolian action, within which vast karst plateaus open up exploited for grazing cattle and flocks. The agricultural landscape is configured in a suggestive system of open fields. The area is characterized by the cultivation of lentils, declared a Protected Geographical Indication in 1999 *(https://www.landscapeunifi.it/2014/05/27/umbria).*

Fig.22 Piani di Castelluccio di Norcia *(https://www.fonterosa.eu/i-piani-di-castelluccio-di-norcia/)*

Currently, the area is under the influence of numerous karst phenomena which have determined the formation of karst structures known by the locals as Mergani, deep sinkholes that furrow the main plain and drain rainwater into underground water tables, which also bring water to the Sordo and Torbidone rivers, of the plain of Santa Scolastica (*https://www.fonterosa.eu/i-piani-di-castelluccio-di-norcia/*). The climate of Umbria, despite the small size, is extremely varied because of the difference in altitude. In the plains and hills it has a sub-littoral or temperate Mediterranean

climate at high altitude, with typical summer drought, while in the mountain areas it is temperate sub-continental. At the highest altitudes, it is cool temperate, with often considerable rainfall mostly in Spring and in Autumn. Average annual temperatures of the most important centers are generally between 11,2°C of Norcia and 15°C of Terni moving to 12,9°C of Spoleto, 13,1°C of Perugia and 14,2°C of Foligno. Altitude plays definitely a key role: Norcia, 604m above the sea level has an average temperature of the coldest month (January) of about 1,1°C while Perugia (493 m s.l.m.) and Spoleto (396 m s.l.m.) has values of almost 3° higher (Perugia 4,0 °C) *(http://www.centrometeo.com/articoli-reportage-approfondimenti/climatologia/5412-clima-umbria)*.

The flowering of greatest interest takes place around the end of May and July as: poppies, daffodils, daisies, violets, cornflowers, wheat, but also from ears of barley and spelt.

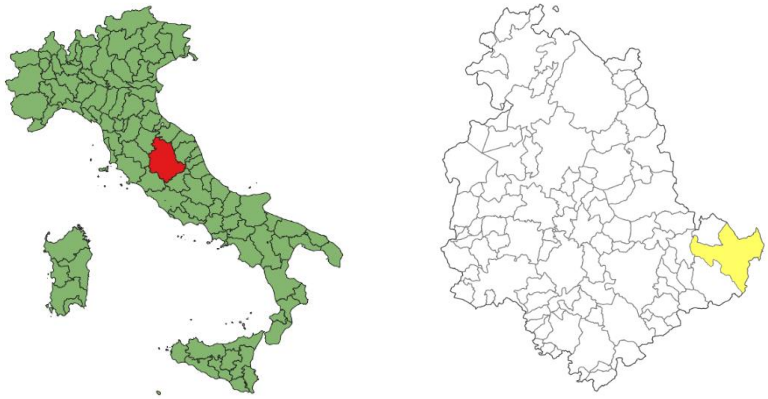

Fig.23 Study area of the Umbria Region in the province of Perugia and framing in the south-east area (QGIS software)

Fig.24 Study area in the province of Perugia (ENVI software)

3.2 Study Area classification

Through Dataset of PlanetScope it is possible to download a land use map for the Umbria Region for the study area of Appenino Umbro-Marchigiano (which constitutes the reality on the ground) marking the natural and wooded areas from the built-up ones, agricultural areas, rivers and waterways, urban centres and roads. The area is studied during June, July and September in order to emphasize the changing of phenological cycles and of cultures in the different months and to understand what causes them. ENVI Program permits to observe the changing of the region of interest in a specific way, focusing on the following areas for all dataset: north area of Norcia **(Fig.25)**, north-east area of Grotti **(Fig.26)**, center-east area of San Pellegrino **(Fig.27)**, and south area of Valcadara-Savelli **(Fig.28)** and the center area of Popoli **(Fig.29)**.

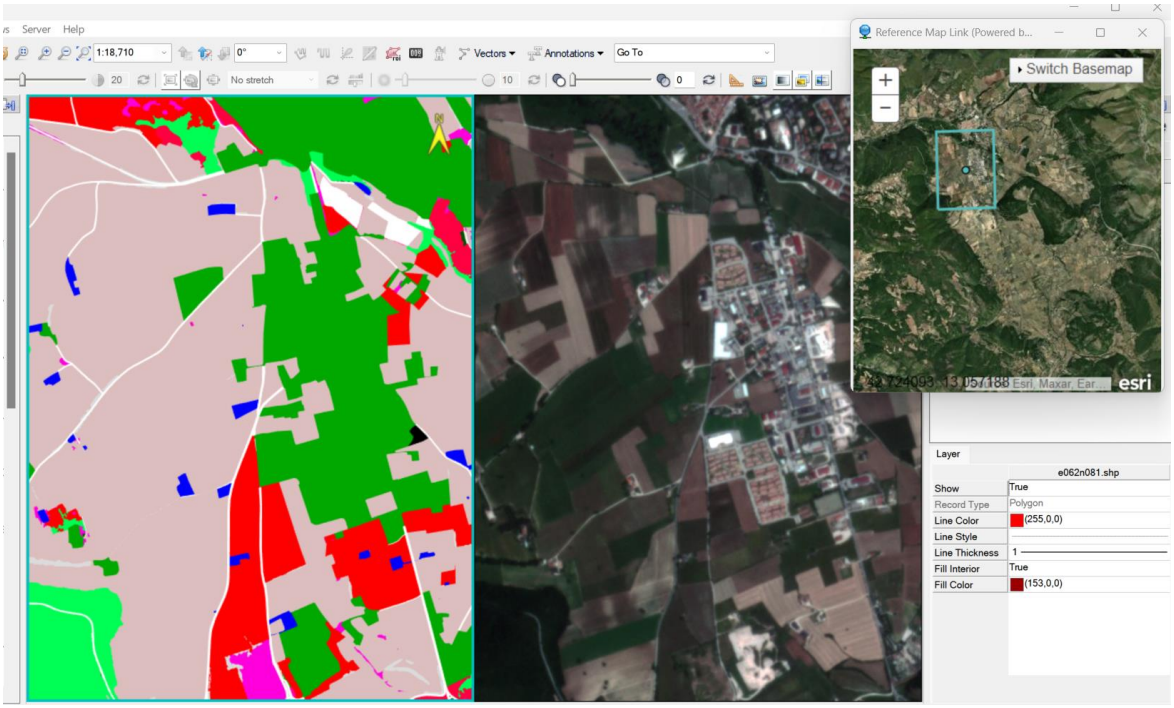

Fig.25 Ground reality map in June for the north area near Norcia (ENVI software)

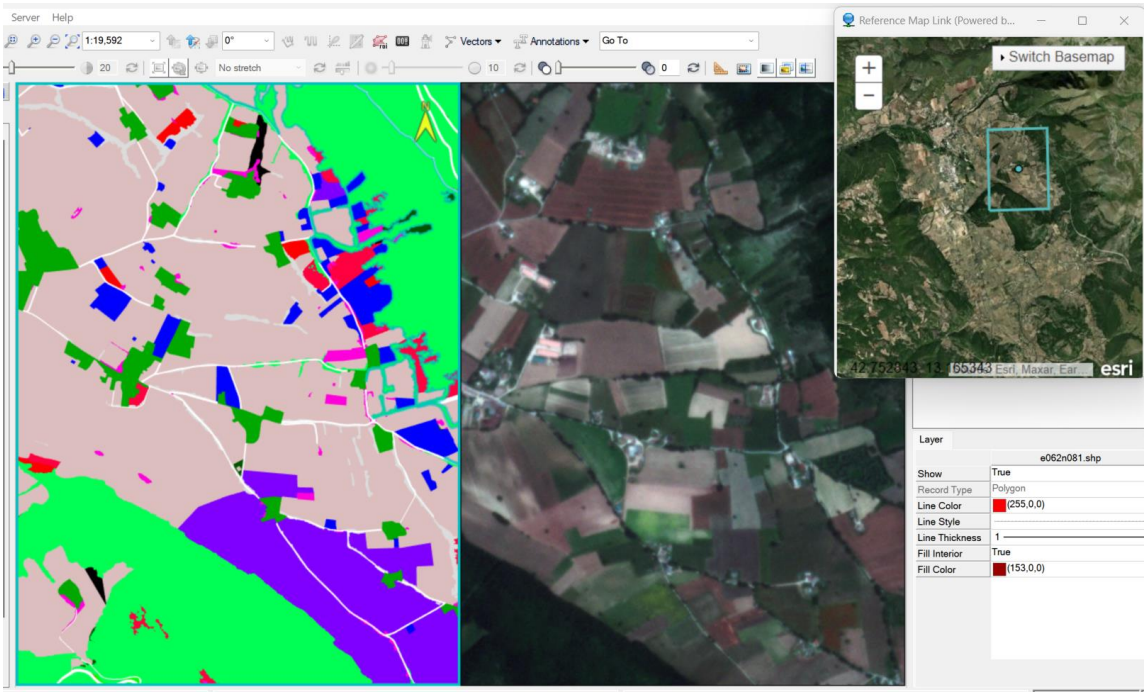

Fig.26 Ground reality map in June for the north-east area near Grotti (ENVI software)

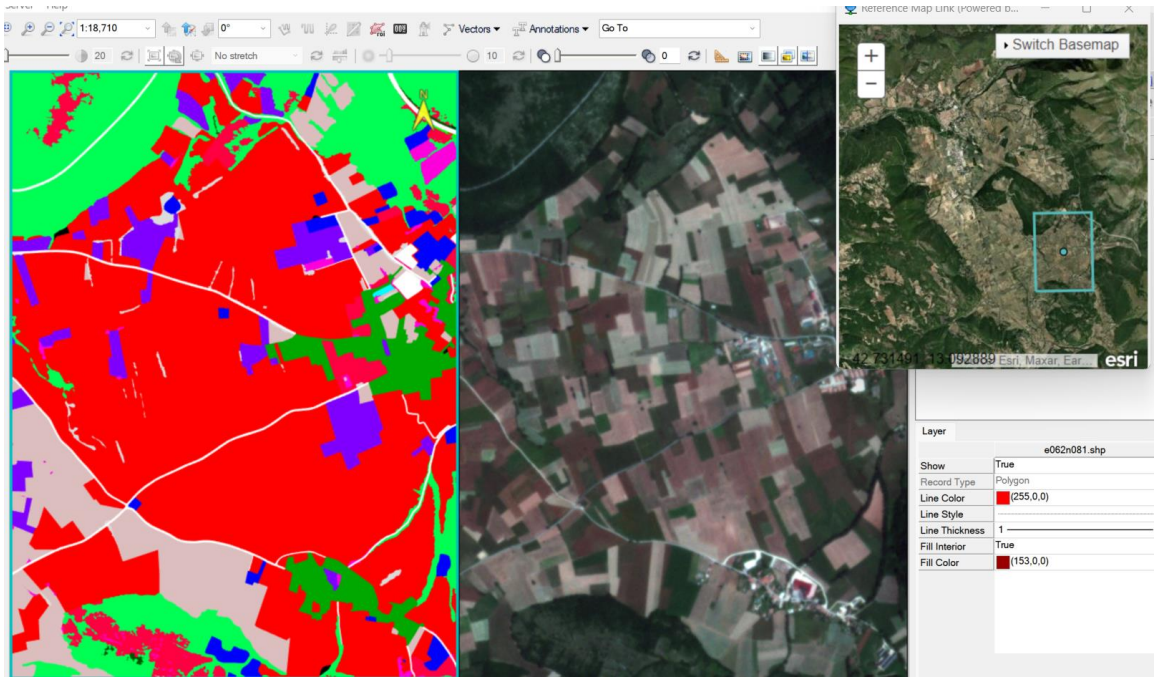

Fig.27 Ground reality map in June for the center-east area near San Pellegrino (ENVI software)

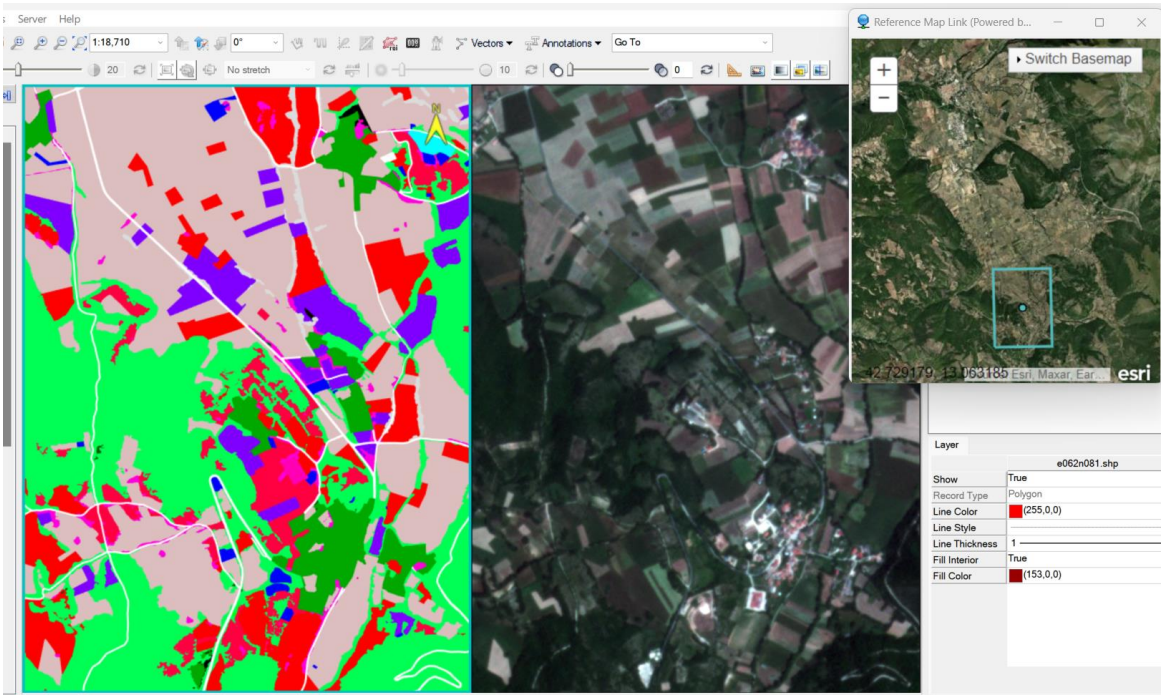

Fig.28 Ground reality map in June for the south area near Valcadara-Savelli (ENVI software)

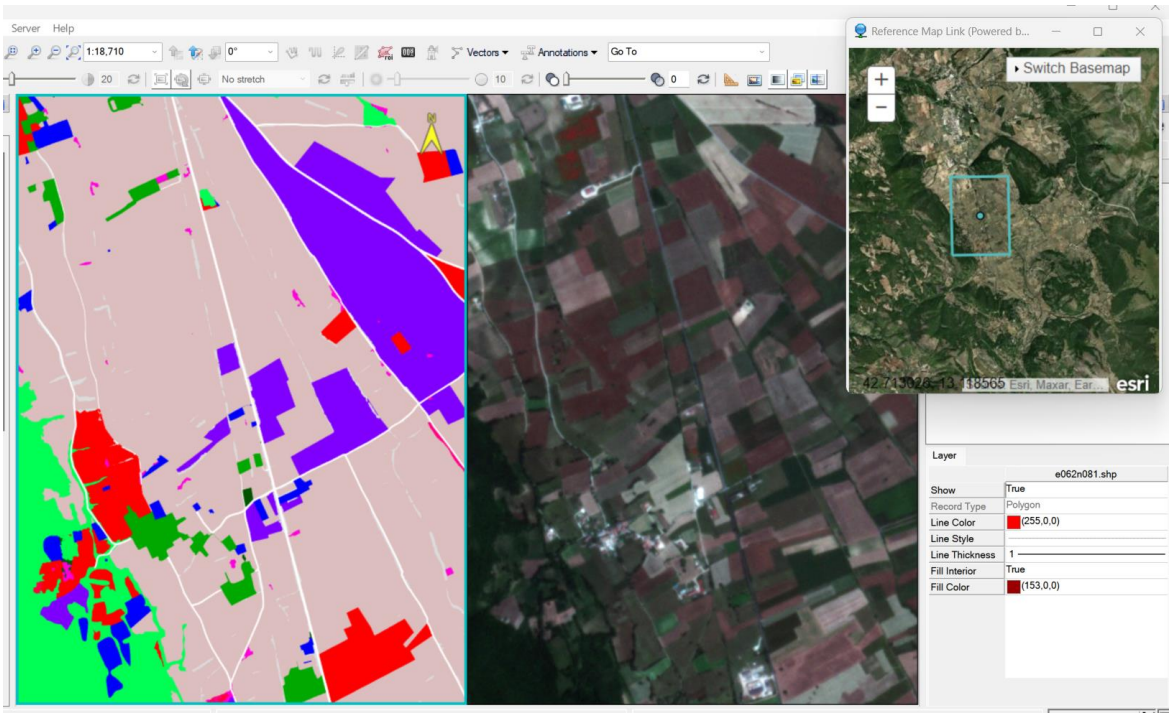

Fig.29 Ground reality map in June for the center area near Popoli (ENVI software)

3.3 Geological and seismic framework of the area

From the geomorphological point of view, as shown in **Fig.30,** the north part towards the city of Norcia and in the center part towards the city of Grotti, there are rather evident alluvial fans of debris and series of carbonate rocks, in particular marls and limestones. In the southern area towards the city of Valcadara there are alluvial fans with terraced detrital deposits. In the western area, carbonate series, alluvial deposits and a small fan belt can be seen, while in the eastern area towards the city of San Pellegrino series of carbonate formations typical of Appennino Umbro-Marchigiano are present, as well as rock formations such as red Scaglia and white Scaglia which are very important for trade in Italy and abroad. Finally, it can be deduced from **Fig**.**30**, that the area is under the influence of a huge formation of alluvial fan which gives the area considerable importance for agriculture from the point of view of agricultural products and crops typical of the Umbria Region.

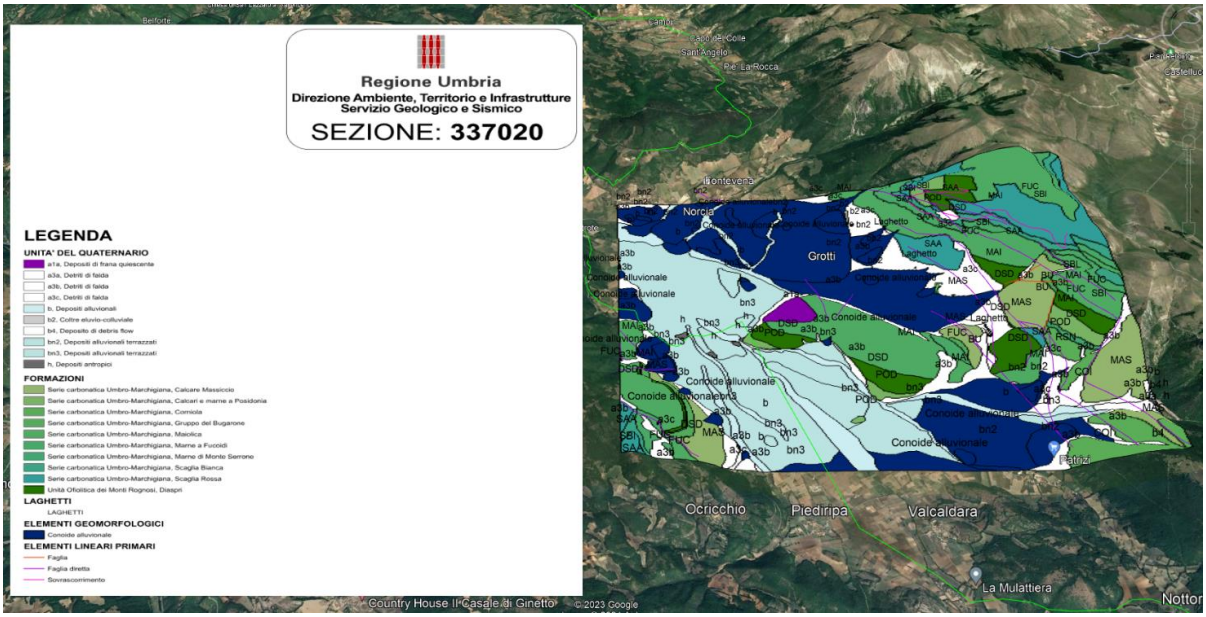

Fig.30 Geological formation of the south-eastern area of the Umbria region for the cities of Norcia to the North, San Pellegrino to the East, Popoli to the West and Valcadara to the South *(https://www.regione.umbria.it/paesaggio-urbanistica/cartografia-geologica)*

From the seismic point of view **(Fig.31)** the area is not affected by strong subsoil movements, the only area where tectonic instability is present is in the central area under the city of Grotti, where landslide deposits are present **(Fig.30)**.

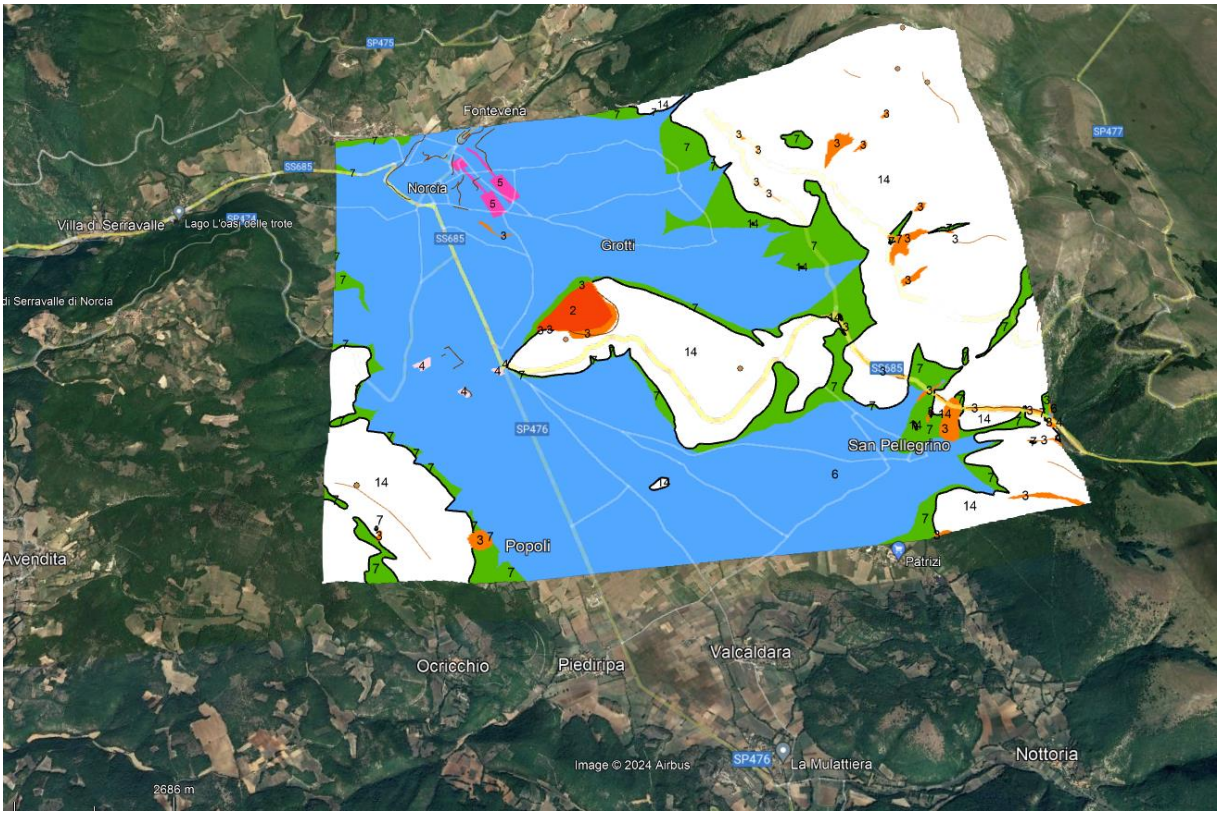

Fig.31 Local seismology of the south-east area of the Umbria Region: the numbers indicate in decreasing order of danger from top to bottom the areas where landslides or instability may occur. In red, unstable areas subject to landslide movements; in blue, areas of alluvial deposits susceptible to seismic amplifications but stable *(http://storicizzati.territorio.regione.umbria.it/Static/PsismicLocaleKmz/Index_kmzMobile.htm)*

3.4 Statistic agricultural dates in Umbria

Biological farming is a method of agricultural production that uses techniques that exclude the use of fertilizers, phytochemicals, synthetic chemical veterinary medicines, and genetically modified organisms, while respecting the fertility of the soil, individual crops, animals and environmental balance. Biological farming helps reduce the risk of pollution and degradation of environmental matrices, water, soil and air, connected to the use of synthetic chemical products and promote the protection and enhancement of biodiversity and the agricultural landscape.

The Umbrian biological area in recent years has increased from 47,369 to 50,936 with an increase of 7.5% compared to the year 2020 (2020-2021 variation) and with a percentage incidence of 15.2 on the national total *(Angelo Frascarelli, Tommaso Cesaretti, 2019).*

Specifically, of the 46,595 hectares of biological farming in Umbria, most are divided between cereals, fodder crops, olive trees and vegetables. In fact, the four categories alone cover about 49% of the entire Umbrian biological area, while at the Italian level they reach almost 52%.

In particular, **Table.2** shows a greater propensity for biological olive growing in the Umbrian territory, historically dedicated to the cultivation of this plant, and less in terms of viticulture and cereal cultivation *(Angelo Frascarelli, Tommaso Cesaretti, 2019).*

Table.2 Division of the cultures present in the Umbria Region

Coltura	Superficie Biologica Umbria		Superficie Biologica Italia	
	ha	%	ha	%
Cereali	6.340	13,6	330.284	16,6
Colture proteiche[1]	386	0,8	47.523	2,4
Piante da radice	67	0,1	3.704	0,2
Colture industriali	1.337	2,9	36.408	1,8
Colture foraggere	8.561	18,4	396.748	19,9
Altre colture da seminativi	222	0,5	23.460	1,2
Ortaggi[2]	1.842	4,0	65.082	3,3
Frutta[3]	139	0,3	37.074	1,9
Frutta in guscio	668	1,4	50.612	2,5
Vite	1.085	2,3	109.423	5,5
Olivo	6.151	13,2	242.708	12,2
Altre colture	19.797	42,5	650.210	32,6
TOTALE	**46.595**	**100,0**	**1.993.236**	**100,0**

3.5 Cultural species in the region of interest

In the Umbria-Marche area taken as a reference, from the land cover map it is possible to highlight many crops present there, also with the help of the orthophoto taken at 20 cm provided by the PlanetScope dataset. Once the crop has been located, it is easy to recognize the details that differentiate it from the others. Below are the crops analyzed and their stages of sowing, growth and maturation up to harvest.

- Wood arboricolture

Fig.32 shows the cultivation of wood arboriculture near the city of Grotti in the studied area.
Fig.33 shows the extension of wood arboriculture.

Fig.32 Wood arboriculture near Grotti

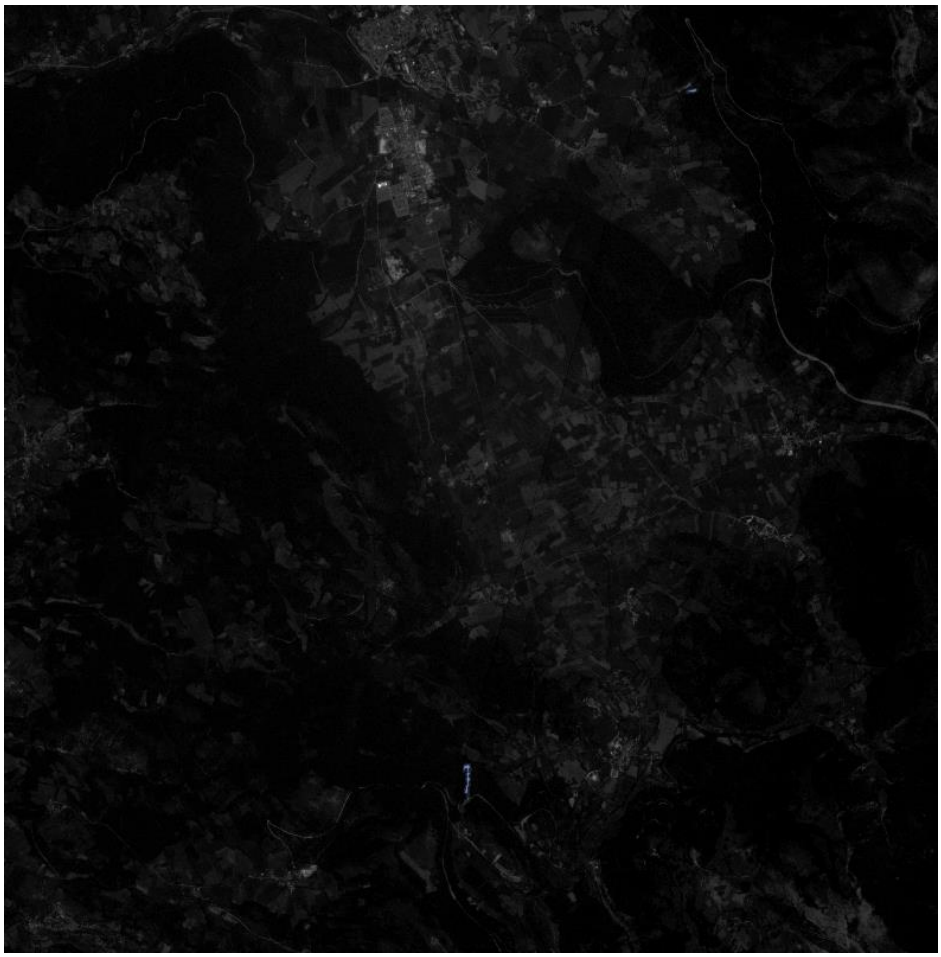

Fig.33 From the land cover map (Palnetscope dataset) the extension of Wood arboriculture is shown in blue (3 species)

Fig.34 Wood arboriculture lands

Definition and classification: "wood arboriculture" refers to the temporary and reversible occupation of agricultural land with the planting of tree species intended to the production of woody masses for predominantly industrial or work use *(Pierpaolo Brenta, Pier Giorgio Terzuolo, 2018).* In arboriculture, the aim can be to obtain valuable timber, woody biomass or both productions on the same plot of land. For woody biomass production, very short cycles are adopted, ranging from 1-2 to 5-7 years with species such as, for example, poplar, willow, black locust, plane, elm, ash, alder, hornbeam or oak. For the production of valuable timber, from 8 years are necessary for poplar to 20 years for species such as, for example, walnut, cherry, ash, oak, maples or rowans *(Enrico Buresti Lattes, Paolo Mori, 2024).*

Location**:** The subject of this study concerning morphology is the area that is predominantly alluvial, halfway between the plain and the river belts, presenting itself as an area of good degree for the growth of this species. The main plain is the best area to grow this crop, in the absence of gravel and sand, risk of erosion and water stagnation. The river belt and therefore the young soils (from the most recent floods), created by the erosion of the river are not suitable for the growth of the wood crop. Even poorly permeable layers of silt and clay are not advisable for the development of wood arable farming. Cultivation occurs mainly in the valley floor, in the north-east area near the city of Grotti and in the south area near the city of Valcadara-Savelli.

Energy: wood biomass can be used for energetic purposes in the form of firewood or wood chips. Trees use the CO2 present in the air to grow, removing it from the atmosphere and, by storing Carbon in the wood, they release oxygen. When wood is burned to produce energy, new carbon is not released into the atmosphere, as happens with fossil fuels, but the same carbon that years before had been immobilized with photosynthesis.

Phenological phases**:** Rooting (growth), sizing (to obtain the appropriate size, soil is worked) and utilization (once the optimal diameter is reached).

- Orchards

Fig.35 shows the cultivation of an orchard near the city of Norcia. **Fig.36** shows the extension of orchards.

Fig.35 Orchards near Norcia

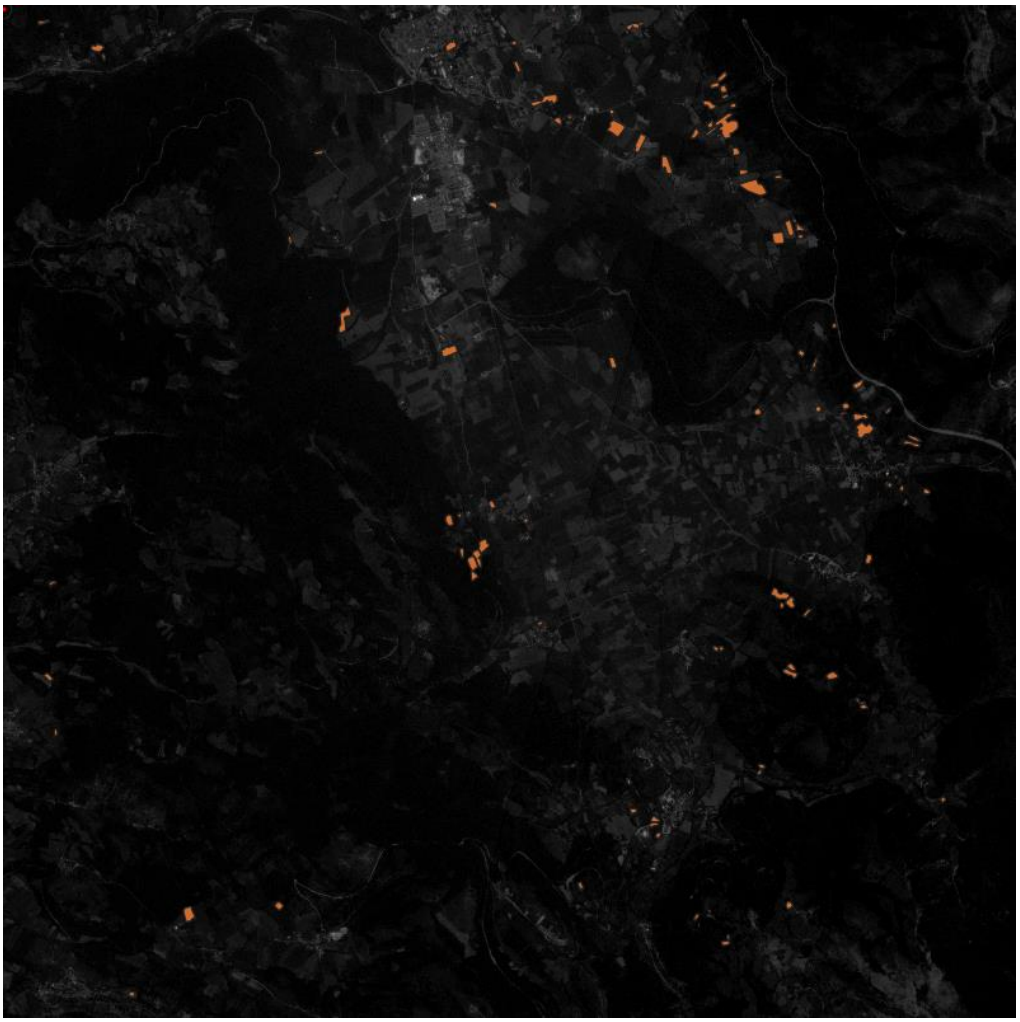

Fig.36 From the land cover map (Palnetscope dataset) the extension of orchards is shown in orange (136 species)

The orchards present in the collection of the Pantalla (PG) and Casalina (PG) areas can be divided in order, by number of species present. Each fruit-bearing plant has a different ripening period *(Mauro Gramaccia, Silvia Spedicato, 2024)*:

1. Apple tree (64): the “Mela Limoncella” typical of the municipality of Cascia and of the entire regional territory was taken into consideration. Flowering occurs in the month of April with the peak around the first, second ten days of the month. Harvest ripening occurs around the middle of October and the fruits are preserved for several months in the fruit store.

Fig.37 Apple tree of Mela Limoncella typical of Cascia city (PG)

Another species is the “Mela Spoletina“**(Fig.38)** found near Norcia (PG): the flowering takes place in the month of April with a peak around the second ten days of the month. The harvest occurs between the first and the second ten days of October. The shelf life of the fruit is good, as it can last for a few months.

Fig.38 Mela Spoletina fruit typical of Norcia city (PG)

1. Pear tree (45): The mother plants of the "Pera Volpina" **(Fig.39)** has been identified in the municipalities of Gualdo Tadino and Gubbio, in the province of Perugia. Flowering

takes place in the third decade of March. The harvest takes place around the month of November, however given the high shelf life of the fruits (a character that guarantees their preservation for many months), fresh consumption must be preceded by a half-time period of a few weeks.

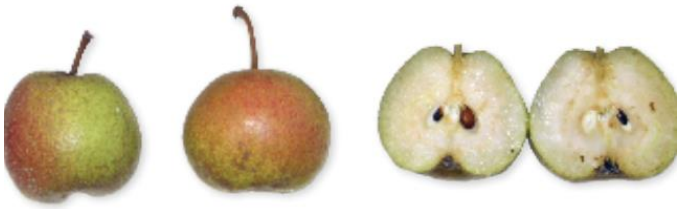

Fig.39 Pera Volpina fruit typical of Gubbio city (PG)

2. Plum tree (17): The "Prugna Agostana" **(Fig.40)** was found in the municipalities of Todi (PG) and Collazzone (PG). Flowering takes place around the first ten days of April. The harvest takes place around the third decade of August; The ripening of the fruits is gradual and consumption, given the easy perishability, is immediate

Fig.40 Prugna Agostana fruit typical of Todi (PG) and Colazzone (PG) cities

3. Fig (9): The "Fico Giallino" **(Fig.41)** has been found particularly in the municipality of Todi (PG) the gradual ripening begins towards the middle of August and lasts until the first ten days of September.

Fig.41 Fico Giallino fruit typical of Todi city (PG)

4. Peach tree (6): The area of probable origin of the "Pesca Marscianese" **(Fig.42)** and of sure diffusion was the Marscianese territory, where the variety was once cultivated and from which it takes the name that identifies it. Currently there are several specimens scattered throughout the territory which are still propagated, as was customary, almost exclusively by seed. Flowering takes place between the third decade of March and the first decade of April, with the peak between the last days of March and the first days of the next. The fruit harvest takes place around the second to third decade of September.

Fig.42 Pesca Marscianese fruit typical of Marscianese territory (PG)

Finally, in the Umbrian territory of this study area there are also fruit trees such as albicocco (2) and cherry (12).

- Vineyard

Fig.43 shows a vineyard system near the city of Norcia. **Fig.44** shows the extension of vineyards.

Fig.43 Vineyards near Norcia (PG)

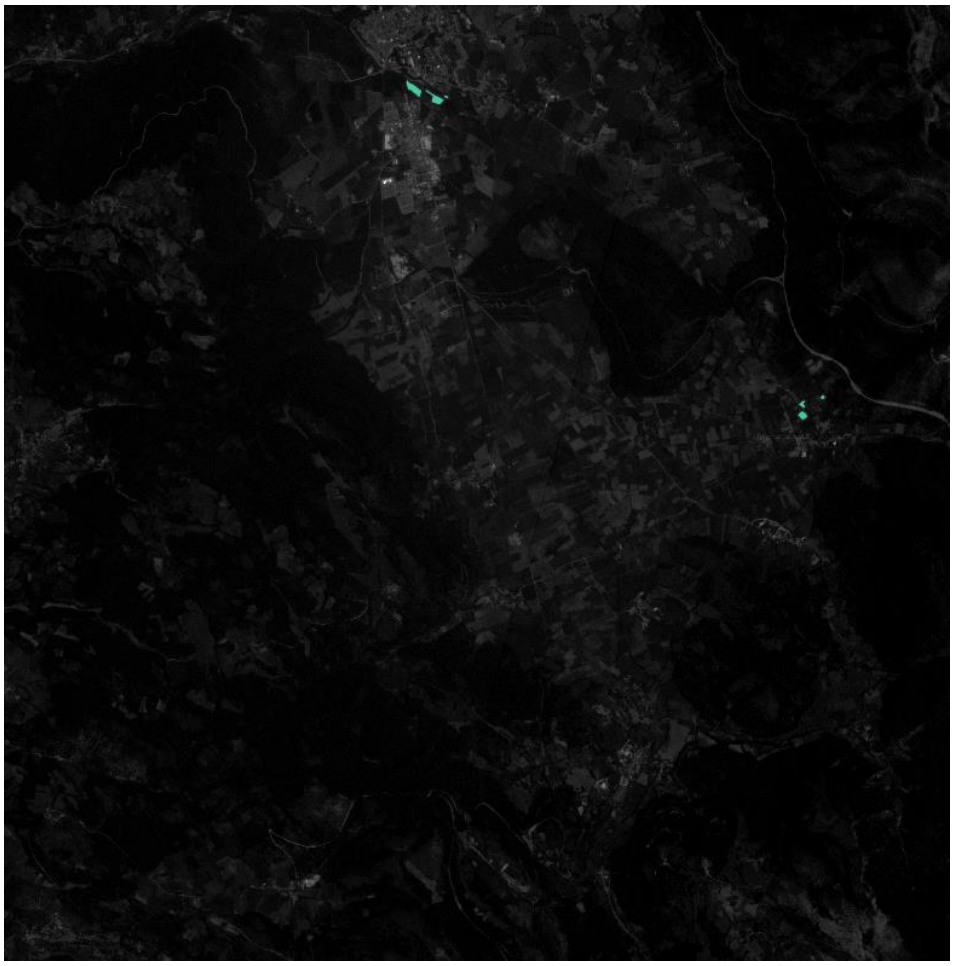

Fig.44 From the land cover map (Palnetscope dataset) the extension of vineyard shown in orange (11 species)

The growing of the vines takes place mainly in the northern area near the city of Norcia **,** the Central-Eastern Zone near the city of San Pellegrino and finally, albeit in traces, in the southern zone near the city of Valcadara-Savelli. The phases of the annual cycle are part of the life cycle: weeping, budding, vegetation, flowering, fruit set, veraison, ripening and winter rest . (*https://tenimenticiva.com/blog/fasi-fenologiche-della-vite/#:~:text=Le%20caratteristiche%20della%20pianta%2C%20la,la%20maturazione%2C%20il%20riposo%20invernale).*

1. Weeping: The long rest of the vine during the cold months is interrupted thanks to the rise in temperature, normally in March.
2. Budding: After weeping, budding occurs, preceded by the swelling of the buds, these open and the first leaves appear. This phase highlights the real vegetative recovery and is affected by the climatic conditions prior to its onset.
3. Vegetative growth: The leaves grow, and new shoots develop. The development of the vegetation extends until August (the period called “agostamento”) in which the shoot matures: from green it becomes brown.

Fig.45 Fruit set of screw

4. Flowering: Between the month of May and June, the flower opens. This phase is very delicate as it can be compromised by a sudden frost or heavy rain.
5. Fruit set: A few days after flowering, small spheres appear: a grape is born from each pollinated flower. With the passage of time the small spheres swell, while the unfertilized flowers fall off, giving rise to the phenomenon of dripping **(Fig.45)**.
6. Veraison: The vegetative activity ends with the beginning of the ripening of the grapes **(Fig.46)**. The berries change color, from green to red or black, depending on the variety, while the white berries show greater transparency of the tissues, taking on a color tending to yellow-green color.

Fig.46 Veraison of screw

Fig.47 Final stage of veraison screw

7. The beginning of ripening is evidenced by veraison and continues for a variable period: about 30 days for early varieties, 50-60 days for late varieties **(Fig.47)**.
8. Once the leaves have fallen, the vine enters the winter rest phase again.

•Chestnut tree

This crop is not very present in the affected area, the only area where its presence can be tested is the central-east zone near the city of San Pellegrino. In the soil map **(Fig.90)** only 1 specie is present.

Fig.48 Chestnut fruits

Soil: The best soils for chestnuts are deep, light and fresh, rich in phosphorus and potassium, those of volcanic origin which, although not acidic, are free of limestone; siliceous soils from the degradation of granites and crystalline schists are also suitable. However, superficial soils can also be used as long as they are light and well supplied with fertilizing elements. Regarding the soil reaction, the pH must be between 5÷6, 5. Traditional chestnut cultivation is widespread along the entire hilly and piedmont area on medium-slope and valley bottom soils previously reserved for cereals and forage crops *(Ginacario Bounous, et.al, 2017).*

Climate: The species is moderately thermophilic, tolerates winter cold, and is suited to environments characterized by an average annual temperature between +8 and +15 °C and with monthly averages above 10 °C for at least 6 months.

Phenological cycle: Budding (maximum flowering of leaves) occurs between March and April, while flowering and fertilization are necessary for pollen germination (fruit production) at temperatures of +27-30 °C and occur in the months between May and July. The fruits reach maturity between September and the beginning of November, in relation to the seasonal trend and, above all, to the genetic characteristics of the tree. For this reason, they are called "late plants" *(Barbara Mariotti, Tatiana Castellotti, 2020).*

- Short-cycle tree crops

The cycle to the production of usable material varies between 8 and 15 years, poplars are the most widespread short-cycle crops. They are present in the Southern Zone near the city of Valcadara-Savelli. Poplar is the most widespread crop for this type. In the soil map **Fig.90** only 3 species are present *(Enrico Buresti Lattes, Paolo Mori, 2016).*

***Phenological cycle*:** The vegetative cycle begins around mid-March with the opening of the wood buds and budding until May. Growth occurs at the end of May until full maturation. It ends with the yellowing and fall of the leaves in the second half of November, that is, at the end of meteorological Autumn *(Giuseppe Frison,2021).*

- Olives

Location: In the area of interest, the presence of olive trees is very scarce if not almost non-existent. In the soil map **(Fig.90)** only 1 specie is present.

Umbria contributes less than 2% of the national oil production. Over 30,000 producers are dedicated to olive growing, operating on a surface area of just over 30,000 hectares (approximately 60% of the regional surface area dedicated to woody crops), of which 20,000 hectares in the Province of Perugia and 10,000 hectares in that of Terni. Olive growing is widespread especially in the hills that close the Terni and Umbrian basins in the Apennine foothills that, starting from Assisi, bends towards Nocera Umbra and extends as far as Spoleto, and also in the area overlooking Lake Trasimeno, at altitudes varying from 150-200 m in the Terni area and up to 500-600 m in the area from Assisi to Spoleto *(Paolo Arice, Dino Biondi, et.al, 2020).*

The olive tree grows very slowly compared to other fruit trees and requires the following phases:

1. Unproductive phase: During this period, production progressively increases, until it reaches its maximum level when the olive tree is about 12-15 years old.
2. Increasing productivity phase: Production continues to be constant for a long period of time, up to 35-40 years.
3. Constant productivity phase: About 35-40 years after planting, production begins to decline at a slow pace.

Temperature: The optimal temperature for the growth of the olive tree is 24-25 °C, the maximum tolerated by this plant is 32-34 °C.

***Phenological cycle*:** The germination occurs between March-April, the flowering at the end of May-June while the harvest in September or in December (table olives), for the olives for oil in September or December *(https://blog.europlantsvivai.com/coltivazione-olivo/#:~:text=Ciclo%20di%20coltivazione,%3A%208%20kg%2F10%20mq).*

Fig.49 Olive landscape in Trevano (PG) and flowering between May and June *(https://blog.euro-plantsvivai.com/coltivazione-olivo/#:~:text=Ciclo%20di%20coltiva-zione,%3A%208%20kg%2F10%20mq)*

- Forage plants

Forage crops are defined as those spontaneous or cultivated plant species that, at a certain stage of their development, can be used as fodder in feeding livestock. Grasslands, pastures, meadows and woods constitute a whole.

In general, forage plants are divided in:

a. Permanent resources: meadows and pastures generally natural and lasting more than 10 years.

b. Temporary resources: grasslands, meadows, cereals and by-products of other crops, generally consisting of sown crops, lasting less than 10 years.

They can be used for harvesting or grazing.

1. Pastures

In **Fig.51** the extension of the pastures is shown in the study area *(Egidio Ciriciofolo, Andrea Onofri, 2003).*

It can be a “permanent” forage formation (usually on plots not suitable for cultivation due to excessive slope, poor profile, outcropping rocks, etc.) or “occasional”, that is, preceded and/or followed by crops other than pasture (for example abandoned arable land, stubble, grassy fallow land, crops for different purposes, etc.).

The type of pasture depends on the crops with which it comes into contact:

- the presence of some species widespread as weeds of cultivated fields (ruderal species, such as Inula viscosa, Stellaria spp., Artemisia campestris, Erigeron spp., Centaurea solstitialis) could indicate that the pasture is rather young and comes from abandoned arable land.
- Instead, the presence of ferns (Pteridium aquilinum) could indicate contact with the forest. The presence of aromatic species (Artemisia, Achillea) or Citisus scoparius, highlight situations of underutilization.

It is essential to know the “livestock load” suitable for the type of pasture for adequate use and conservation of the grass cover and the soil. The modification of the floristic composition is due not only to the “incorrect load” but also to mineral fertilization. Every contribution of nutritional elements should be considered a factor that disrupts the pre-existing balance, because it is able to modify the growth rate.

Fig.50 Pastures near the hills in the area of interest

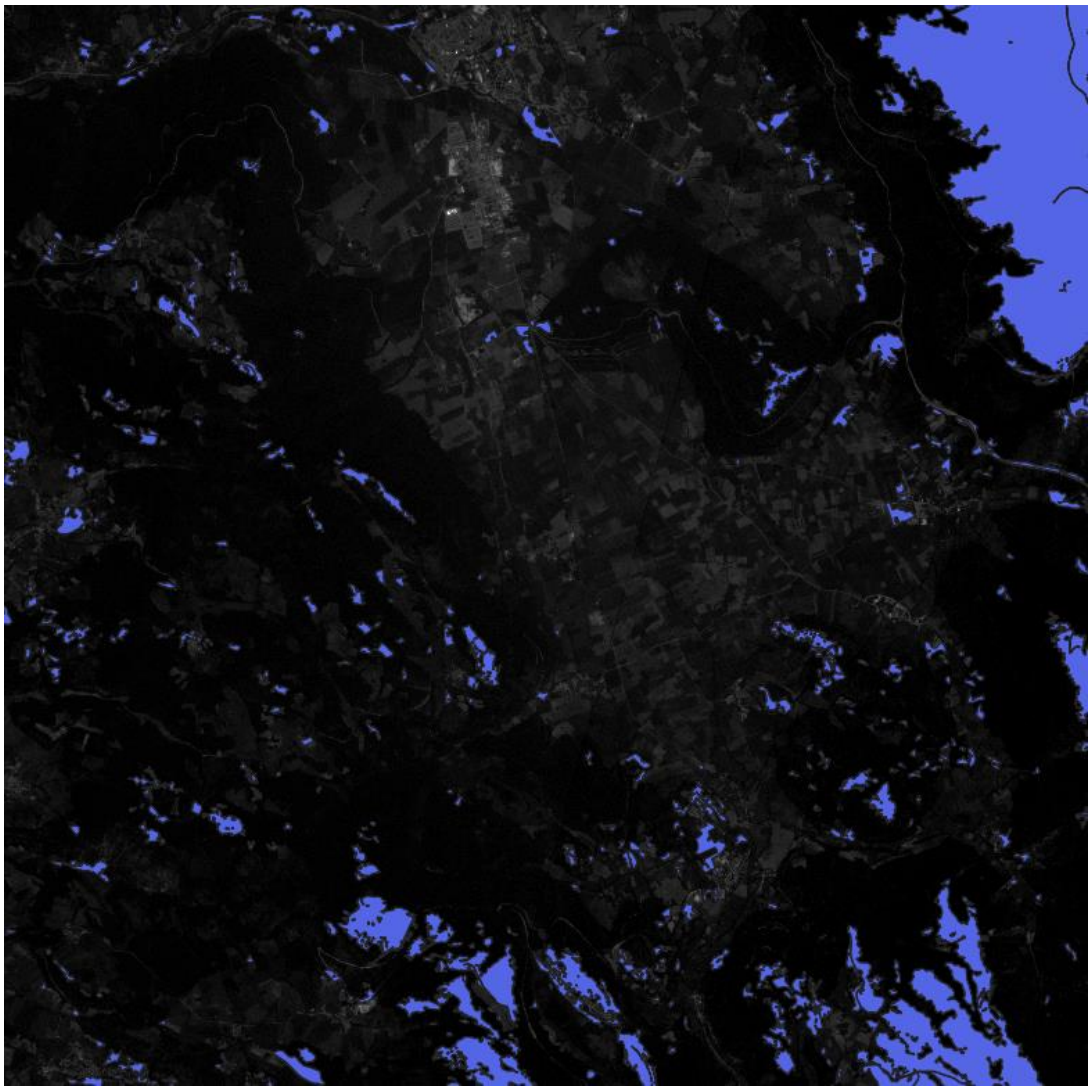

Fig.51 From the land cover map (Palnetscope dataset) the extension of pastures is shown in blue

2. Meadows

In **Fig**.**53** the extension of the meadow is shown in the study area.

These are perennial forage crops (average duration 2 to 5 years) that are planted to produce forage, to be used after harvesting (mowing).

The importance of meadows as a basis for livestock feeding was very strong in the past, but has significantly reduced in recent times, due to the increase in the cultivation of annual species such as corn and ryegrass which allow for much higher productivity. Generally, meadows are rotated, that is, they follow and precede another crop, usually a cereal. It should be remembered that rotation is an agronomic practice that consists of rotating crops in a certain plot, in order to maintain its fertility unaltered.

In addition to rotated meadows, there are also permanent grassland crops, which instead remain on the same land for a duration of more than 10 years. Gramineae and legumes are two types of crops that make up meadows.

Phenological phases: ear emergence, ear flowering and harvesting (mowing).

Fig.52 Grass and legume meadows: two types of crops

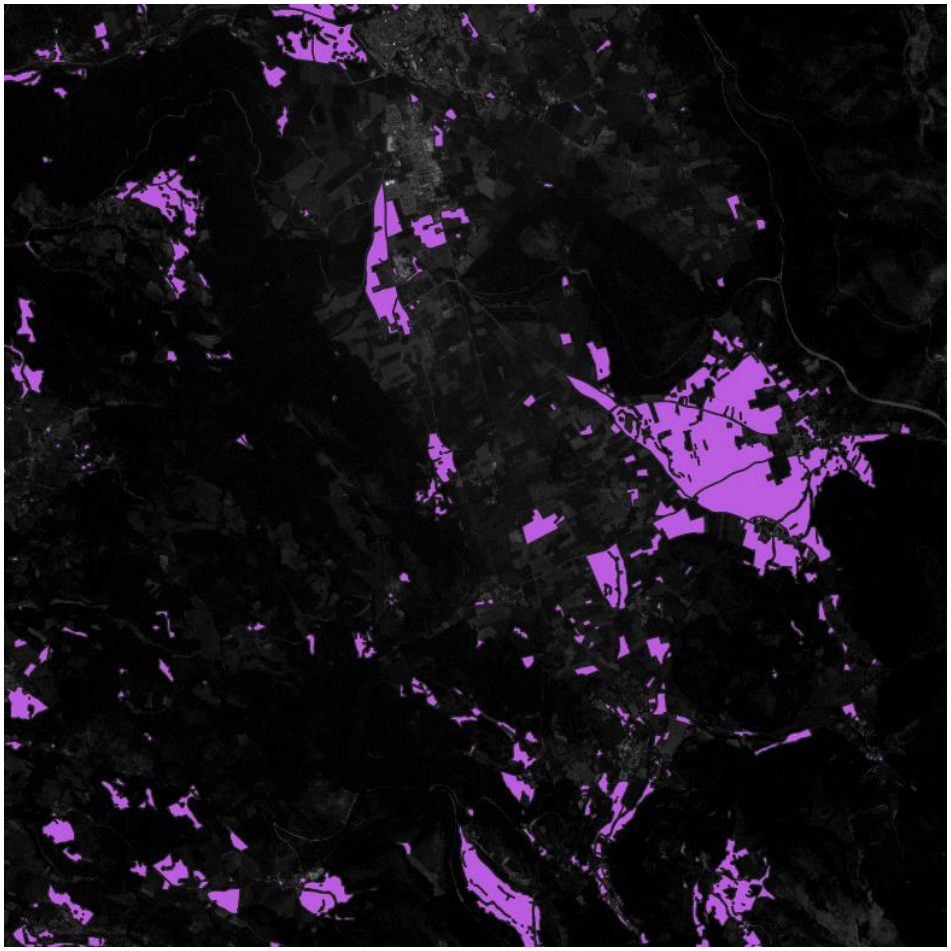

Fig.53 From the land cover map (Palnetscope dataset) the extension of meadows is shown in blue

3. Grasslands

Grasslands are short-cycle forage crops, lasting a maximum of one year. It is the type of use that makes them grasslands. In **Fig.58** the extension of grasslands is shown for the study area.

For example, wheat can be grown as a cereal: in this case it is harvested at the end of its biological cycle and only the grain is used either for human consumption (for example for bread production) or for livestock feed. If, on the other hand, wheat is harvested at milky/waxy maturity, chopped and ensiled (technique for conserving the plant mass in silos or round bales with pH acidification to avoid plant growth. A forage crop is shown in **Fig.54**.

Fig.54 Example of a grassland with the silage technique

Unlike meadows, which have been divided on the basis of botanical species (grasses and legumes), for grasslands it will be better to adopt a division based on the period of forage production:

1. Autun-winter grasslands

Autumn-winter grasslands are characterized by a biological cycle that takes place during the autumn-winter season and ends in spring. The main interest of these grasslands is linked to the fact that they are practiced in a normally rainy season and therefore do not require any irrigation. They are therefore suitable for all agriculture, including extensive hillside agriculture. The forage species that can be used for autumn-spring grasslands belong to the families of graminaceae, legumes and crucifers. Among the graminaceae there are all the species normally used as cereals (wheat, barley, oats and rye) **(Table.3)**. Loeissa is a forage species also very suitable for the constitution of grasslands, used on an annual basis **(Fig.55)**.

Table.3 Summary of the characteristics of some cereals used as autumn grass

CARATTERISTICHE	FRUMENTO TENERO	ORZO	AVENA	SEGALE	LOIESSA
PRODUTTIVITA' *(t ha^{-1} di granella)*	3 - 7	2 - 6	2 - 5	2 – 3 *(Ambienti difficili)*	-
PRODUTTIVITA' *(t ha^{-1} di foraggio secco)*	8-10 (mat. cerosa) 5-6 (spigatura)	8-10 (mat. cerosa) 5-6 (spigatura)	8-10 (mat. cerosa) 5-6 (spigatura)	- 4-5 (spigatura)	- 8-10
PRECOCITA'	media	alta	media	molto alta	alta
ADATTABILITA' CLIMI CALDO-ARIDI	buona	media *(ma favorito dalla precocità)*	media *(alti cons. idrici)*	medio-bassa *(ma favorito dalla precocità)*	media
ADATTABILITA' A CLIMI FREDDI	buona	media *(ma favorito dalla precocità)*	media	molto alta *(montagna)*	buona
RESISTENZA RISTOPPIO	buona	molto-buona	molto-buona	molto-buona	-
ADATTABILITA' A TERRENI ARGILLOSI	buona	buona	molto-buona	buona	buona
ADATTABILITA' A TERRENI SCIOLTI	buona	molto-buona	molto buona *(purchè umidi)*	molto-buona *(sopr. Acidi)*	buona
U.F. (granella)	1.1 UF/kg	1 UF/kg	0.7 UF/kg	0.7 UF/kg	-
ATTITUDINE AL PASCOLAMENTO	-	media	buona	buona	buona *(ricacci)*
ATTITUDINE AL FORAGGIAMENTO VERDE	buona	buona	buona	buona	buona
ATTITUDINE ALL'INSILAMENTO	-	molto buona	bassa	bassa	buona

Fig.55 Type of grassland: Loeissa

2. Spring-summer grasslands

The group of spring-summer forage crops includes all species sown in late Winter-early Spring and harvested during the summer season.

These are species with considerable productivity, but also with high water requirements, which severely limit their diffusion in the central and southern areas of Italy. The most interesting species as forage crops is corn **(Fig.56)** which is subjected to two types of cultivation: densely cultivated forage crop and sparsely cultivated forage crop and sorghum, capable of entering vegetative stasis during periods of more intense drought and being able to survive **(Fig.57)**. For corn forage crops, fertilization and fertigation are carried out between June and July while harvesting takes place in September *(https://agrispoleto.wordpress.com/mais/).*

Fig.56 Type of grassland: corn field

Fig.57 Type of grassland: sorghum field

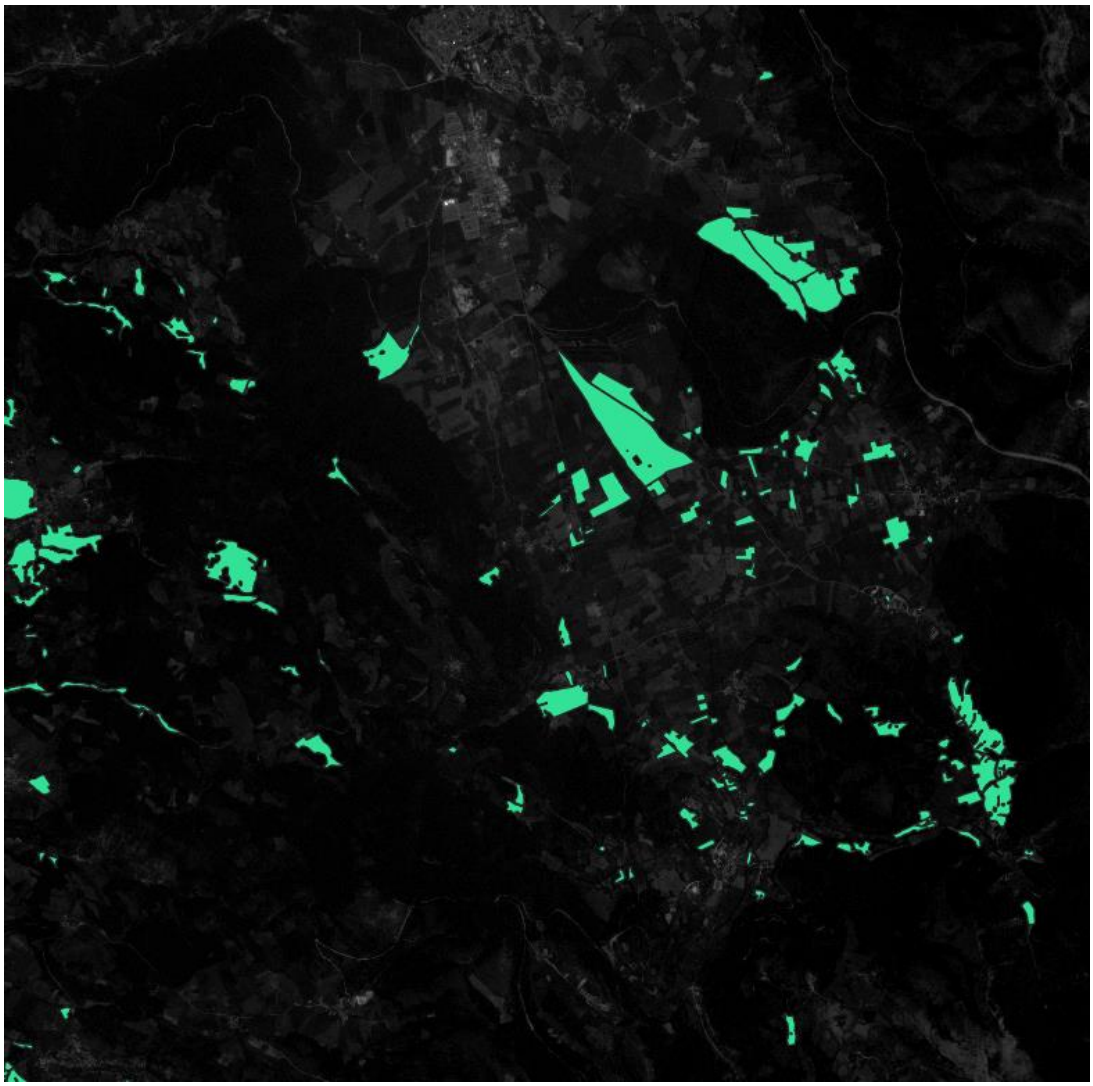

Fig.58 From the land cover map (PlanetScope dataset) the extension of grassland is shown in cyan

- Arable land

In **Fig.61** from the soil map it is possible to represent the extension of the arable fields in the territory of interest.

The arable fields can be divided into:
(https://cloud.ldpgis.it/sanvincenzo/sites/sanvincenzo/files/ps/RAC%20Schede%20uso%20del%20suolo_Pag29-44.pdf)

1. Simple arable land: Land subject to intensive herbaceous cultivation of cereals, legumes and horticultural crops in the field **(Fig.59)**. Cultivated areas, regularly ploughed and subjected to a crop rotation system.

Fig.59 Simple arable land

2. Arborized arable land: Land having the same characteristics as simple arable land but characterized by the presence of arboreal plants compared to herbaceous crops belonging to the class of forage crops. An example of arborized arable land is the agricultural surface used for the growth of olive trees **(Fig.60)**.

Fig.60 Arable land with trees

Phenological cycle: In the territories of Umbria, sowing takes place in Spring, as soon as, the snow cover has melted. Re-seeding occurs in September, while the growth of the crops and flowering occur in the months of June or July.

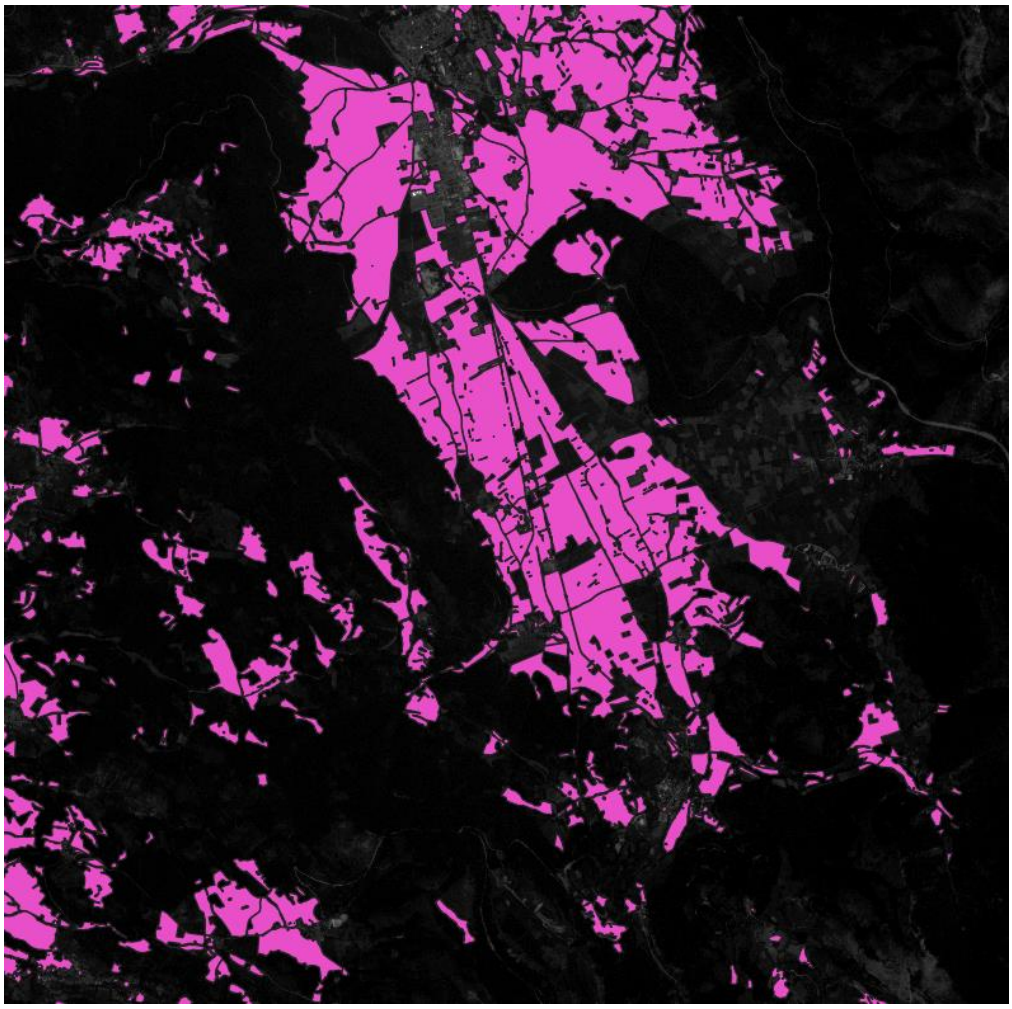

Fig.61 From the land cover map (PlanetScope dataset) the extension of sown fields in purple color

- Nuts

Fig.62 shows a plant for the cultivation of nuts near the city of Grotti where there are 5 species of nuts.

Fig.62 Nut growing plant near Grotti

In the study area concerned, some specimens of shell fruit were found in the north-east area near Grotti. Some examples of shell fruit plants that can be found in the Umbria Region:

1. Almond tree

The almond tree is a fruit tree belonging to the Rosaceae family. The almond is its seed, it has a slow growth and it is very long-lived, it can become centuries-old. The harvest is mainly done by hand after the almonds fall to the ground. The detachment from the plant is facilitated by olive harvesters, therefore tools that are banged on the plant to shake the branches and make the fruit fall *(https://it.wikipedia.org/wiki/Prunus_amygdalus).*

Phenological cycle: Flowering occurs in March. Harvest between July and September **(Fig.63)** *(https://www.elaisian.com/2022/09/22/la-raccolta-delle-mandorle/#:~:text=La%20raccolta%20avviene%20tra%20luglio,caduta%20delle%20mandorle%20a%20terra).*

Fig.63 Almond fruit and plant

Fig.64 Almond blossom

1. The hazelnut

The hazelnut does not tolerate water stagnation but appreciates a minimum amount of humidity in the first 50-60 cm of soil depth *(Moreno Moraldi, 2021).*

Phenological cycle: flowering occurs in March. The fruit ripens between September and October and then the harvest **(Fig.65)**.

In **Fig.66** two different types of cultivation are shown for the growth of the plant and the maturation of the hazelnut. For the cultivation of the bush plant the operation of harvesting the fruit and cutting the turf is called “spullonatura”. The mechanized harvesting of the fruit is less easy than that of the tree.

Fig.65 Hazelnut fruit and plant

Fig.66 Hazelnut grove grown as a small tree and as a bush

CHAPTER 4

4. Dataset

4.1 Satellite data acquisition in the study area

Three images were collected covering the period June, July and September. They represent the soil reality. In the images in **Fig.67** there are some differences between the crops and the vegetation. From PlanetScope data *(PlanetScope-Earth Online esa.int),* an orthophoto at 20 cm of resolution was acquired **(Fig.69)** and constitutes itself an instrument to study in a better way the cultures present in the study area, recognizable from the color, the shape and the position of the crops. In the orthophoto the measure of the crops as the reality is possible, in scale 1:1. Planet scope images are supplied as 100 km × 100 km tiles or those projected in the WGS84 UTM reference frame, UTM, zone 33 North. Comparing true color image with the False color images **(Fig.68)**, composing the multispectral bands at different wavelengths (in the ENVI program), it is possible to see better the characteristics of the vegetation and soil and the image constitutive classes.

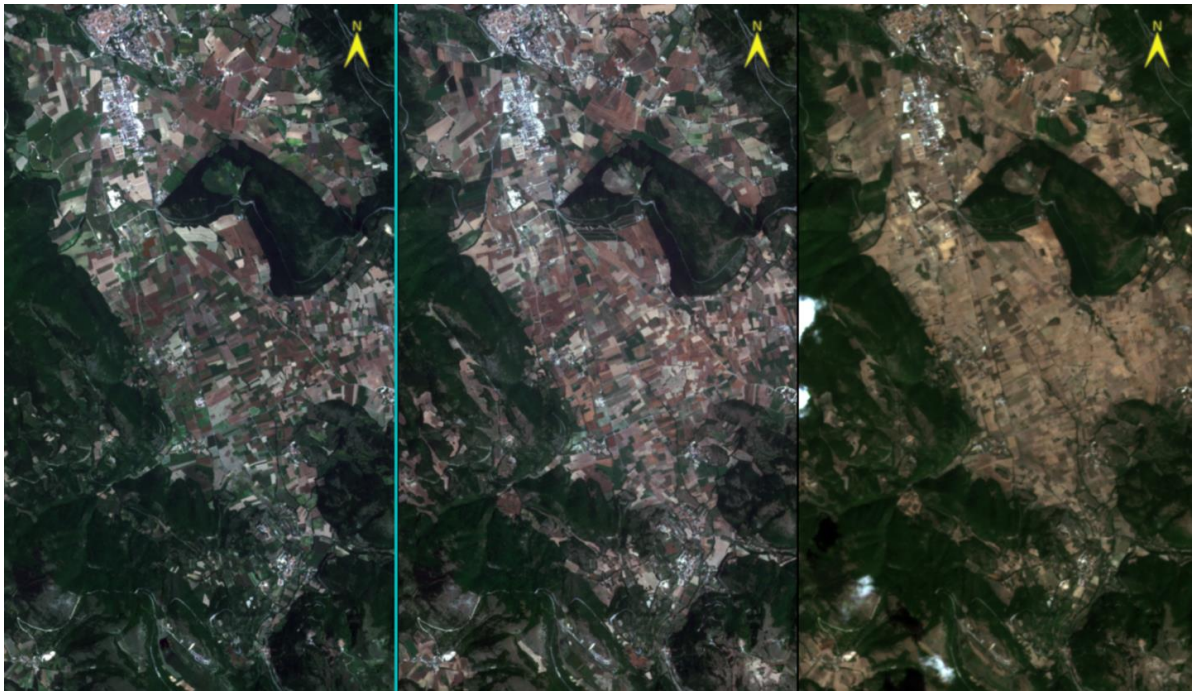

Fig.67 Acquisition from the PlanetScope server of three multispectral images for the study area concerned in the months of June, July and September.

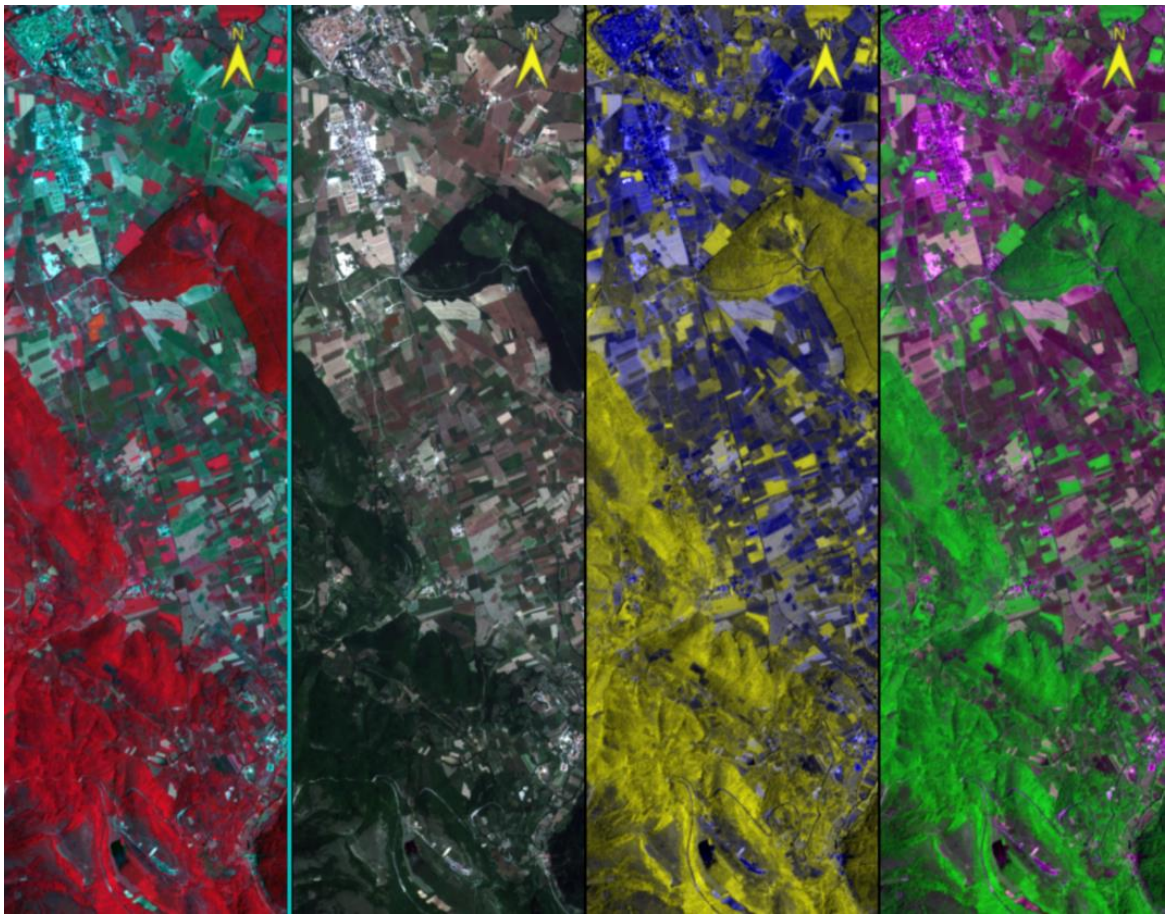

Fig.68 Combination of spectral bands (ENVI program) for the study area: True color (RED, BLUE, GREEN), False color (NIR, RED, GREEN), False color (NIR, NIR, RED) , False color (YELLOW, NIR, COASTAL BLUE).

Fig.69 Representative orthophoto, purchased at 20 cm, of the locality of Norcia, San Pellegrino, Popoli and Valcadara in the Umbria Region

4.2 PlanetScope satellite constellation

The PlanetScope satellite constellation consists of multiple launches of groups of individual satellites. Each PlanetScope satellite is a CubeSat ~3U form factor (10 cm by 10 cm by 30 cm). As of October 2021, Planet operates a fleet of over 200 satellites whose dual purpose is to acquire important time sensitive imagery on demand and at high spatial resolution. The first objective is supported by Planet's fleet of Dove satellites which passively collect images over the Earth's land mass on a continuous basis, providing near daily monitoring of any location. The Doves are medium resolution cube sats with a ground sampling distance (GSD) of ~4 meters **(Table.5)**, have a swath width of 25-32.5 km, and image in nadir pointing mode for nominal image collection. The second objective is supported by Planet's fleet of SkySat high resolution (< 1 meter GSD) satellites **(Table.4)**. SkySats are larger, maneuverable and can be tasked to image any location on the planet at any view angle. To date, three major generations of Dove satellites are in orbit collecting images: Dove classic, Dove-R, Super-Dove. These medium resolution satellites have been launched over an extended period of time in groups referred as “flocks.” Given the Dove’s small swath width and large number of individual satellites combined with the inclusion of high-resolution,

Sky-Sat imagery, consistent image processing and scaled radiometric calibration are a key requirement for producing a usable dataset across space and time **(Fig.70)** *(Alan Collison, Arin Jumpasut, Hannah Bourne, 2022).* Planet's constellation of satellites orbits the poles every 90 minutes, capturing the entire Earth's landmass every day. The satellite constellation system is composed of approximately 200 satellites including: PlanteScope (180), Rapideye (5) and Skysat (21).

Table.4 Planet Satellites (*https://www.planet.com/products/satellite-imagery-of-earth/)*

	PLANETSCOPE	RAPIDEYE	SKYSAT
Bands	8 (RGB, NIR)	5 (RGB, red edge, NIR)	5 (RGB, NIR, pan)
Products	Color enhanced Visual Analytic	Color enhanced Visual Analytic	Visual Panchromatic Pansharpened multispectral Analytic
Pixel Resampled	3 m	5 m	Visual, panchromatic, pansharpened multispectral: 0.5m
Radiometric Resolution	Visual: 8 bit Analytic: 16 bit		Visual: 8 bit Analytic, panchromatic, and pansharpened multispectral: 16 bit
Positional Accuracy	< 10 M RMSE		
File Format	GeoTIFF		

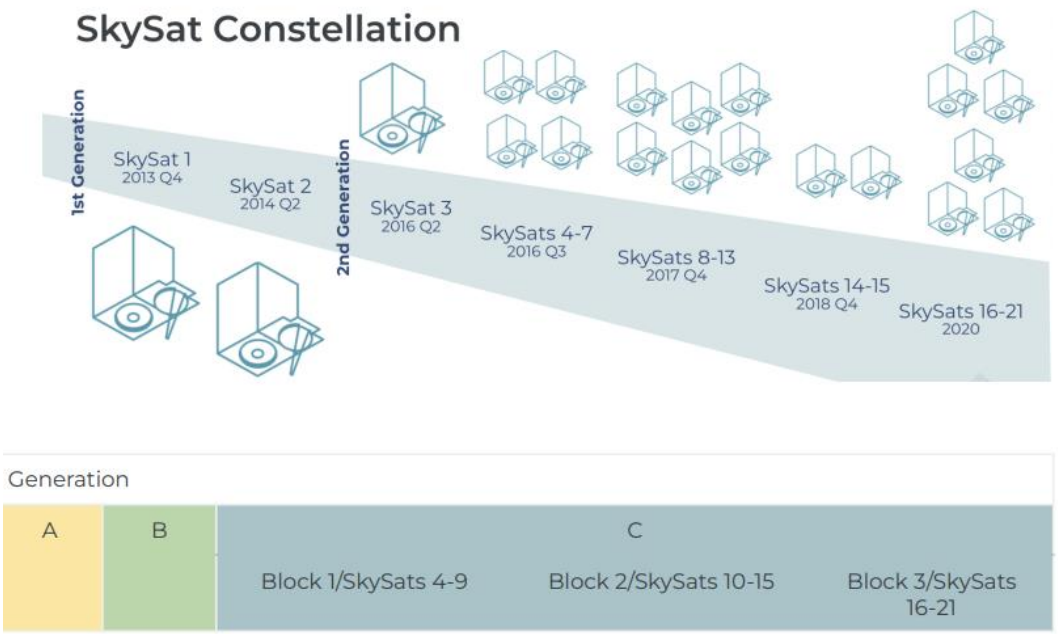

Fig.70 SkySat generations and launches over the years *(Alan Collison, Arin Jumpasut, Hannah Bourne, 2022)*

Table.5 PlanetScope Constellation and Sensor Specifications

CONSTELLATION OVERVIEW: PLANETSCOPE			
Mission Characteristics	Sun-synchronous Orbit		
Instrument	**PS2**	**PS2.SD**	**PSB.SD**
Orbit Altitude (reference)	450 - 580 km (~98° inclination)		475 - 525 km (~98° inclination)
Field of View	3.0° (swath) 1.0° (scene length)	3.0° (swath) 2.0° (scene length)	4.0° (swath) 2.3° (scene length)
Max/Min Latitude Coverage	±81.5° (dependent on season)		
Equator Crossing Time	7:30 - 11:30 am (local solar time)		
Sensor Type	Four-band frame Imager with a split-frame VIS+NIR filter	Four-band frame imager with butcher-block filter providing blue, green, red, and NIR stripes	Eight-band frame imager with butcher-block filter providing coastal blue, blue, green I, green, yellow, red, red-edge, and NIR stripes
Spectral Bands	Blue: 455 - 515 nm Green: 500 - 590 nm Red: 590 - 670 nm NIR: 780 - 860 nm	Blue: 464 - 517 nm Green: 547 - 585 nm Red: 650 - 682 nm NIR: 846 - 888 nm	Coastal Blue 431-452 nm Blue: 465-515 nm Green I: 513. - 549 nm Green: 547. - 583 nm Yellow: 600-620 nm Red: 650 - 680 nm Red-Edge: 697 - 713 nm NIR: 845 - 885 nm
Ground Sample Distance (nadir)	3.0 m-4.1 m (approximate, altitude dependent)		3.7 m-4.2 m (approximate, altitude dependent)
Off-Nadir Angle	0° - 5° (latitude dependent)		
Frame Size	24 km x 8 km (approximate)	24 km x 16 km (approximate)	32.5 km x 19.6 km (approximate)
Maximum Image Strip per orbit	20,000 sq km		
Revisit Time	Daily at nadir		
Image Capture Capacity	200 million sq km/day		
Imagery Bit Depth	12-bit		
Availability Date	July 2014 - April 2022	March 2019 - April 2022	March 2020 - present

4.3 PlanetScope Satellite sensors

PlanetScope satellites launched in November 2018 have sensor characteristics that improved the spatial and spectral resolution *(https://developers.planet.com/docs/data/planetscope/).* PlanetScope images are taken from three different sensors: PS2, PS2.SD, and PSB.SB. Sensors PS2 and PS2.SD deliver four bands: red, green, blue, and near infrared. PSB.SD sensor has an additional four bands: green I, yellow, coastal blue, and red edge. Depending on the scene product, re-

quested (3-band, 4-band, or 8-band) imagery can come back from a combination of different sensors. **Table.5** provides the frequencies of the imagery returned from the three sensors. The spatial resolution of the PlanteScope system for the PS2 and PS2.SD sensor is 3-4.1 m coinciding with the Ground Sample Distance (GSD), the size of the pixel on the ground. For the PSD.SB sensor the GSD is 3.7-4.2 m *(https://www.planet.com/products/satellite-imagery-of-earth/).*

4.3.1 PS2 sensor

In **Fig.71**, the PS2 satellites carry instruments consisting of a telescope paired with a 2D frame detector having a spatial resolution of 6600 pixels across by 4400 lines down. This sensor captures red, green, blue, and near infrared channels. It produces Scene products which are approximately 25.0 x 11.5 sq km. Earliest imagery available on July, 2014 to April 29, 2022. The detector has a Bayer pattern filter separating the wavelengths of light into blue, green, and red channels. On top of the Bayer pattern filter is a “2-stripe” filter. The top half blocks the NIR wavelengths, thus allowing only the blue, green, and red light to pass through. The bottom half allows only the NIR wavelengths of light to pass through. In **Fig.72** each frame acquired by the PS2 instrument consists of a top half that is an RGB image and a bottom half that is an NIR image. The RGB half of each frame is then combined with the NIR half of the adjacent frame in order to generate the resulting 4-band image.

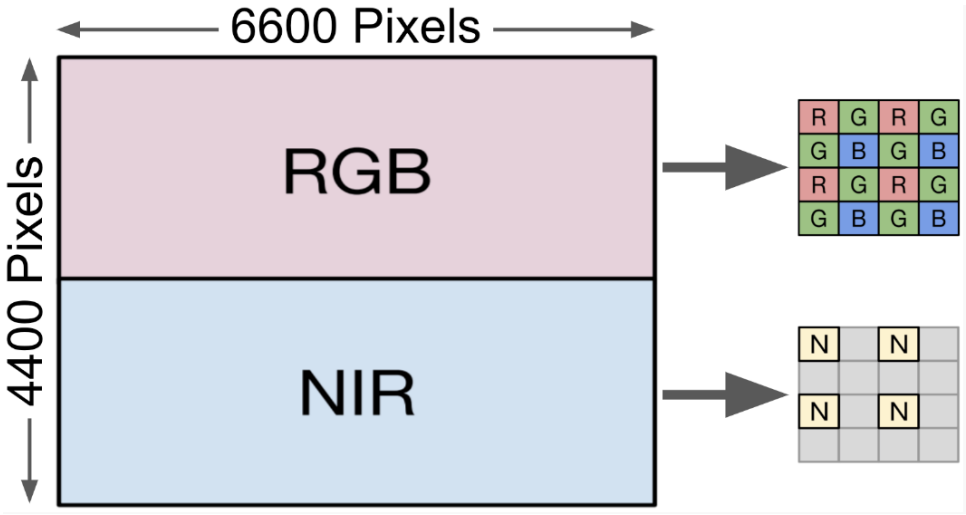

Fig.71 PS2 filter system *(https://developers.planet.com/docs/apis/data/sensors/)*

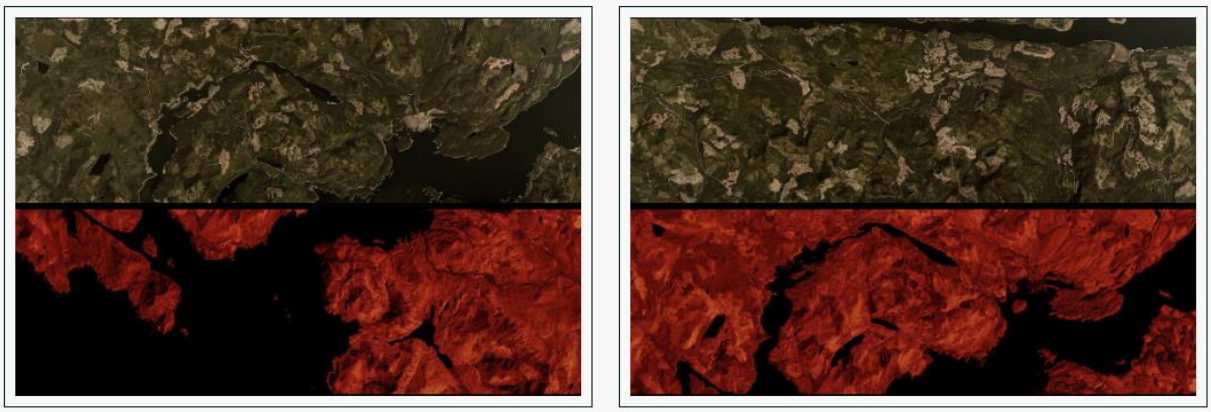

Fig.72 4-band image with PS2 system *(https://developers.planet.com/docs/apis/data/sensors/)*

4.3.2 PS2.SD sensor

The **PS2.SD** instrument is composed of the same “PS2” telescope which has a sensor camera large 47 megapixel, and has the same 2D frame detector as used in PS2. This instrument captures red, green, blue, and near infrared channels. It produces Scene which are approximately 25.0 x 23.0 sq km. Earliest imagery available is in March, 2019 to April 22, 2022. A sensor plane is divided into four separate horizontal stripes (one per radiometric band) along the track of the flight path. The Bayer pattern filter and pass-band filters in the PS2 satellites have been replaced with a high-performance butcher-block filter. In **Fig.73** The PS2.SD filter is made up of 4 individual pass-band filters that separate the light into each of the blue, green, red, and NIR channels. The choice of the pass-band filters for PS2.SD match closely Sentinel-2 satellite.

In **Fig.74** each frame acquired by the PS2.SD instrument consists of 4 stripes, as seen below. In order to generate the final 4-band image, we stack together a number of consecutive frames on either side of a given frame.

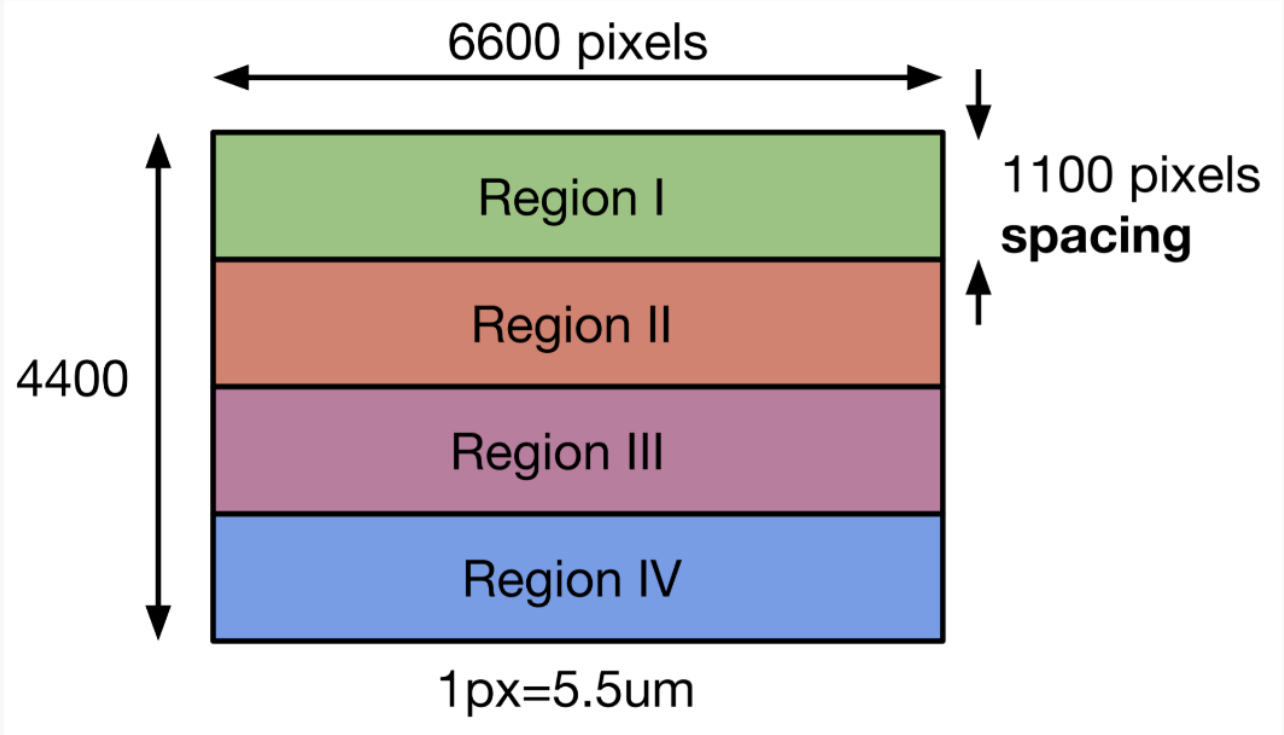

Fig.73 PS2.SD filter system *(https://developers.planet.com/docs/apis/data/sensors/)*

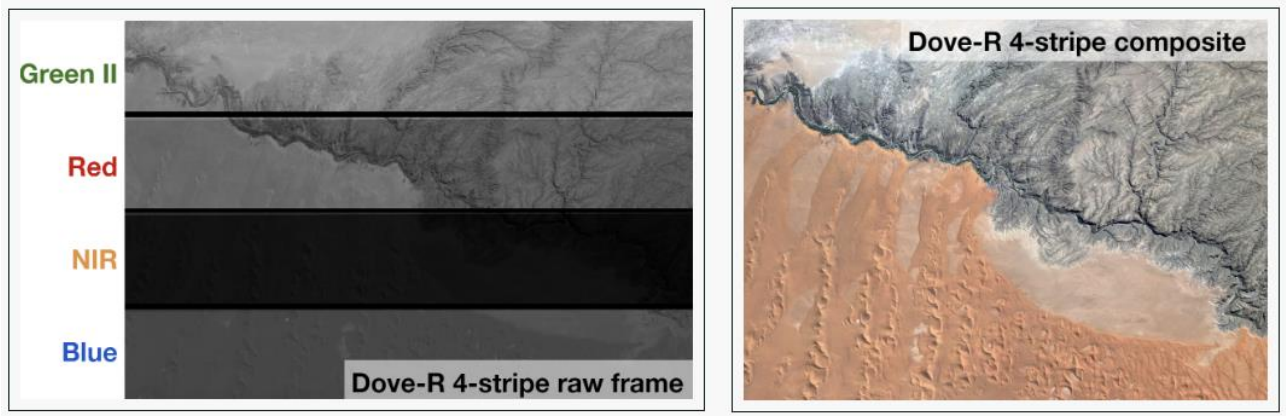

Fig.74 4-band image with PS2.SD system *(https://developers.planet.com/docs/apis/data/sensors/)*

4.3.2 PSB.SB sensor

"PSB.SB" sensor has the same filter response as PS2.SD instrument, this sensor captures in 8 spectral bands: red, green, blue, near infrared, as well as a new red edge, green I, coastal blue, and yellow channel. It produces Scene products which are approximately 32.5 x 19.6 sq km. Earliest imagery available is mid-March, 2020 to current monitoring **(Table.6)**.

Table.6 PSB.SB spectral absorption range for each band *(https://developers.planet.com/docs/apis/data/sensors/)*

Band	Name	Wavelength (fwhm)	Interoperable with Sentinel-2
1	Coastal Blue	443 (20)	Yes - with Sentinel-2 band 1
2	Blue	490 (50)	Yes - with Sentinel-2 band 2
3	Green I	531 (36)	No equivalent with Sentinel-2
4	Green	565 (36)	Yes - with Sentinel-2 band 3
5	Yellow	610 (20)	No equivalent with Sentinel-2
6	Red	665 (31)	Yes - with Sentinel-2 band 4
7	Red Edge	705 (15)	Yes - with Sentinel-2 band 5
8	NIR	865 (40)	Yes - with Sentinel-2 band 8a

There is a new, larger sensor on the PSB.SD payload, meaning that the framing of scene products is larger in both directions when compared to PS2.SD and Dove Classic scene products. Each frame consists of eight stripes, as seen below. In order to generate the final 8-band image, we stack together a number of consecutive frames on either side of a given frame **(Fig.75)**.

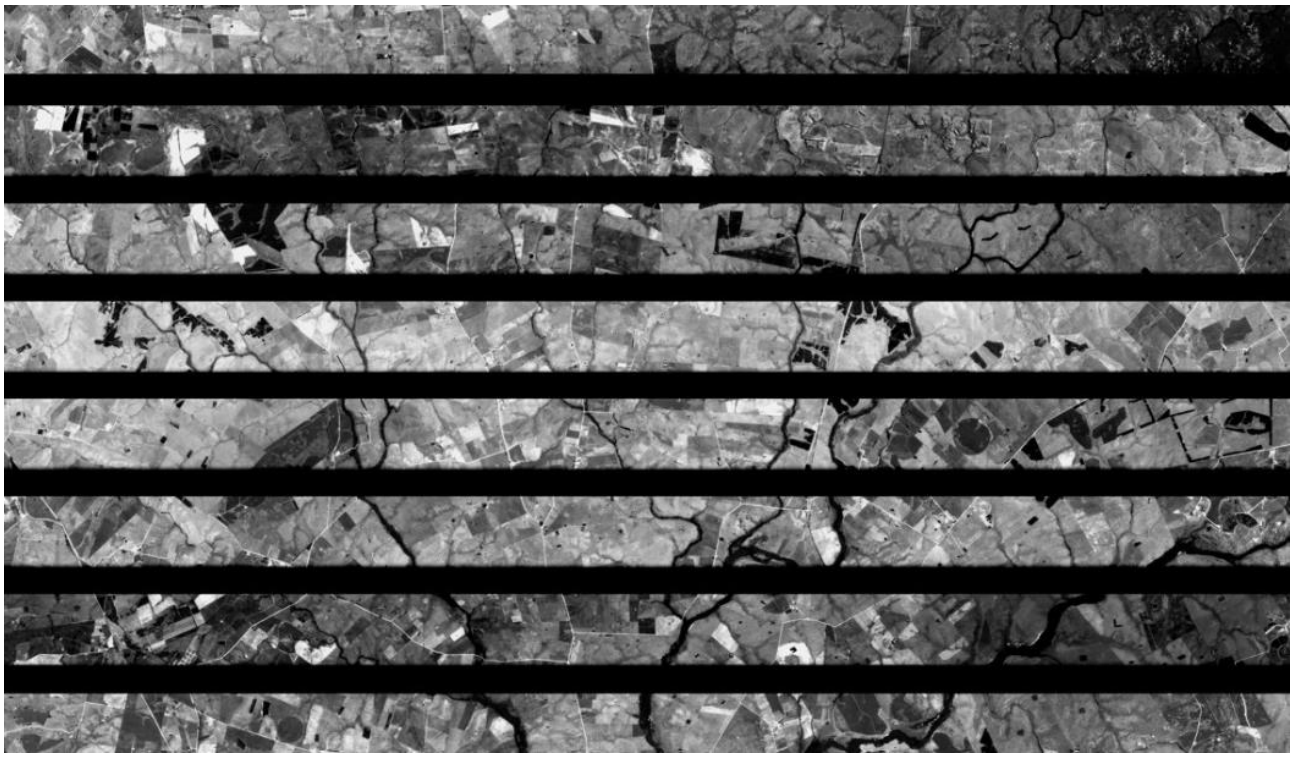

Fig.75 Frames of a scene generated from "PSB.SB" sensor *(https://developers.planet.com/docs/apis/data/sensors/)*

4.4 Calibration reference

To achieve this consistency, all calibrations across Planet's fleets are based on gathering a dataset of near simultaneous crossovers with Sentinel 2 as the reference satellite, with a < 5% radiometric accuracy. Sentinel-2 is a multi-spectral instrument that images in 13 spectral bands that 3 range from the visible to the short-wave infrared. The spatial resolution of Sentinel-2 spectral band ranges from 10 to 60 m. Absolute radiometric calibration for Sentinel is performed every month using a diffuser fitted inside the calibration and shutter mechanism. Sentinel 2 uses several methods to validate radiometric calibration, including measurements over Pseudo Invariant Calibration (PIC).

4.4.1 Radiometric resolution accuracy

Analytic products are scaled to Top of Atmosphere Radiance. Validation of radiometric accuracy of the on-orbit calibration has been measured at 5% using vicarious collects in the Railroad Valley calibration site. Furthermore, each band is maintained within a range of +/- 2.5% from the band mean value across the constellation and over the satellite's lifetime. All RapidEye satellite images were collected at a bit depth of 12 bits and on-board the satellites, the least significant bit is removed, and thus 11 bits are stored and downloaded.

4.4.2 Radiometric calibration

The radiometric resolution of multispectral PlanetScope system is 16 bits, the visual PlanetScope system is 8 bits *(https://www.planet.com/products/satellite-imagery-of-earth/).*

PlantetScope radiometric corrections are as follows:

Darkfield/Offset Correction: Corrects for sensor bias and dark noise. Master offset tables are created by averaging on-orbit darkfield collects across 5-10 degrees temperature bins and applied to scenes during processing based on the CCD temperature at acquisition time.

Flat Field Correction: Flat fields are collected for each optical instrument prior to launch. These fields are used to correct image lighting and CCD element effects to match the optimal response area of the sensor. Flat fields are routinely updated on-orbit during the satellite lifetime.

Camera Acquisition Parameter Correction: Determines a common radiometric response for each image (regardless of exposure time, number of TDI stages, gain, camera temperature and other camera parameters).

Absolute Calibration: As a last step, the spatially and temporally adjusted datasets are transformed from digital number values into physical based radiance values (scaled to W/(m²*str*µm)*100).

On the ground, the bit shift is reversed by a multiplication factor of 2. During on-ground processing, radiometric corrections are applied, and all images are scaled to a 16-bit dynamic range. This scaling converts the (relative) pixel DNs coming directly from the sensor into values directly related to absolute at sensor radiances. The scaling factor is applied so that the resultant single DN values correspond to 1/100th of a W/(m²*sr*µm). The DNs of the RapidEye image pixels represent the absolute calibrated radiance values for the image. To convert the pixel values of the Analytic products to radiance, it is necessary to multiply the DN value by the radiometric scale factor,

$$RAD(i) = DN(i) * \text{radiometric Scale Factor}(i)$$

Where radiometric Scale Factor(i) = 0.01

The resulting value is the at-sensor radiance of that pixel in watts per steradian per square meter (W/m²*sr*µm).

It is possible to neglect the influence of the atmosphere by calculating the Top Of Atmosphere (TOA) reflectance taking into consideration only the sun distance and the geometry of the incoming solar radiation. The formula to calculate the TOA reflectance not taking into account any atmospheric influence is as follows *(https://assets.planet.com/docs/Planet_Combined_Imagery_Product_Specs_letter_screen.pdf):*

$$REF(i) = RAD(i)\frac{\pi * SunDist^2}{EAI(i) * \cos(SolarZenith)}$$

with:

- I = Number of the spectral band

- REF = Reflectance value

- RAD = Radiance value

- Sun Distance = Earth-Sun Distance at the day of acquisition in Astronomical Units. Note: This value is not fixed, it varies between 0.9832898912 AU and 1.0167103335 AU and has to be calculated for the image acquisition point in time.

- EAI = Exo-Atmospheric Irradiance

- SolarZenith = Solar Zenith angle in degrees (= 90° – sun elevation)

In brief, the radiometric corrections applied:

● Correction of relative differences of the radiometric response between detectors

● Non-responsive detector filling which fills null values from detectors that are no longer responding (This isn't currently done because there are no non-responsive detectors)

● Conversion to absolute radiometric values based on calibration coefficients

4.4.3 Example: Satellite crops comparing

Geographic based framing **(Fig.76)**: a geographic region is defined by two corners. The product width is close to the full image swath as observed by all bands (77 km at nadir, subject to minor trimming of up to 3 km during processing) with a product length that does not exceed 300 km with a minimum length of 50 km and around a 10km overlap.

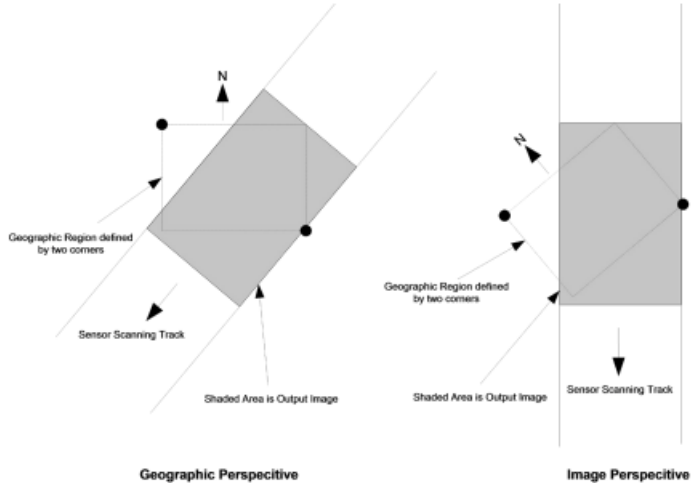

Fig.76 Geographic based framing *(Alan Collison, Arin Jumpasut, 2022)*

Example time series plots of the derived NDVI vegetation index for an alfalfa field in the Imperial Valley area of California and a grassy field in California's Central Valley are provided in **Fig.77** for the summer months of 2019. Image collections were made by both Dove and Dove-R and are displayed by capture date. Dips and spikes in the curves generally represent clouds/shadows in or near the scene which causes additional atmospheric scattering that is not corrected for. The

curves illustrate the usefulness of daily collects where sharp drops in index value are evident during harvesting time with some collects captured in the middle of the process. The low values of NDVI for Dove satellite collects during the peaks in alfalfa and grass growth are the result of the wide red band for those satellite sensors.

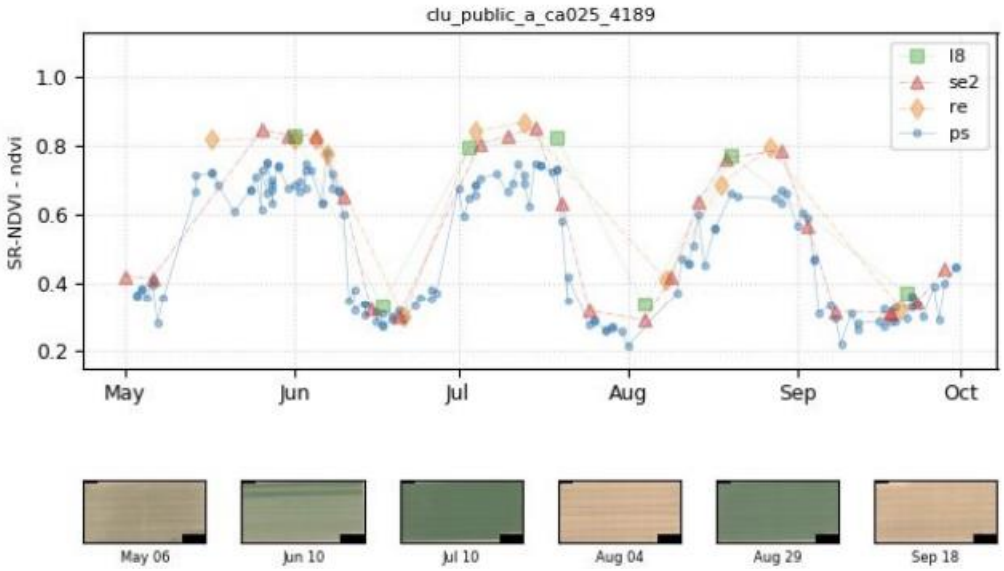

Fig.77 NDVI response curves for crop classification of Sentinel and PlanetDove satellites *(Alan Collison, Arin Jumpasut, 2022)*

Fig.77 shows a single set of collections near growth peak further illustrating the agreement between Dove-R satellite and both Landsat and Sentinel satellites. In **Fig.78** a comparison is provided showing average per-band surface reflectance for the field in the Sacramento Valley at different points of the growing season. Each plot is a single Dove-R scene and a corresponding Landsat 8 and Sentinel-2 scene for the closest crossover date. As can be seen, the general shape of both the Planet, Landsat 8 and Sentinel-2 spectra agree as the surface cover changes over the Summer with small differences partly due to the non-simultaneity of the collects.

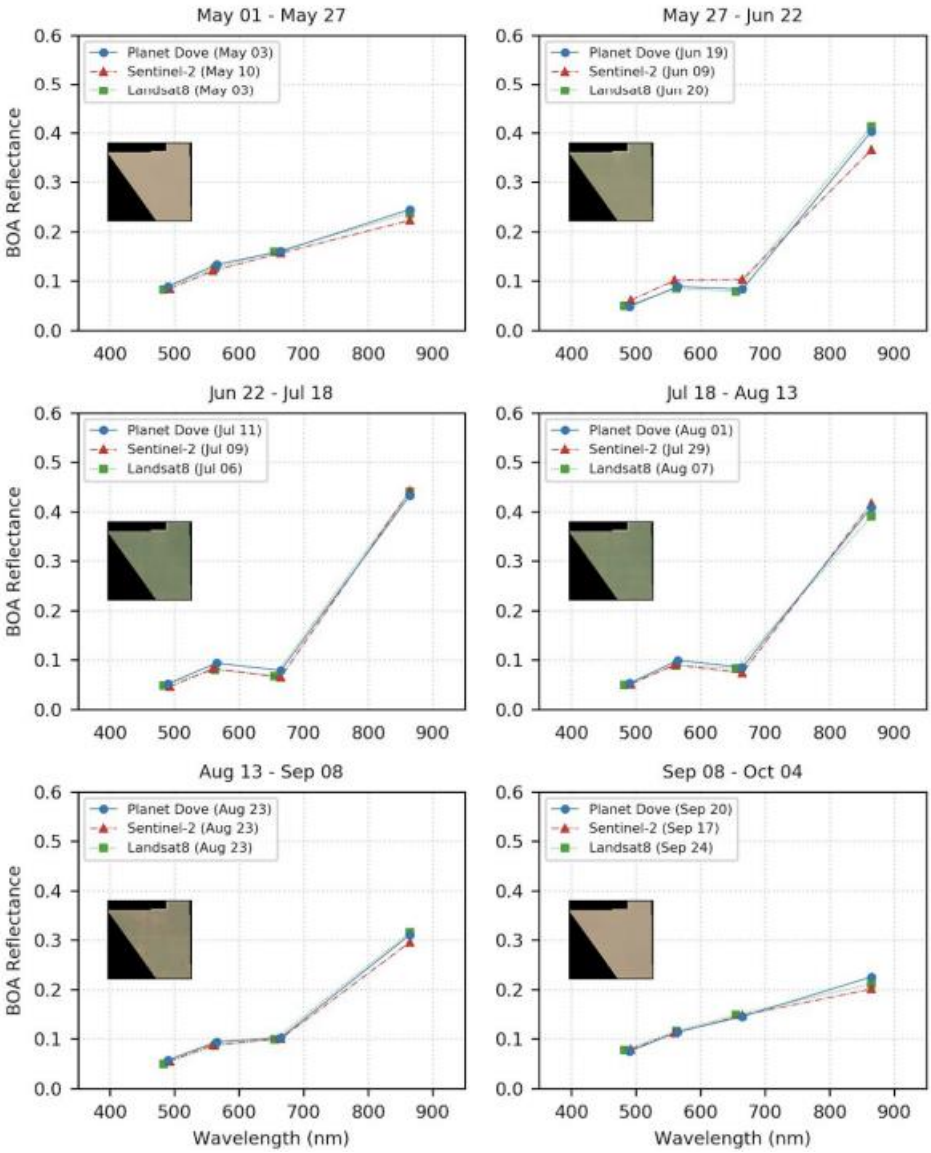

Fig.78 A comparison of Planet and Landsat 8 spectra for a field in the Sacramento Valley for the Summer of 2017 *(Alan Collison, Arin Jumpasut, 2022)*

Results demonstrate that the absolute SR values are closely aligned between coincident image products with both Landsat 8 and Sentinel-2, and temporal analysis of derived vegetation indices show the datasets are highly correlated.

4.5 Sentinel-2 characteristics

Constellation: The orbital swath width is 290 km. The Sentinel-2 mission consists of two identical satellites, Sentinel-2A and Sentinel-2B, that were launched using the European VEGA launcher. Each of these satellites weighs approximately 1.2 tones. The two Sentinel-2 satellites operate simultaneously, phased at 180° to each other, in a sun-synchronous orbit at a mean altitude of 786 km. The position of each Sentinel-2 satellite in its orbit is measured by a dual-frequency Global Navigation Satellite System (GNSS) receiver. Orbital accuracy is maintained by a dedicated propulsion system.

Temporal resolution: is the revisit frequency of the satellite to a particular location. The revisit frequency of each single Sentinel-2 satellite is 10 days and the combined constellation revisit is 5 days.

Spatial resolution: is dependent on the particular spectral band. Sentinel-2 carries an optical instrument payload that samples 13 spectral bands: four bands at 10 m, six bands at 20 m and three bands at 60 m spatial resolution.

Spectral resolution: is defined as a measure of the ability of the instrument to distinguish features in the electromagnetic spectrum.

The 13 spectral bands of Sentinel-2 range from the Visible (VNIR) and Near Infra-Red (NIR) to the Short Wave Infra-Red (SWIR):

- 4 x 10 meter Bands: the three classical RGB bands (Blue (~493nm), Green (560nm), and Red (~665 nm)) and a Near Infra-Red (~833 nm) band.
- 6 x 20 meter Bands: 4 narrow Bands in the VNIR vegetation red edge spectral domain (~704 nm,~740 nm, ~783 nm and ~865 nm) and 2 wider SWIR bands (~1610 nm and ~2190 nm) for applications such as snow/ice/cloud detection, or vegetation moisture stress assessment.
- 3 x 60 meter Bands mainly focused towards cloud screening and atmospheric correction (~443 nm for aerosols and ~945 nm for water vapor) and cirrus detection (~1374 nm).

Radiometric resolution: is the capacity of the instrument to distinguish differences in light intensity or reflectance. The greater the radiometric resolution, the more accurate the sensed image will be. Radiometric resolution is routinely expressed as a bit number, typically in the range of 8 to 16 bits. The radiometric resolution of the MSI instrument is 12 bit, enabling the image to be acquired over a range of 0 to 4095 potential light intensity values. The radiometric accuracy is less than 5% (goal 3%). Radiometric resolution is also dependent upon the Signal to Noise Ratio (SNR) of the detector.

4.6 Sentinel-2 and PlanetScope

Planet offers Analysis-Ready PlanetScope (ARPS) imagery as a 3 meter orthorectified (corrected for terrain distortions) surface reflectance product (ARP-SR). The surface reflectance product is accompanied by a Quality Assurance product (ARP-QA) in GeoTIFF format. Analysis-Ready PlanetScope products are projected in the UTM zone intersected by their extent using the WGS-84 horizontal datum. Enhanced geometric performance includes temporal positional accuracy of <4m RMSE PCTL90.

The similarity of spectral bands between Dove-R, SuperDove and Sentinel 2 is a calculated design choice to allow Sentinel 2 to be leveraged as a reference for on-orbit calibration utilizing simultaneous, intersecting crossovers. As the relative spectral responses (RSRs) between Sentinel 2 and Dove-R/SuperDove are very similar, we can collect crossover scenes from anywhere in the world to perform the on-orbit calibration and are not just limited to well characterized calibration sites where a spectral band adjustment factor (SBAF) can be calculated. Because of the shared spectral bands with Sentinel 2, Planet's Dove-Rs and SuperDoves crossover comparisons avoid the need of RSR adjustments and therefore can be collected anywhere in the world. This allows collection of

sufficient simultaneous crossovers to allow rapid on-orbit calibration for commissioning after launch. It also allows longer term monitoring and calibration adjustments while providing data spanning the full dynamic range of the satellite sensor. Since significant RSR differences between Dove CLassic satellites and Sentinel 2 are present, SBAF corrections are still necessary to directly compare TOA reflectance values. This restricts the usable simultaneous crossovers to well-characterized calibration sites. Because these sites are limited in number and are mostly composed of bright, pseudo invariant desert regions, this not only limits both the number of usable crossovers that can be collected in a short period of time, but also largely limits the measurements to high TOA reflectance values. Any improvement in the characterization of these sites and the addition of more covering a wider dynamic range of reflectance's would be beneficial to calibrations *(https://assets.planet.com/docs/radiometric_calibration_white_paper.pdf).*

For Planet's Dove satellites, each generation has a different sensor design with each Dove having its own unique relative spectral response. The **Fig.79** shows the original Dove design, the Dove Classic, and it has a sensor with four wide overlapping bands in blue, green, red and near infrared. The Dove-R satellites also have 4 spectral bands, but they are narrow, non-overlapping and chosen to closely match the corresponding ones from Sentinel 2. The most recent Planet payload, the SuperDove, has eight narrow, well defined spectral bands, four of which match the VNIR bands of Dove-R. Overall, 6 of the SuperDove bands are shared with Sentinel-2 *(Alan Collison, Arin Jumpasut, 2022).*

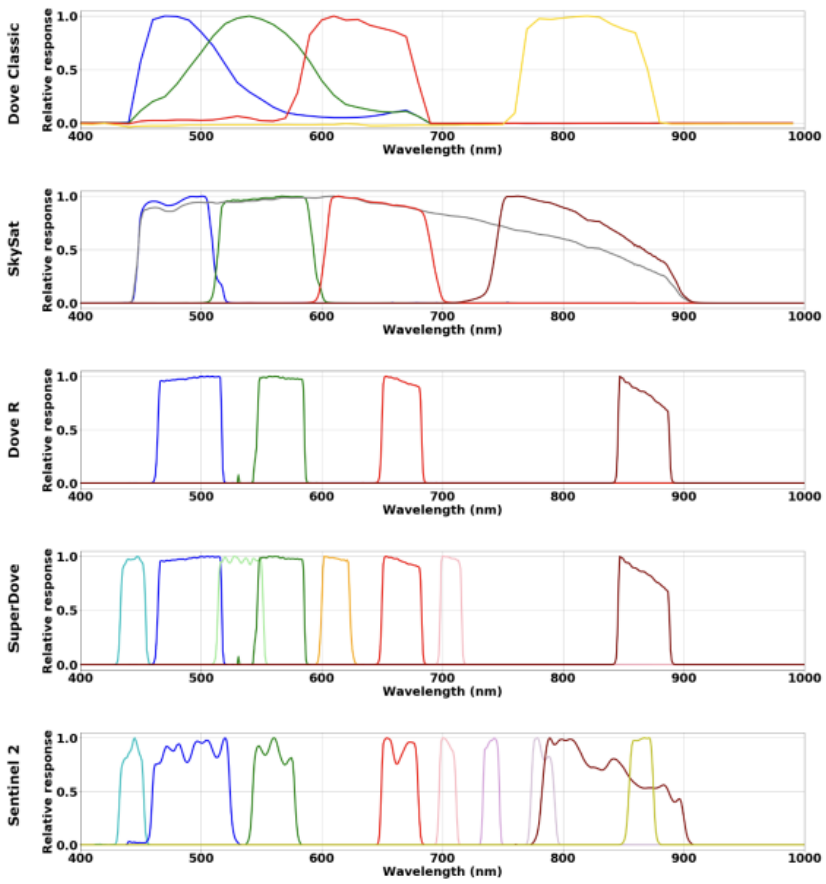

Fig.79 Spectral response for PlanetDove generations and Sentinel-2 satellites *(Alan Collison, Arin Jumpasut, 2022)*

4.7 Calibration process image

Geo-Spatial Aid Application service (GSAA) contains all information about fields that Common Agricultural Policy (CAP) contributions are requested for (e.g., location, size, crop types, etc.).

A problem that can occur in the acquisition of data via satellite in the agricultural context is the interpretation of the geometry of the agricultural land present on the ground and the size, in fact the effect of distortions that can occur can lead to spectral measurements being unreliable. To improve the effect of distortions, a sensor records the intensity of the electromagnetic radiation for each pixel as a digital number (DN), these digital numbers can be converted to more meaningful real world units like radiance, reflectance or brightness temperature *(https://gsp.humboldt.edu/olm/Courses/GSP_216/online/lesson7/radiometric.html).* It is necessary to calibrate the images with the "top of the atmosphere" and "no selective scattering" adjustments **(Fig.80)**, reducing the average of the variations and the standard deviation, increasing the precision of the data and of the DN (digital number) present in the image.

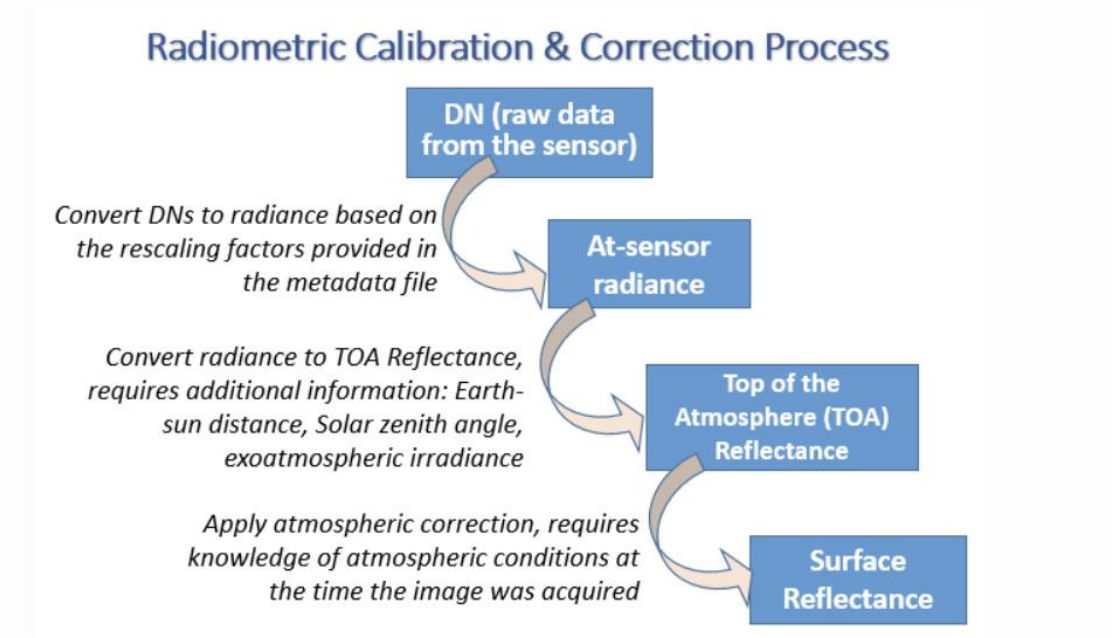

Fig.80 Radiometric calibration process
(*https://gsp.humboldt.edu/olm/Courses/GSP_216/online/lesson7/radiometric.html)*

4.8 Calibration Map

It is possible to highlight more accurately the presence of crops **(Fig.81, Fig.83, Fig.85)** thanks to the image calibration process in **Fig.80**. Furthermore, the Max and Min values of the DN (Digital Number) associated with the different bands in which the image was studied are more coherent in an ordered range and no longer random as it can be seen in the histograms in **Fig.82** for the month of June. Differently for the months of July and September in which the effect of the distortions does not seem to be attenuated even after the calibration, as can be deduced from the graphs of the standard deviations **(Fig.84, Fig.86)**; the correction of the radiometric tone through the calibration technique depends on how the images were acquired and on the geometric resolution. From the geophysical point of view, the electromagnetic radiation measured by the sensor depends on the radiation reflected on the surface and that dispersed by the particles present in

the atmosphere. The dispersion of light depends on the atmosphere, the elevation of the sun and the alternation of the seasons. The Geo-Spatial Aid Application (GSAA) data that are processed with greater precision are based on larger and well-structured terrain dimensions. Geometric resolution plays a fundamental role in this context, to study more clearly and precisely the data that are made available by the GSAA. Consequently, to take care of that important issue, supplied GSAA polygons were analyzed while the corresponding area and shape index (SI) were computed by ordinary Geographic Information System (GIS). The shape index (SI) is dependent on perimeter and area of the polygon.

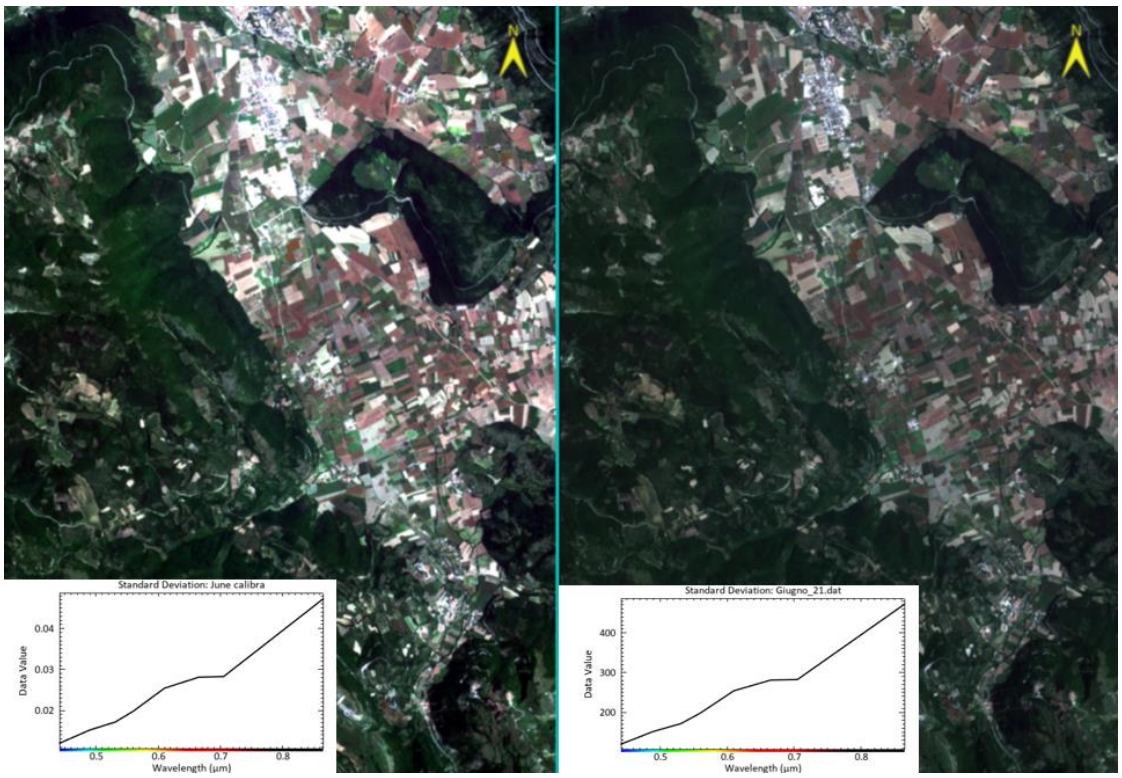

Fig.81 Radiometric calibration technique for the month of June (at left) and standard deviation

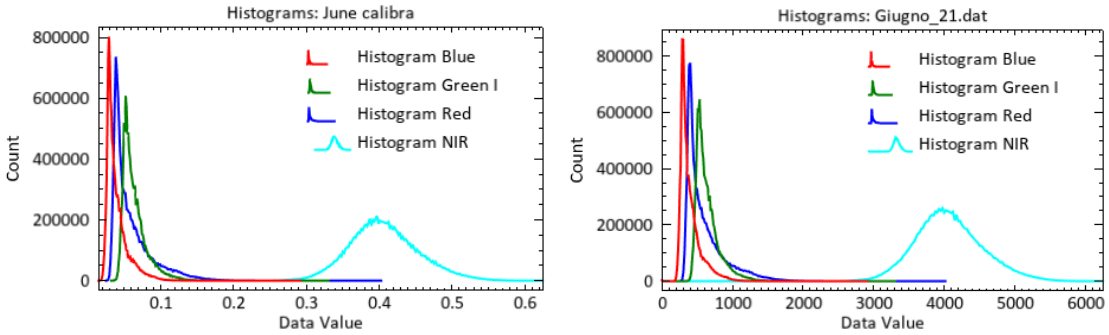

Fig.82 Spectral profiles of Radiometric calibrated image of June month

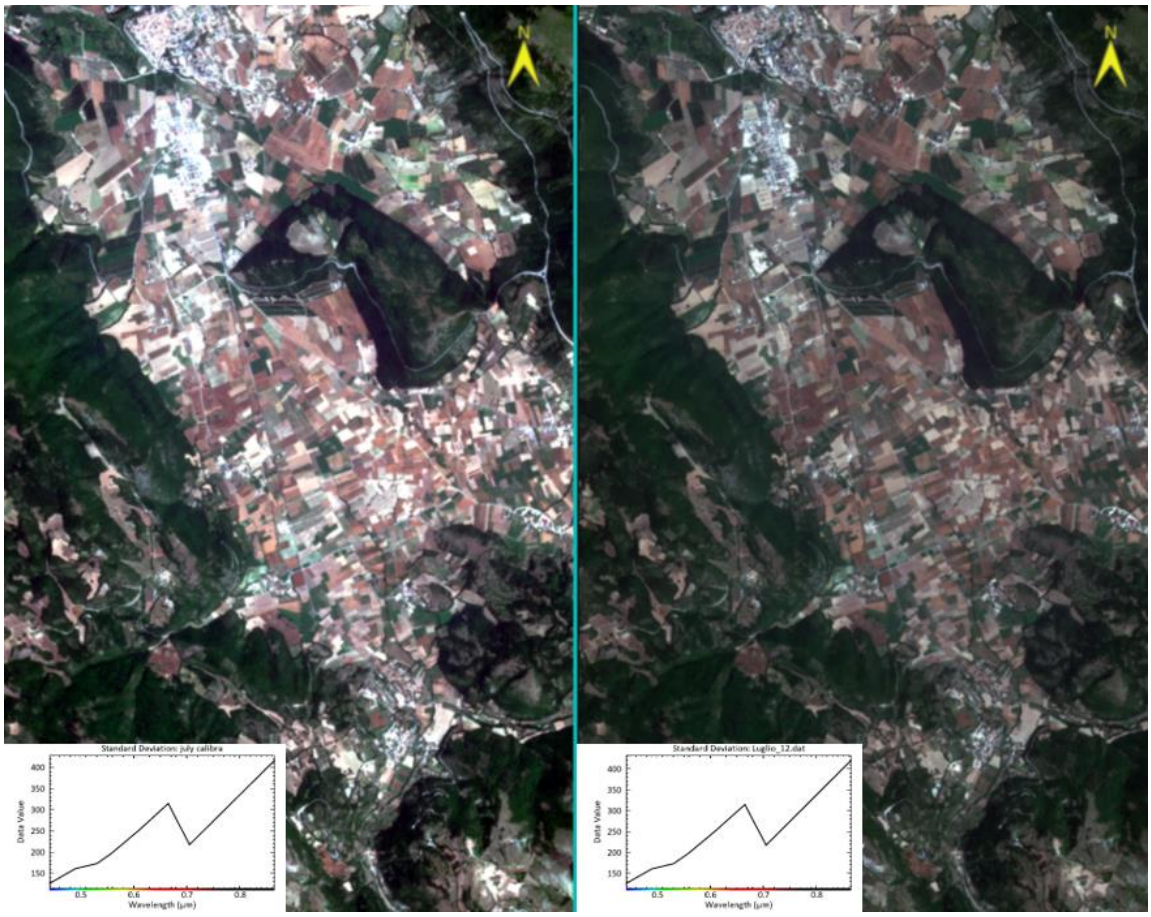

Fig.83 Radiometric calibration technique for the month of July (at left) and standard deviation

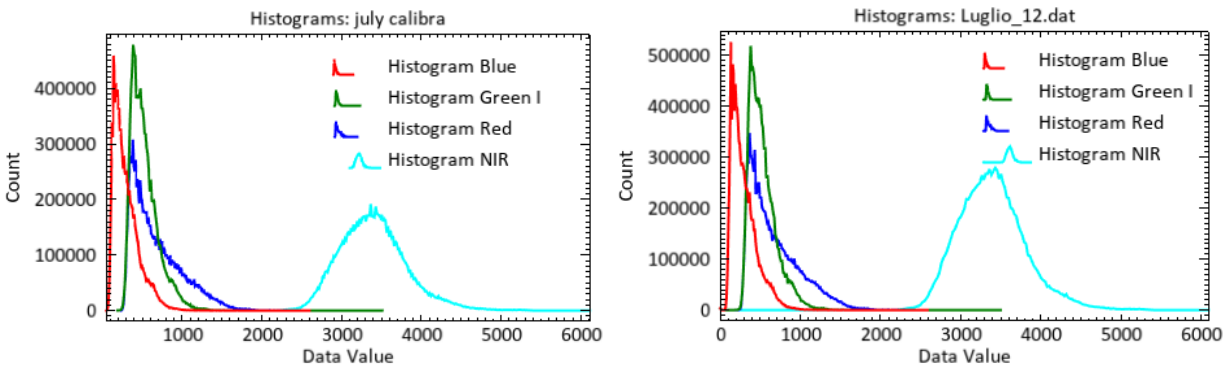

Fig.84 Spectral profiles of Radiometric calibrated image of July month

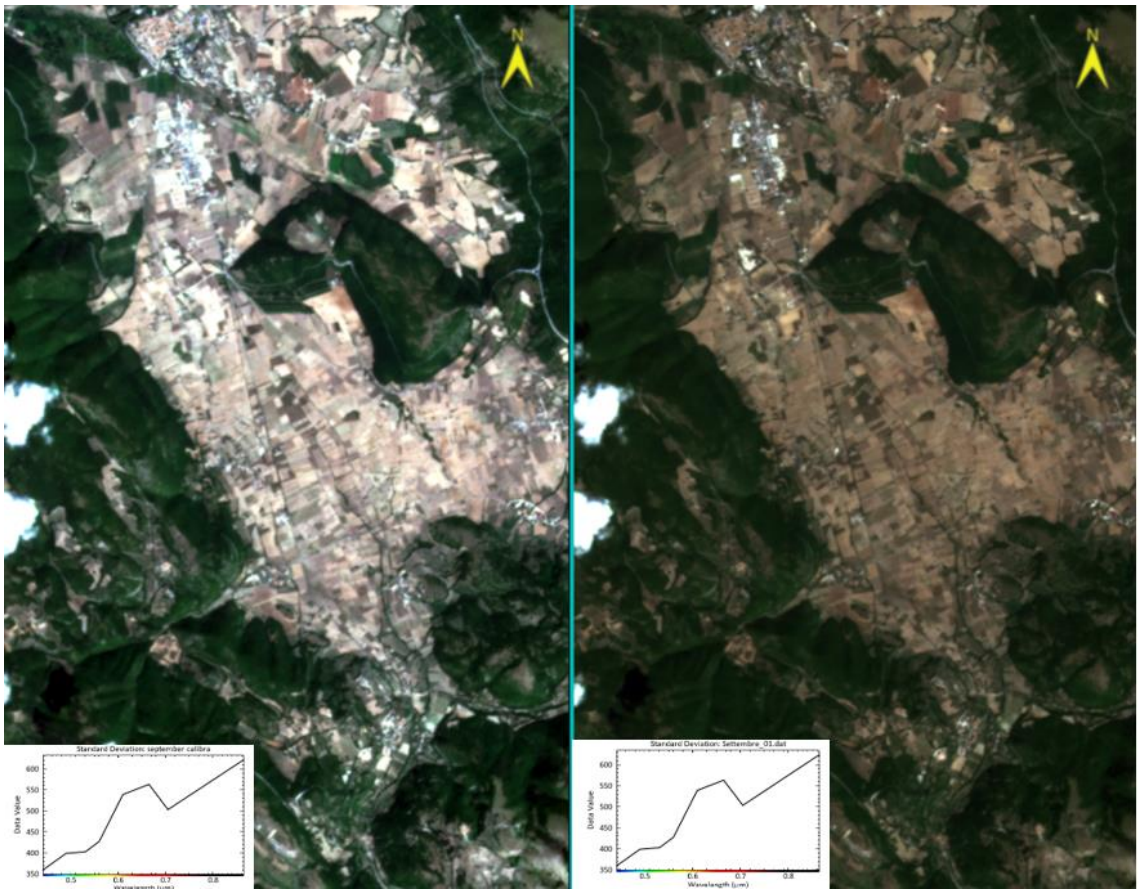

Fig.85 Radiometric calibration technique for the month of September (at left) and standard deviation

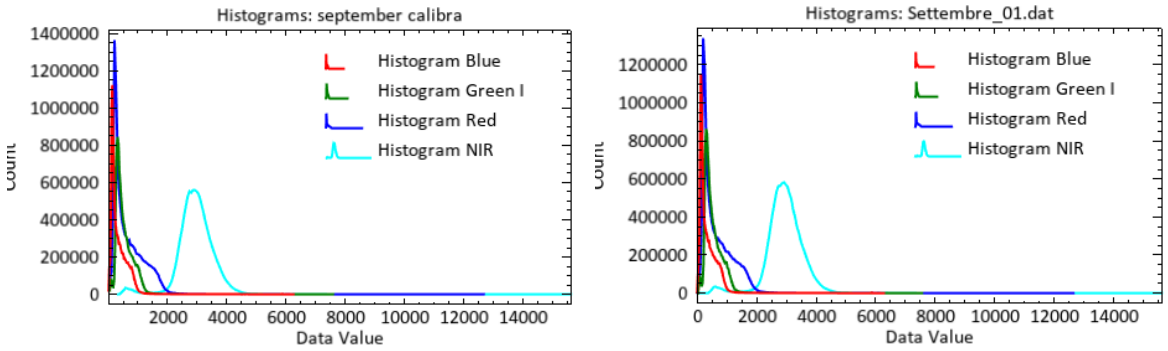

Fig.86 Spectral profiles of Radiometric calibrated image of September month

4.9 NIR and True color image: differences

In **Fig.87, Fig.88** and **Fig.89** two types of images are shown for the months of June, July and September in the study area: false color (NIR band, Red band, Green band) and real acquired in the visible (red, green, blue). The vegetation reflects in the NIR band (0.865 um) and not in the visible. At the centre of the area it can be noted that not all the fields are red, therefore they are not reflected in the NIR band, but only in the visible and they do not represent the vegetation. In general, it can be seen from the comparison of the false color and visible images that the presence of meadows and green areas decreases from the month of June towards September and the mowing phase begins for meadows and grasslands. The harvest is followed by mowing, for the crops sown in the months of April-May and the reseeding of new crops, according to the crop rotation technique. After harvesting the main crops, the soil is covered by cover crops that provide nutrients to the soil, preventing leaching. A good crop rotation technique allows the killing of microorganisms present in the soil, increasing the profitability of the soil and that of the crop. Furthermore, for all acquisitions there are no clouds or shadows that obstruct the scene.

Fig.87 Comparison between False color image (NIR, Red, Green) and acquisition in the visible band (Red, Green, Blue) for the month of June

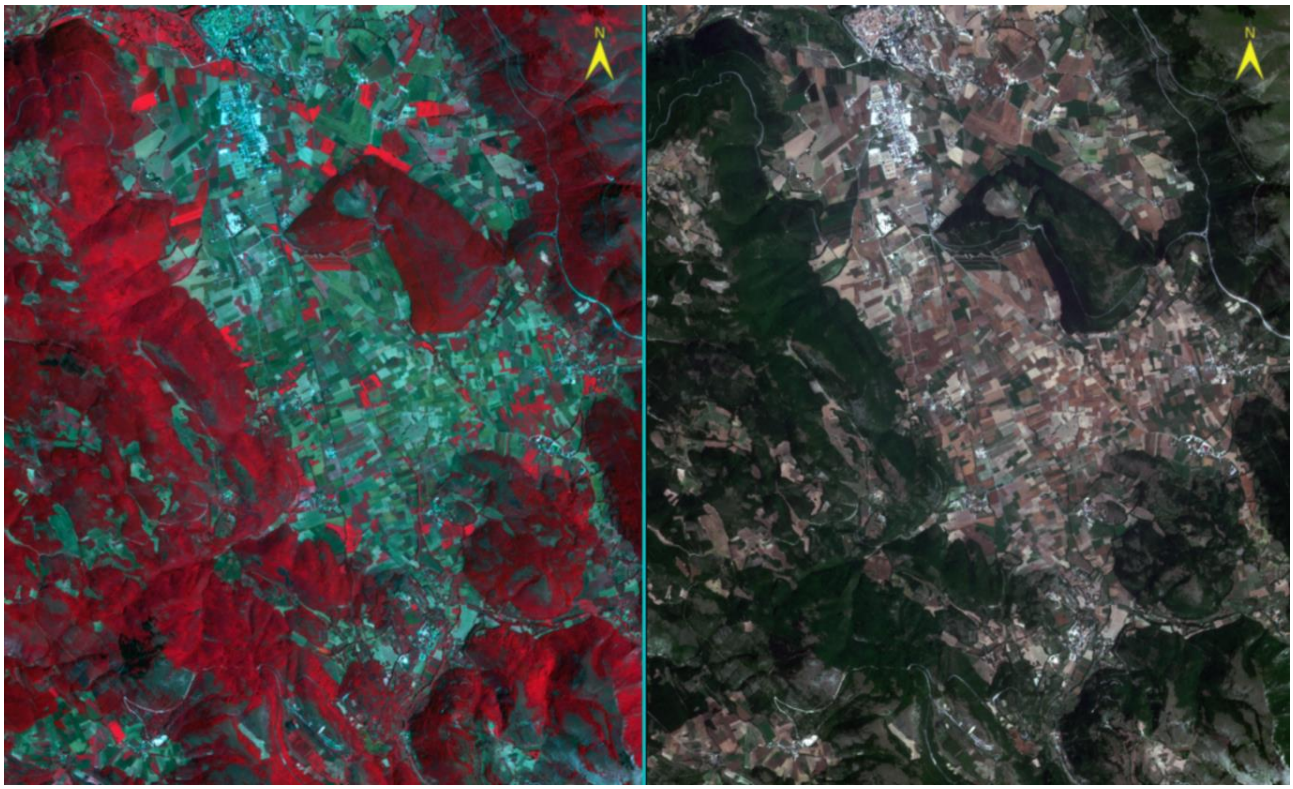

Fig.88 Comparison between False color image (NIR, Red, Green) and acquisition in the visible band (Red, Green, Blue) for the month of July

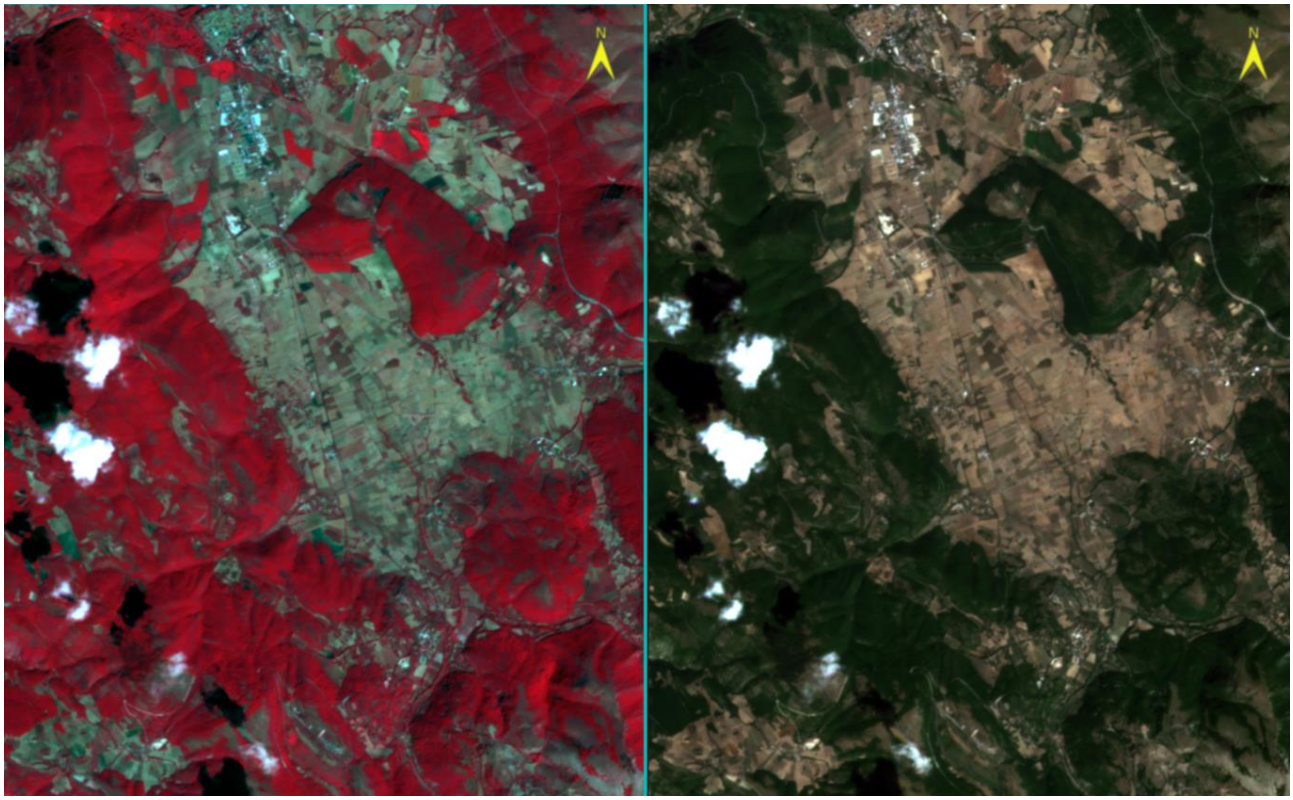

Fig.89 Comparison between False color image (NIR, Red, Green) and acquisition in the visible band (Red, Green, Blue) for the month of July

CHAPTER 5

5. Results

5.1 Spectral profiles cultures comparing in the summer months

Using the land cover map in **Fig.90** (provided by the PlanetScope dataset), it is possible to highlight the presence, through appropriate colors, of the crops that cover the studied area, but without having information on the life cycle of the crops represented. Each color represents a different crop and by comparing it with the images acquired in the months of June, July and September it is possible to highlight the changes in the seasons through the extraction of spectral profiles using the ENVI software. The spectral profiles explain how the light that reflects on the surfaces emits a sequential signal, which through the software algorithms is converted into data (Data Value). The signal reflects more in one spectral band than another, for example the vegetation reflects more in the near infrared and the water in the visible band, the wavelength of the blue color. Following graphs show the spectral profiles for the months of June, July and September in the VIS (0.4-0.75 um) and NIR (0.75-0.9 um) bands.

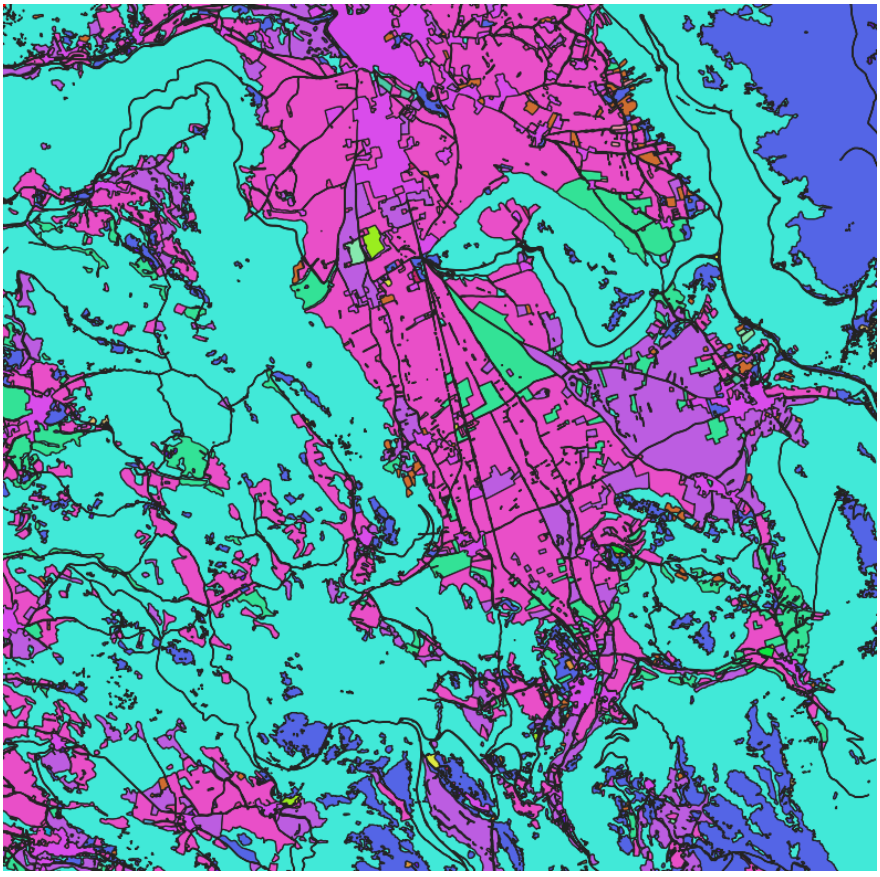

Fig.90 Land cover map *(https://earth.esa.int/eogateway/missions/planetscope)*

- In **Fig.91** the presence of the class of trees and groves is depicted. From the spectral profiles it can be seen that the vegetation reflects more in the month of June than in July and September in the NIR band. Furthermore, in the month of September, the reflection of the vegetation in the NIR band is very poor.

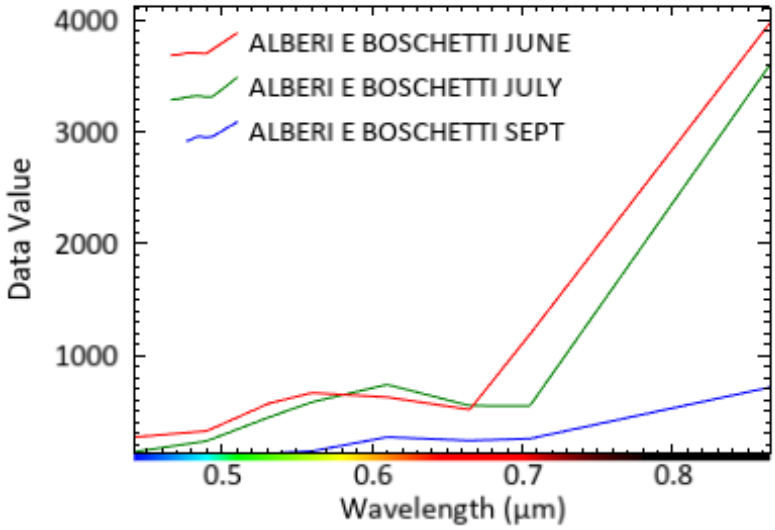

Fig.91 Spectral profiles for the class of trees and groves

- **Fig.92** shows the presence of the class of Wood Arboriculture (cultivation of tree and/or shrub species, reversible, aimed at the production of specific woody assortments). From the spectral profiles it can be seen that the vegetation reflects more in the month of June than in July and September in the NIR band. The spectral response in the month of September in the NIR band is very good, almost as good as that of the other two months.

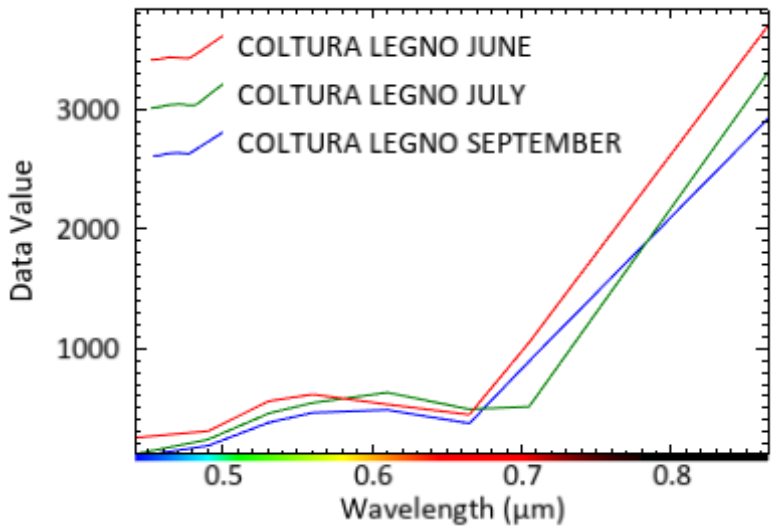

Fig.92 Spectral profiles for the class of Arboriculture for wood

- In **Fig.93** the presence of the mixed forest class is depicted. From the spectral profiles it can be seen that the vegetation reflects more in the month of June than in that of July and September in the NIR band, on the contrary in the VIS. The spectral response in the months of July and September in the NIR band is very good.

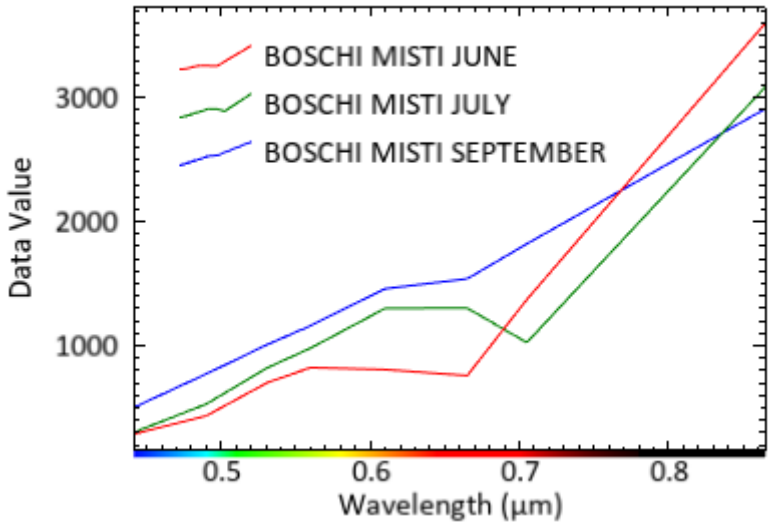

Fig.93 Spectral profiles for the Mixed Forests class

- **Fig.94** shows the presence of the chestnut class and the extraction of the spectral profiles related to this class. It can be noted in **Fig.94** that the spectral signature of the chestnut is similar for all three different spectral profiles in the visible bands (VIS), differently in the near infrared (NIR), in fact it is mostly present in the month of June. The chestnut cultivation is not very widespread in the area studied by the soil map, moreover it blends in with the surrounding vegetation.

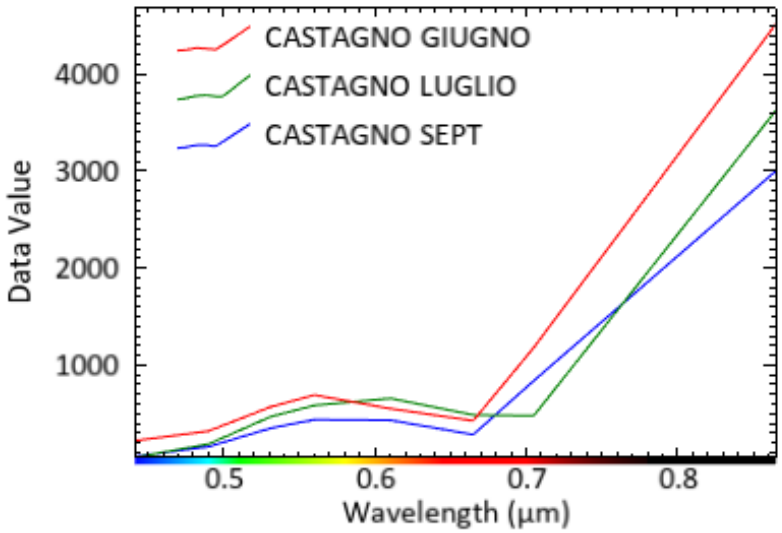

Fig. 94 Spectral profiles for the chestnut class

- **Fig.95** shows the presence of the class of short-cycle tree crops (non-woody in which the vegetative cultivation cycle takes place in a few months) and the extraction of the spectral profiles relating to this class. From the spectral profiles it can be seen that the vegetation reflects more in the month of June than in July and September in the NIR band.

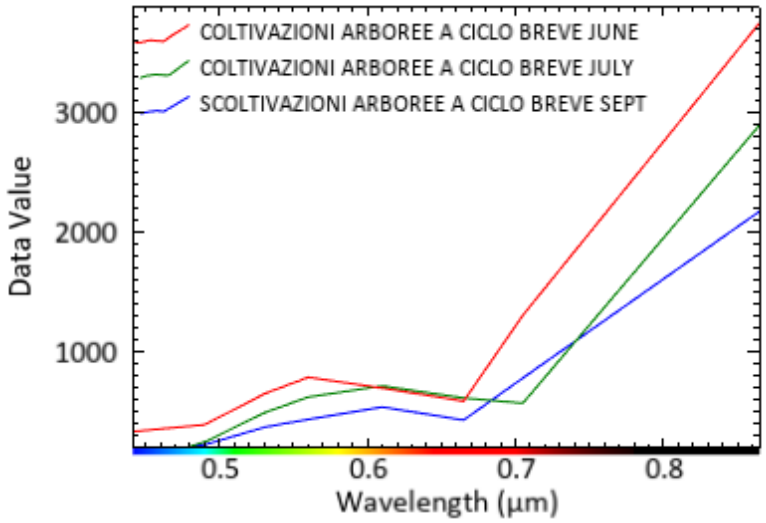

Fig.95 Spectral profiles for short-cycle tree crops

- **Fig.96** shows the presence of the grassland class and the change in the different months and the extraction of the spectral profiles related to this class. From the spectral profiles it can be seen that the vegetation reflects more in the month of June than in July and September in the NIR band. In the NIR band between 0.7-0.8 um the spectral response in the month of September is greater than that of July and June. Differently in the VIS band, the grassland vegetation reflects more in the month of September.

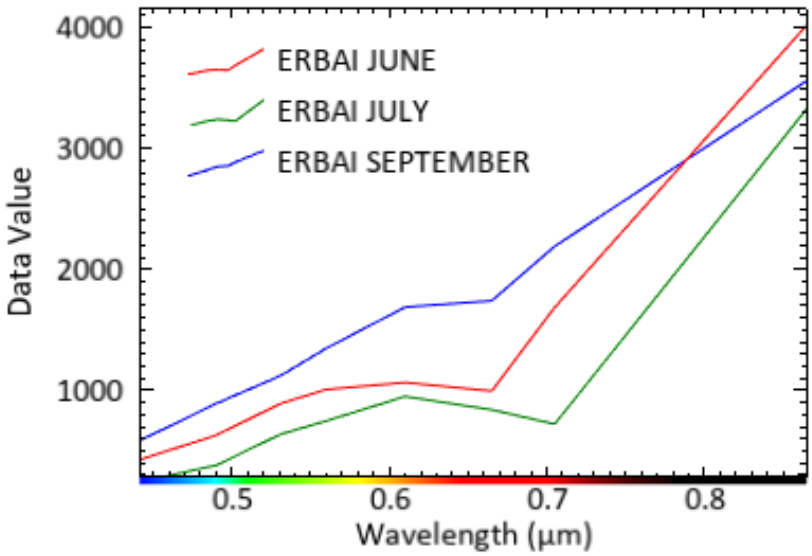

Fig.96 Spectral profiles for the grass class

- In **Fig.97** the presence of the orchard crop, the change in the different months and the extraction of the spectral profiles related to this crop are depicted. From the spectral profiles it can be seen that the vegetation reflects more in the month of June than in July and September in the NIR band. In the NIR band between 0.73-0.78 um the spectral response in the month of September is greater than that of July but not of June. Differently in the VIS band, the vegetation of the grasslands reflects more in the month of September.

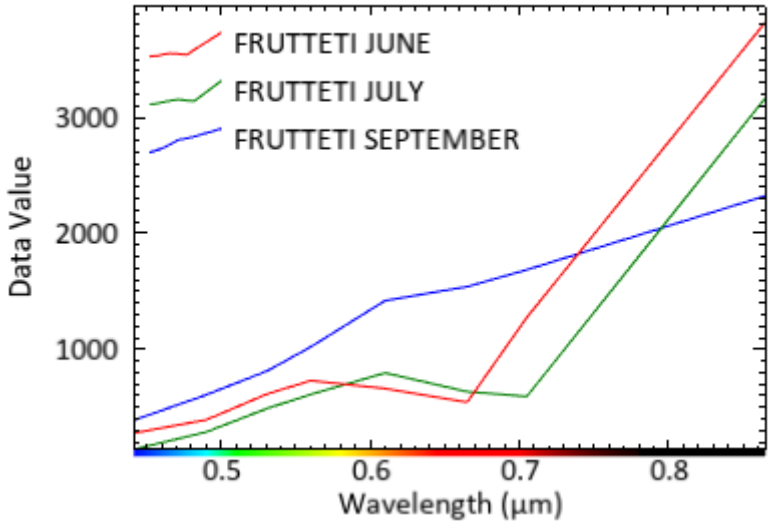

Fig.97 Spectral profiles for orchard cultivation

- **Fig.98** shows the presence of the class of areas subject to grazing and the change in the different months and the extraction of the spectral profiles referred to this class. From the spectral profiles it can be seen that the vegetation reflects more in the month of June compared to that of July and September in the NIR band.

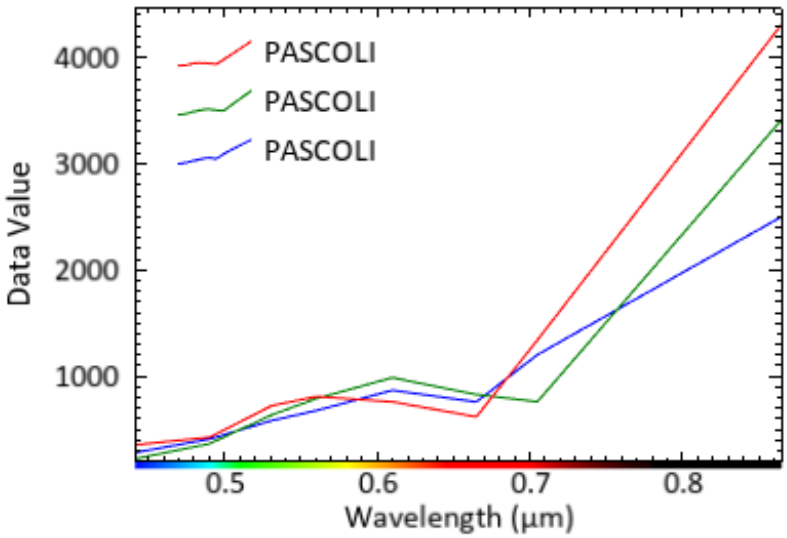

Fig.98 Spectral profiles for grazing areas

- **Fig.99** shows the presence of the sowing class, the change in the different months and the extraction of the spectral profiles related to this class. The areas subject to sowing cover most of the studied territory. In the NIR 0.75-0.8 um band the spectral profile of the month of September has higher values, but the slope tends to decrease towards the medium IR. Therefore, the vegetation reflects well in the month of September.

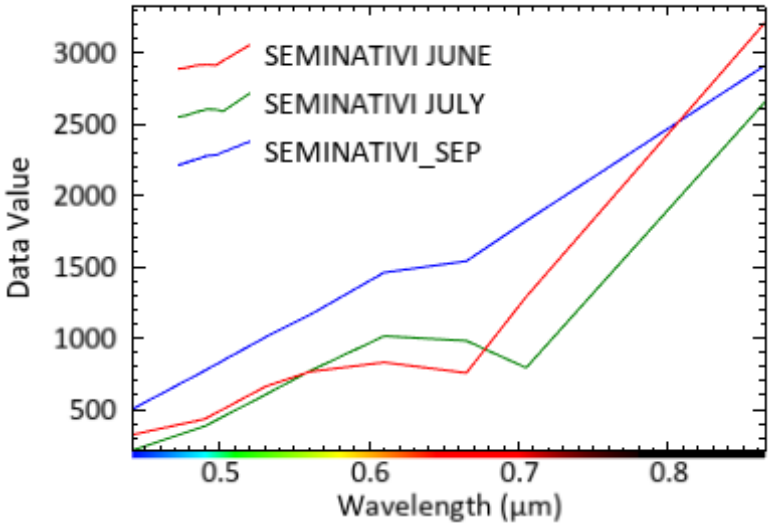

Fig.99 Spectral profiles for areas subject to sowing

- **Fig.100** shows the presence of the hedges and tree-lined strips class and the change in the different months and the extraction of the spectral profiles related to this class. It can be noted from the spectral profiles in the NIR band that the presence of the hedges and tree-lined strips class in the month of June together with that of September is greater than in the month of July.

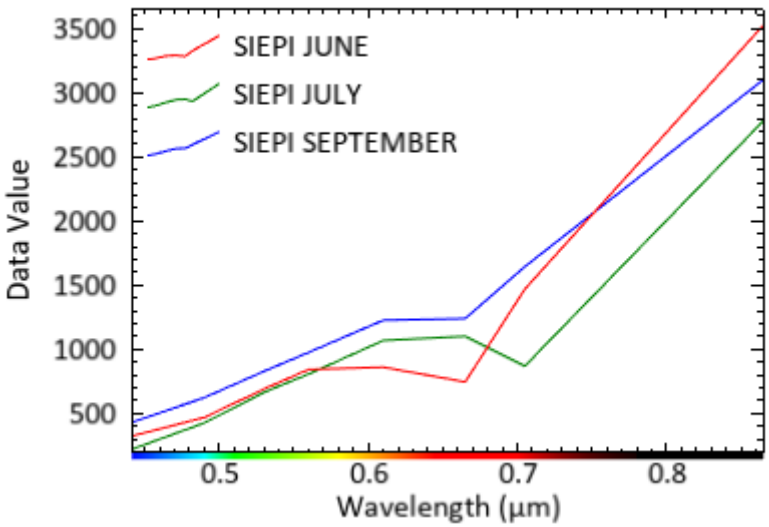

Fig.100 Spectral profiles for the hedge and tree-lined strip class

- **Fig.101** shows the presence of the vine class and the extraction of the spectral profiles related to this class. The cultivation of the vine in the studied area is very widespread, furthermore it is important from the fruit-growing point of view. In particular, in the months of September and July the spectral signature in the NIR band assumes high values and slopes (in the growth phase) compared to the month of June.

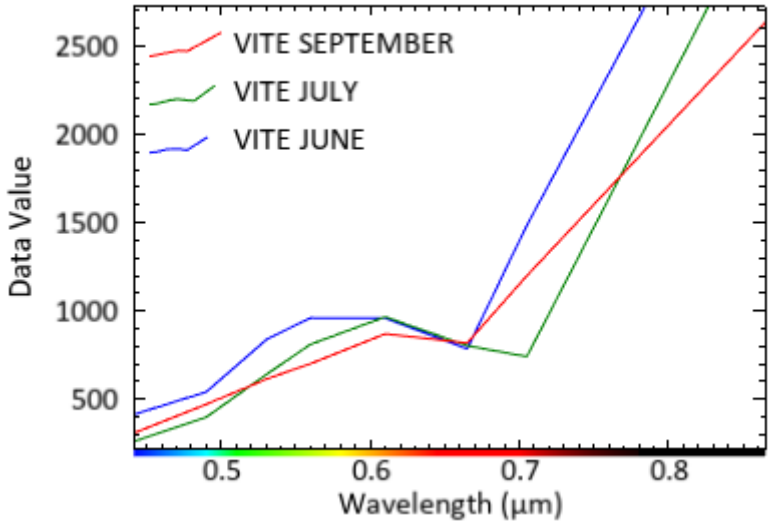

Fig.101 Spectral profiles for the grapevine crop class

- **Fig.102** shows the presence of the uncultivated land class and the extraction of the spectral profiles related to this class. It is possible to note that in the NIR band, the spectral profile of September assumes high values with a decreasing slope towards the medium IR. On the contrary, in the months of June and July the profile increases and assumes high values.

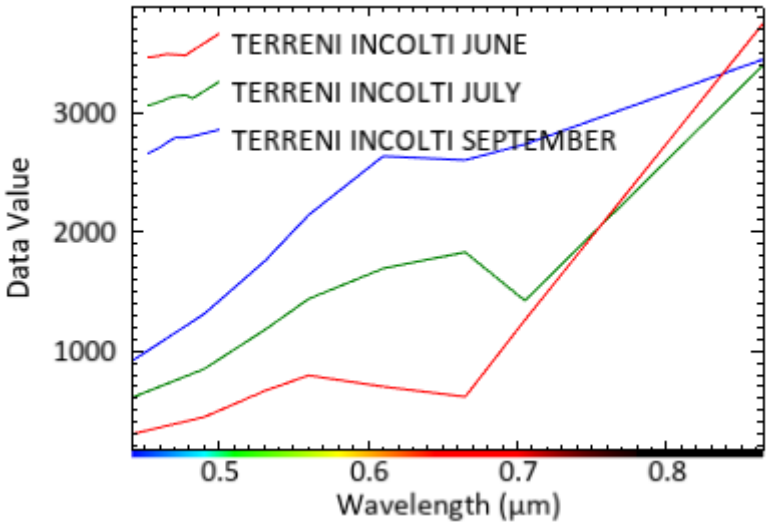

Fig.102 Spectral profiles for the uncultivated land class

5.2 NDVI Index

The Normalized Difference Vegetation Index (NDVI) is a graphical indicator that can be used to analyze measurements obtained from remote sensing, typically but not necessarily from a dedicated satellite. Moreover, NDVI can evaluate whether the observed area contains more vigorous vegetation. To detect and monitor crops, the basic operational requirements are important:

(a) an adequate “Geometric resolution” with respect to fields size

(b) high “Temporal resolution” for phenological phases detection

(c) spectral bands sensitive to crop parameters (biomass, photosynthetic activity)

(d) Decrease in clouds and shadows

(e) Costs compatible with agronomic sector

The calculation of the vegetation index NDVI is calculated as follows:

$$\mathrm{NDVI} = (\mathrm{NIR} - \mathrm{VIS})/(\mathrm{NIR} + \mathrm{VIS})$$

VIS and NIR stand for spectral reflectance measurements acquired in the visible (red) and near-infrared regions, respectively. According to the definition, the NDVI itself therefore varies between -1 and +1. It can be seen from its mathematical definition that the NDVI of an area containing dense vegetation will tend to give positive (0.3-0.8) values, while negative values are given if clouds are present *(https://it.wikipedia.org/wiki/Normalized_Difference_Vegetation_Index).*

In **Table.7** NDVI index was calculated to measure the vigor of vegetation. The colors range from blue (which corresponds to low values, just above 0) to green (higher values, up to a value of 0.6) passing through yellow (intermediate values, around 0.5) and then red (values equal to 1) in which the vegetation is more luxuriant**.**

The color scale of the NDVI index **(Table.8)** is done with raster color slice technique and **r**eflects reality that goes from gray (which corresponds to low values, just above 0) to yellow (higher values, up to a value of 0.35) passing through brown (intermediate values, around 0.5) and then green (values equal to 1) in which the vegetation is more luxuriant. **Fig.103**, **Fig.104** and **Fig.105** show the variation of the NDVI index in the area of interest for June, July and September.

Table.7 Legend NDVI index false color

Classes	NDVI	Value
1	Health	0.71 to 1
2	Medium	0.63 to 0.71
3	Minimum	0.56 to 0.63
4	Low	0.27 to 0.56
5	Very Low	-1 to 0.27

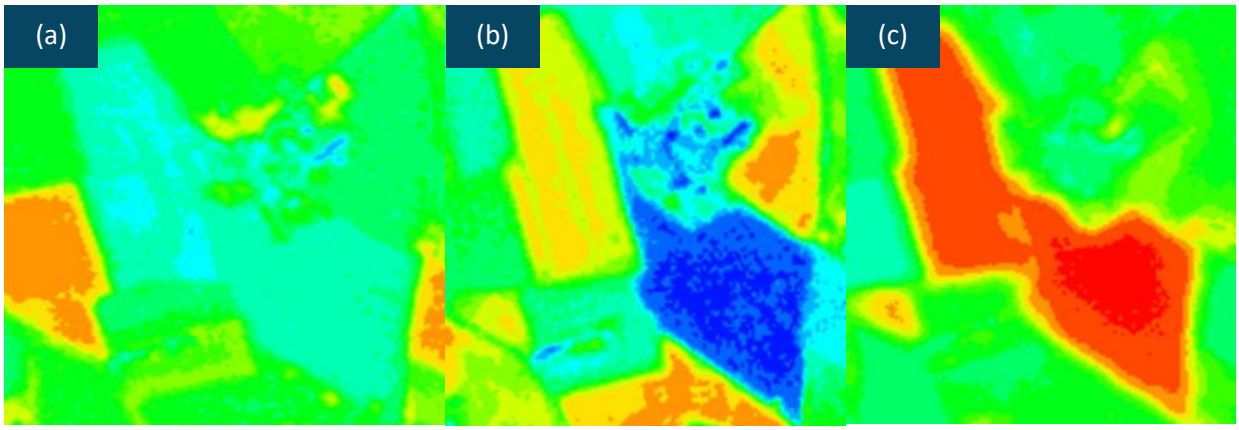

Fig.103 Normalized Difference Vegetation Index (NDVI) comparing in the images of June(a), July(b) and September(c)

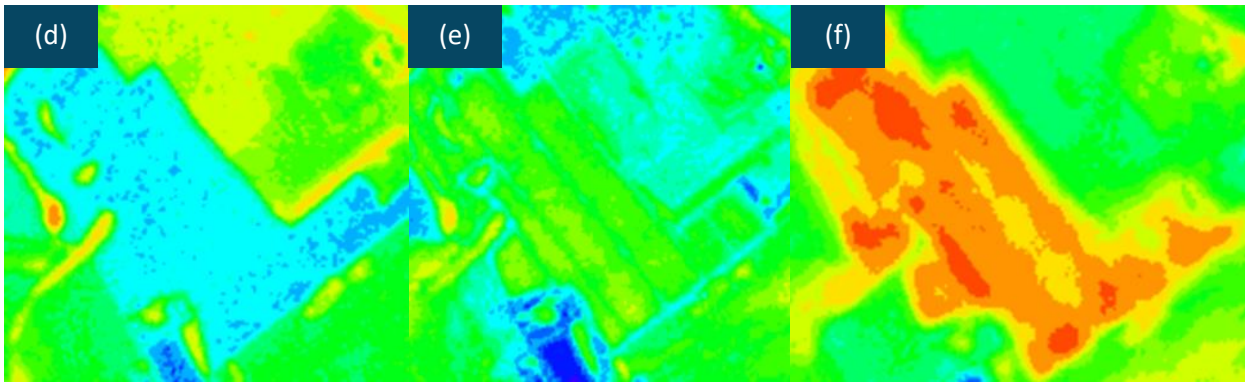

Fig.104 Normalized Difference Vegetation Index (NDVI) comparing in the images of June(d), July(e) and September(f)

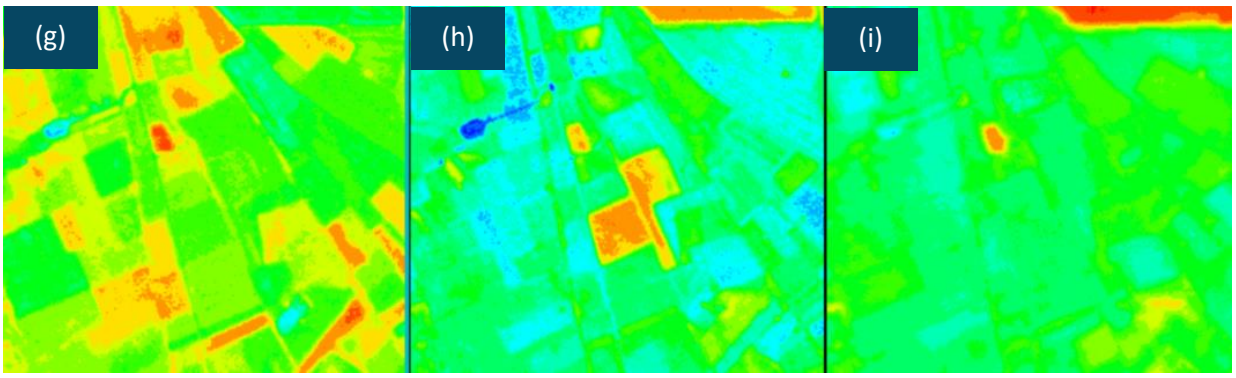

Fig.105 Normalized Difference Vegetation Index (NDVI) comparing in the images of June(g), July(h) and September(i)

Table.8 Legend NDVI index in real colors

Classes	NDVI	Value
1	Health	0.78 to 1
2	Medium	0.53 to 0.78
3	Minimum	0.35 to 0.53
4	Low	0.24 to 0.35
5	Very Low	-1 to 0.24

In general, **Fig.106, Fig.108, Fig.110** show the classes with an NDVI index from the minimum value (class 5) to the maximum value (class 1), which corresponds to a higher vegetation vigor index.

In **Fig.106** the comparison of the NDVI index for the health of vegetation in the month of June is presented between the two real color images on the right and the non-real ones on the left. From the real color image on the right, the green vegetation is very present as there is a high number of arable land left fallow, but most of the vegetation is covered by the class of woods and meadows with an NDVI index between 0.70-1, the brown color represents the arable fields with a beginning of vegetation growth (NDVI range between 0.5-0.65) while in yellow color the arable fields where the soil must be worked or sown and grasslands with round bales. In **Fig.107, Fig.109, Fig.111** the NDVI indices for the real color images and the black and white panchromatic image for the months of June, July and September are shown.

In **Fig.108** the comparison of the NDVI index for the health of vegetation in the month of July is presented between the two real color images on the right and non-real on the left. From the real color image on the right, green vegetation is always present, in particular the class of woods and groves with an NDVI index equal to about 1, but in smaller quantities than in the month of June, the arable fields left fallow decrease slightly. The number of grasslands with round bales and arable land tend to remain almost as in the month of June.

Fig.110 shows the comparison of the NDVI index for vegetation health in the month of September between the two real color images on the right and the non-real ones on the left. From the real color image on the right, the woods begin to lose vigor, giving way to evergreen crops such as pastures and meadows with an NDVI index between 0.5-0.8. It can be clearly seen that the amount of grassland with round bales and arable land where reseeding must take place has increased, covering a wider range of values (between 0.2-0.4). The arable land where reseeding takes place, compared to the previous months, covers a range of NDVI values between 0.4-0.5.

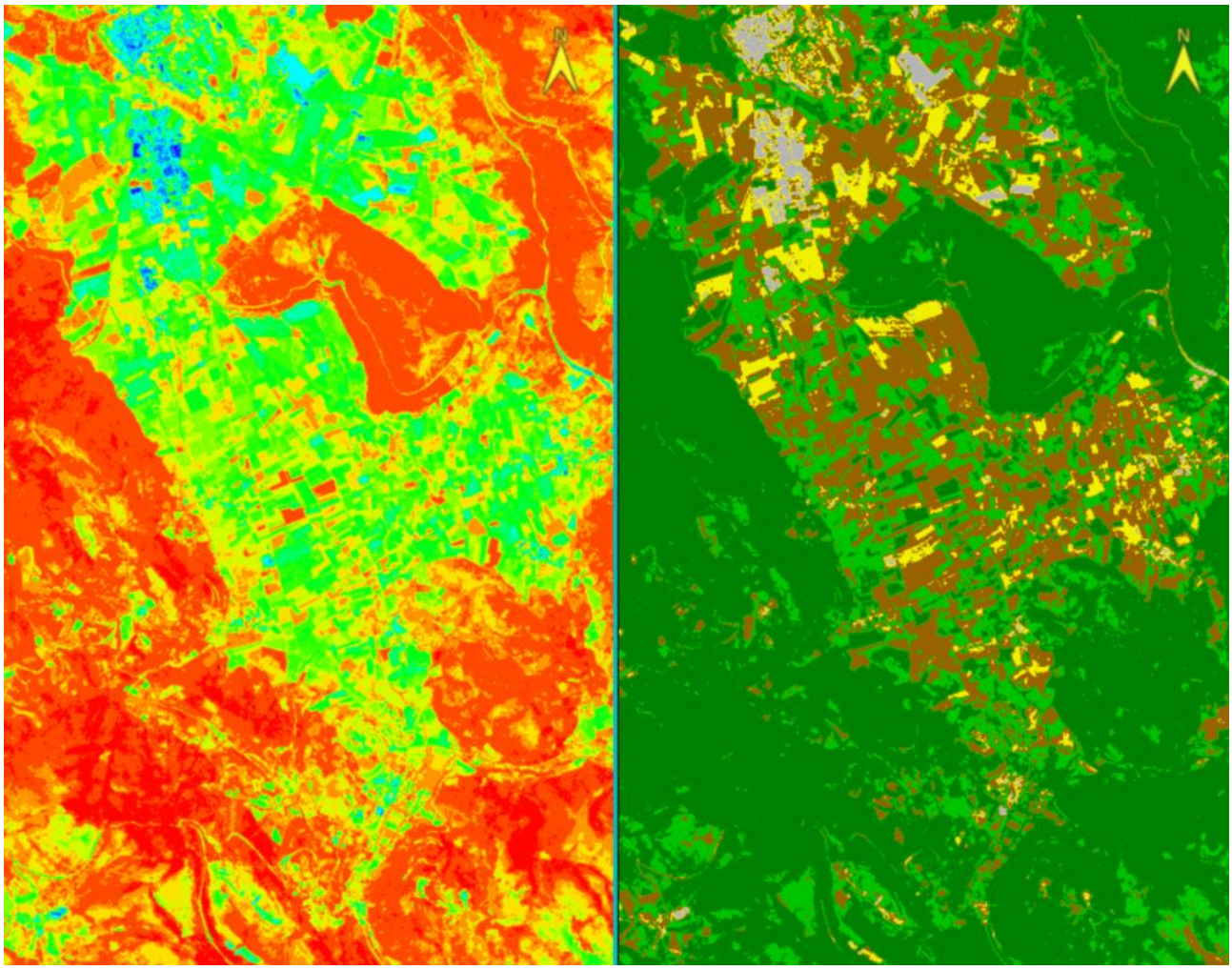

Fig.106 Normalized Difference Vegetation Index (NDVI) crops comparing using the raster color slice function (ENVI Program) in June

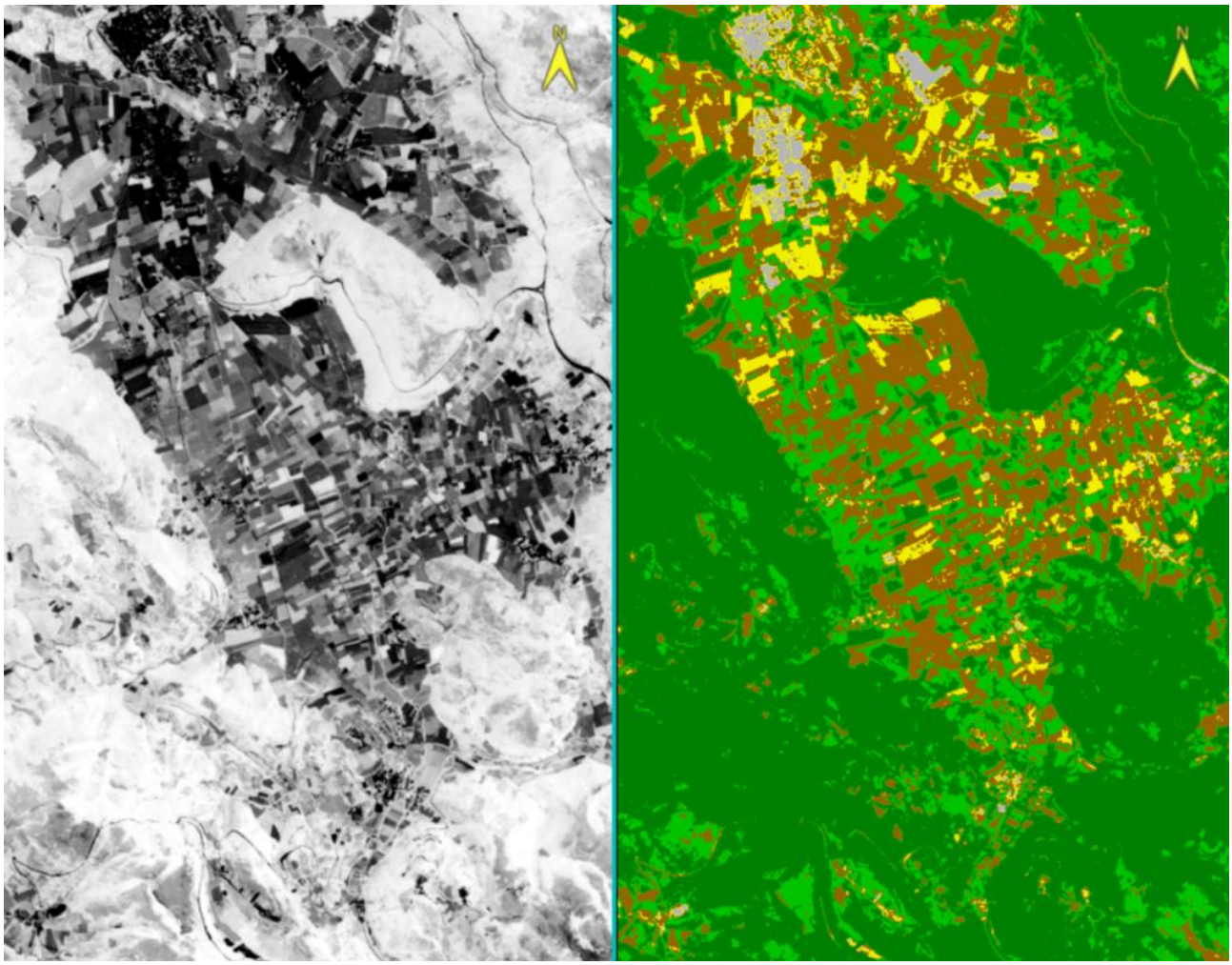

Fig.107 Normalized Difference Vegetation Index (NDVI) crops comparing with panchromatic image in June

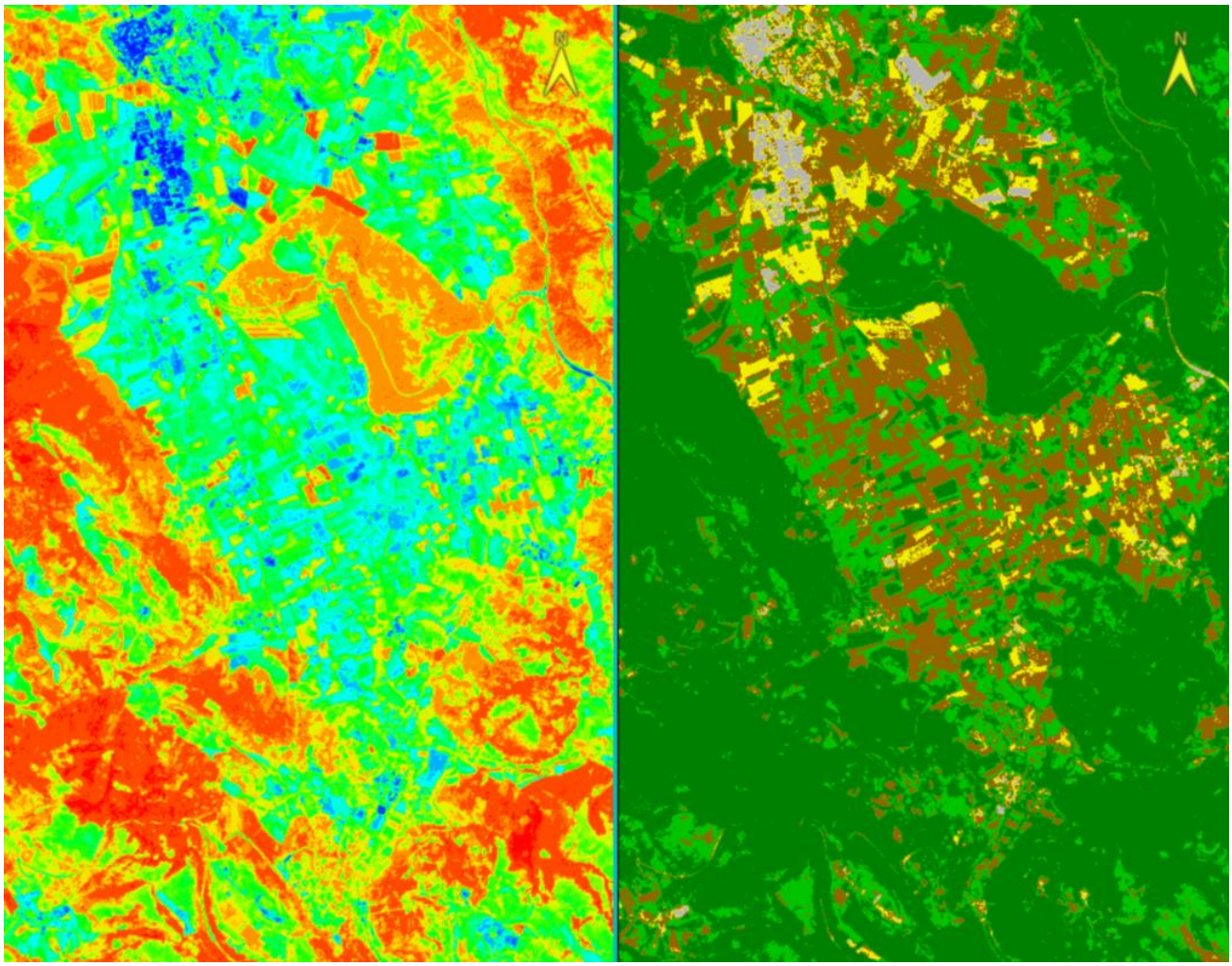

Fig.108 Normalized Difference Vegetation Index (NDVI) crops comparing using the raster color slice function (ENVI Program) in July

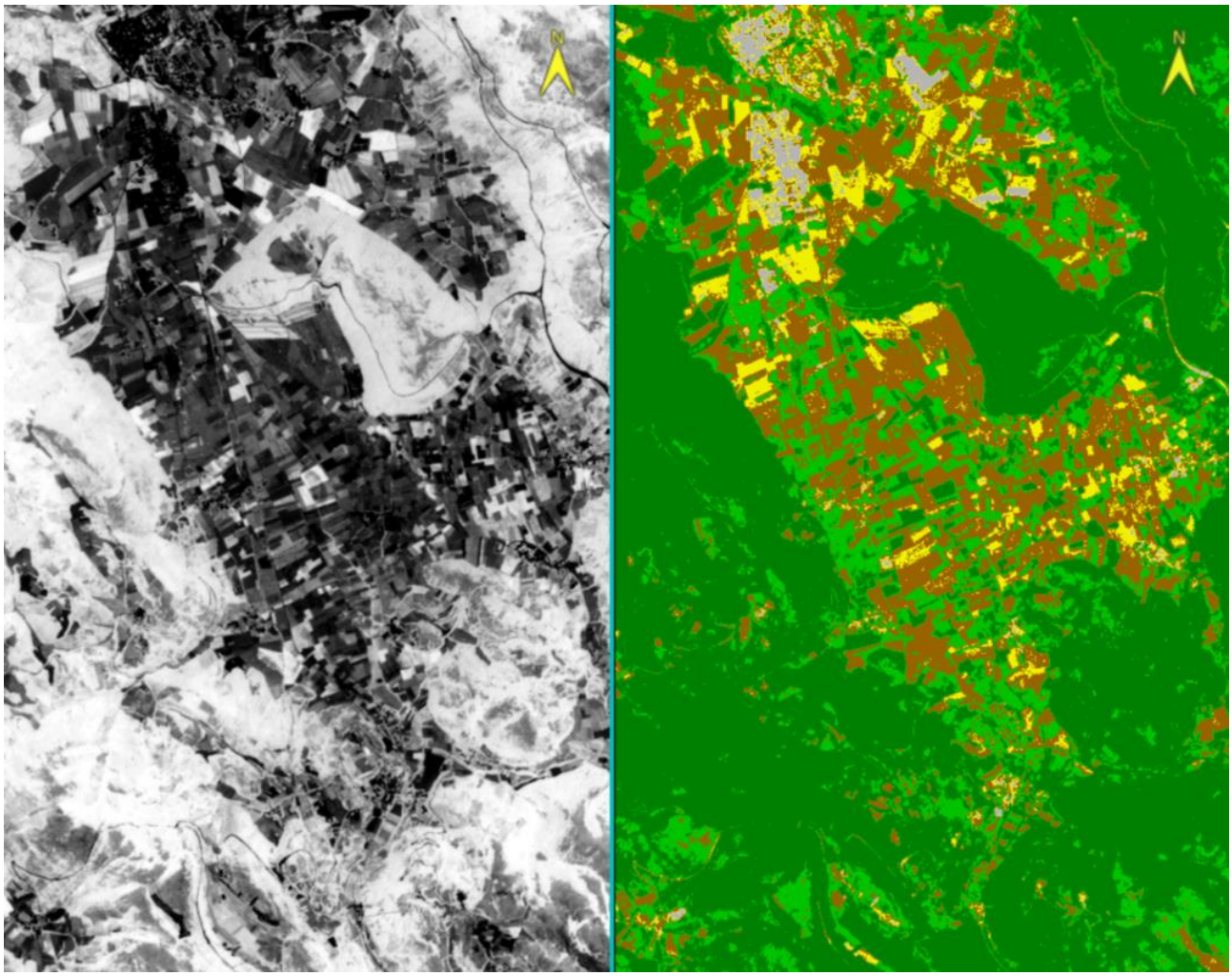

Fig.109 Normalized Difference Vegetation Index (NDVI) crops comparing with panchromatic image in July

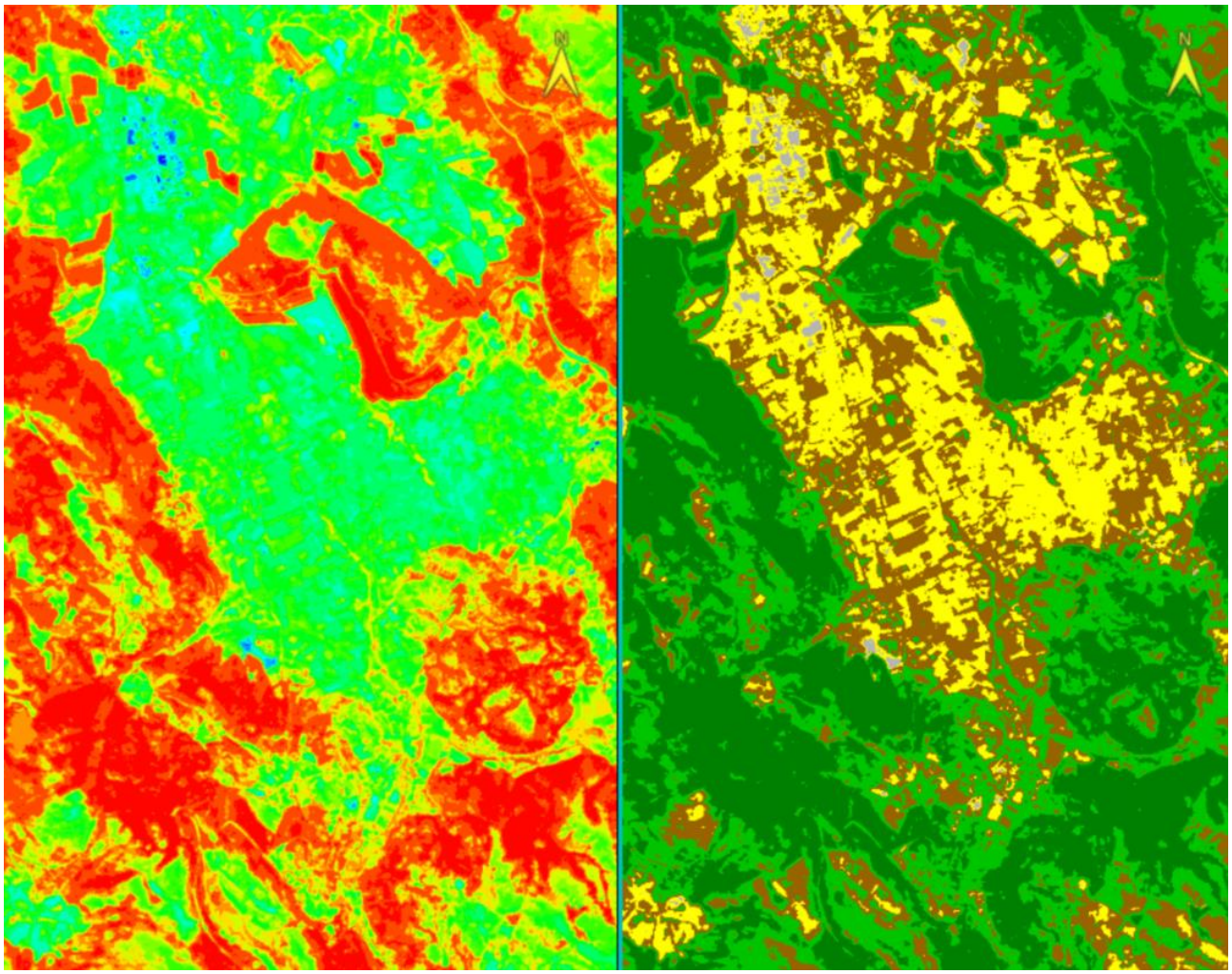

Fig.110 Normalized Difference Vegetation Index (NDVI) crops comparing using the raster color slice function (ENVI Program) in September

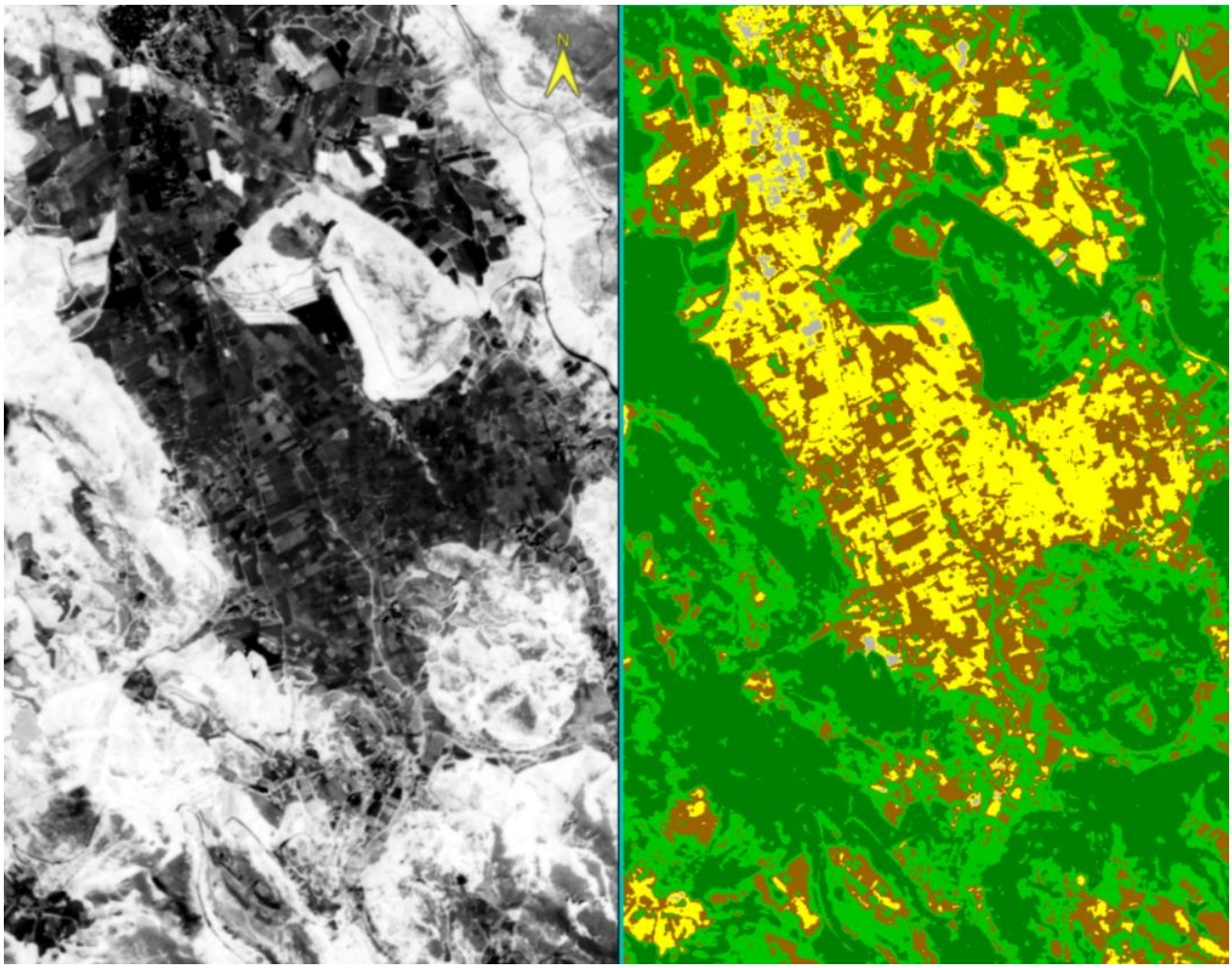

Fig.111 Normalized Difference Vegetation Index (NDVI) crops comparing with panchromatic image in September

5.3 NDVI radiometric spectra for cultures

Through the ENVI program algorithm (layer stack function) it is possible to study the phenological cycle of crops, grouping all the PlanetScope datasets and representing them in histogram-shaped graphs (spectral profiles) as a function of time. In this case the following crops are analyzed for the months of June, July and September determining the Normalized Difference Vegetation Index (NDVI) spectral signature that allows to clearly understand the life cycle.

The following crops were analyzed in the area of interest:

- WOOD ARBORICULTURE

In **Fig.112** it is noted that vegetation is more developed in the month of June, compared to July and September because the Normalized Difference Vegetation Index (NDVI) assumes higher values. In **Fig.113** from a graphic point of view, the highest peak referred to the month of June is taken as a reference (NDVI = 0.77) in which vegetation is more developed, followed by a decrease in the curve in the month of July up to a minimum (NDVI = 0.65) and a rise in the month of September (NDVI = 0.73).

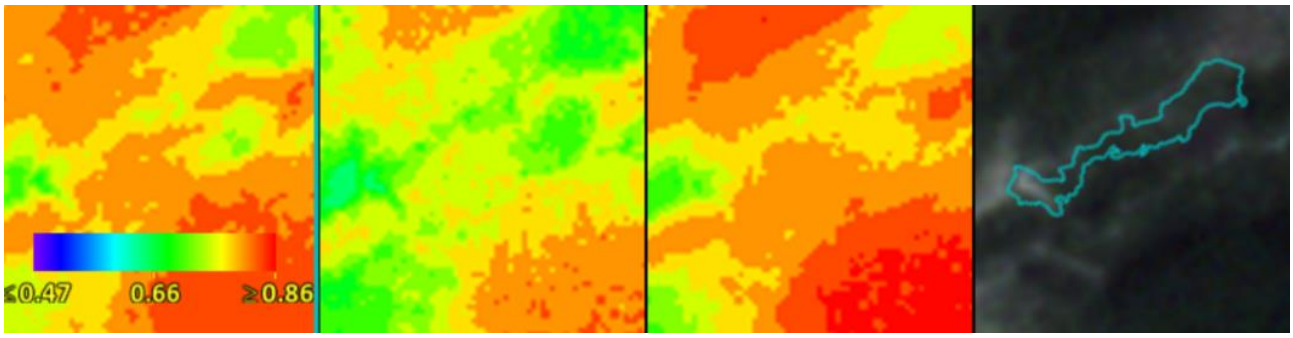

Fig.112 Comparison of Normalized Difference Vegetation Index (NDVI) in the months of June, July and September for woody arboriculture

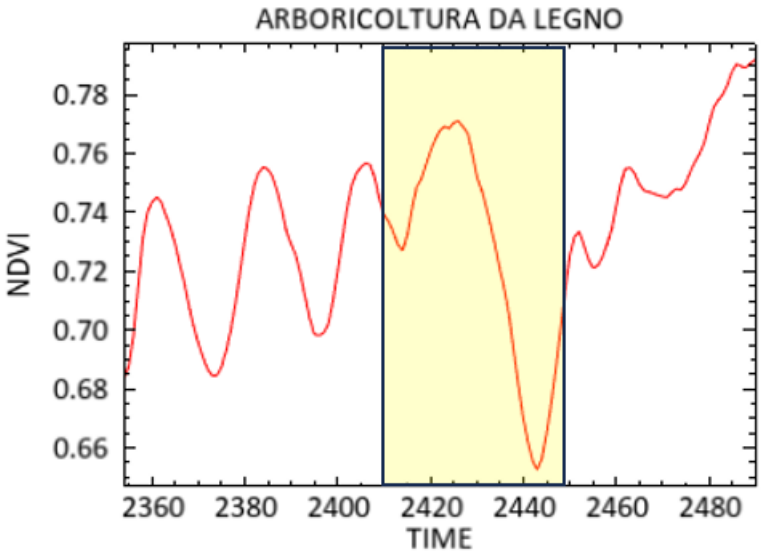

Fig.113 Normalized Difference Vegetation Index (NDVI) histogram in the months of June, July and September for wood tree cultivation

- ORCHARDS

In **Fig.114** it can be seen that the vegetation is more developed in the month of June, compared to July and September because the NDVI assumes higher values. From the spectral profile in **Fig.115** the highest peak referred to the month of June (NDVI = 0.77) is taken as a reference in which the vegetation is more developed, followed by a decrease in the curve in the month of July up to a minimum (NDVI = 0.40) and a rise in the month of September (NDVI = 0.5).

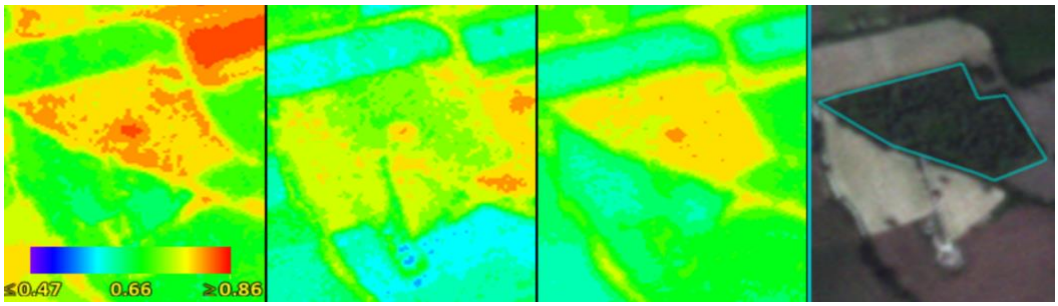

Fig.114 Comparison of Normalized Difference Vegetation Index (NDVI) in the months of June, July and September for orchard cultivation

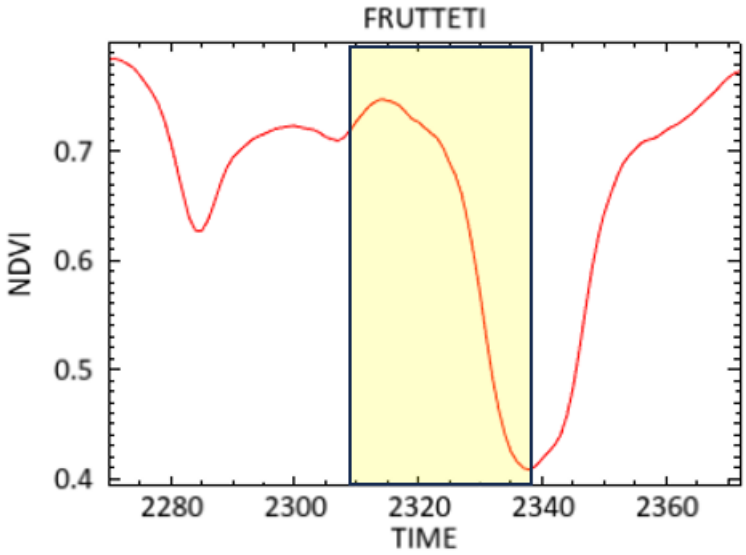

Fig.115 Normalized Difference Vegetation Index (NDVI) histogram in the months of June, July and September for orchard cultivation

- SCREW

In **Fig.116** it can be seen that the vegetation is more developed in the month of September, compared to June and July because the NDVI assumes higher values. From the spectral profile in **Fig.117** the highest peak referred to the month of September is taken as a reference (NDVI=0.72) in which the vegetation is more developed, preceding the months of July and June with a decrease in the curve (NDVI=0.5 and NDVI=0.44 respectively).

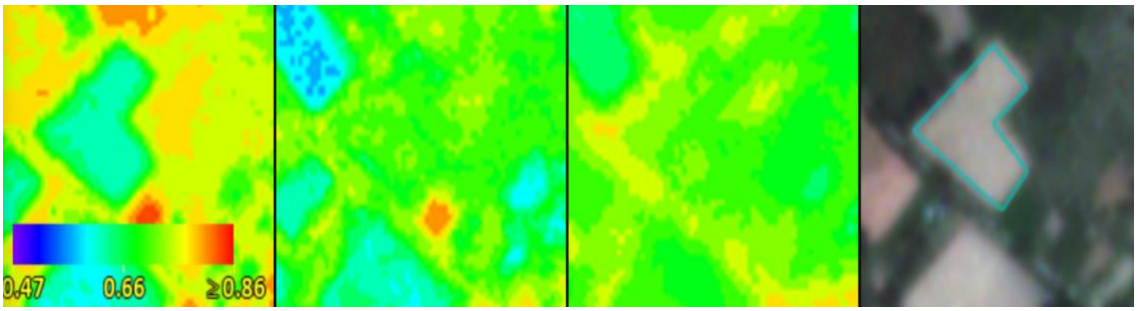

Fig.116 Comparison of the Normalized Difference Vegetation Index (NDVI) in the months of June, July and September for vine cultivation

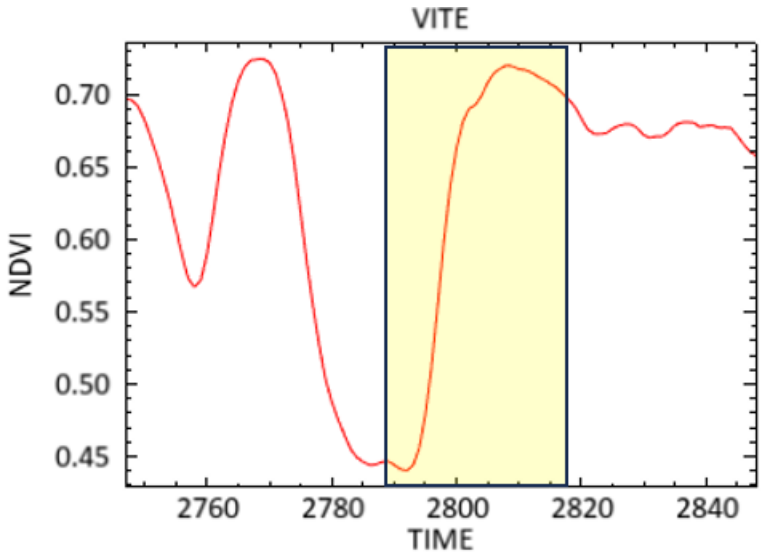

Fig.117 Normalized Difference Vegetation Index (NDVI) index histogram in the months of June, July and September for vine cultivation

- SHORT CYCLE TREE CROPS

In **Fig.118** it is clearly noted that the vegetation is more developed in the month of September and subsequently in the month of June and then July. In the month of July, the NDVI index assumes lower values because the vegetation is less vigorous. In **Fig.119** the behavior of the crop is depicted (through the NDVI histogram for the summer months of reference) from a graphic point of view. Following the trend of the spectral profile it is seen that the month of June is not the most developed (NDVI = 0.78). The peak that assumes higher values is in the month of September (NDVI = 0.85). The minimum is in the month of July in which the vegetation is less intense (NDVI = 0.75).

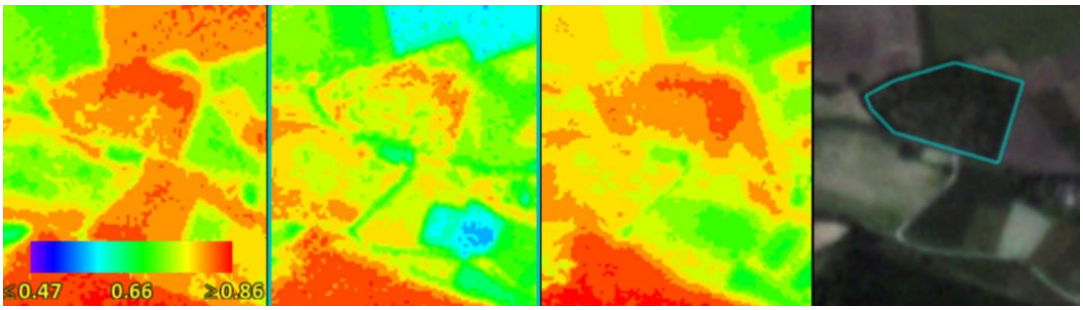

Fig.118 Comparison of Normalized Difference Vegetation Index (NDVI) in the months of June, July and September for short-cycle tree crops

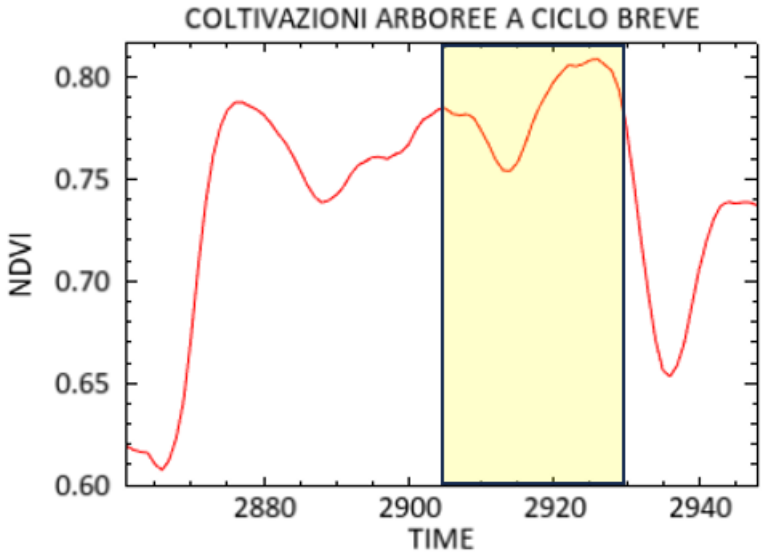

Fig.119 Normalized Difference Vegetation Index (NDVI) histogram in the months of June, July and September for short-cycle tree crops

- NUTS

Fig.120 shows the scale of variation of the NDVI index for the cultivation of nuts. It is clearly noted that the vegetation is more developed in the month of June. In the month of July, the curve tends to decrease and the NDVI index assumes lower values since the vegetation is less vigorous. **Fig.121** shows (through the NDVI histogram for the summer months of reference) the behavior of the crop from a graphic point of view. The peak that assumes higher values is in the month of June (NDVI = 0.76) the curve decreases in the month of July (NDVI = 0.65) until it rises slightly reaching a relative maximum in the month of September (NDVI = 0.58).

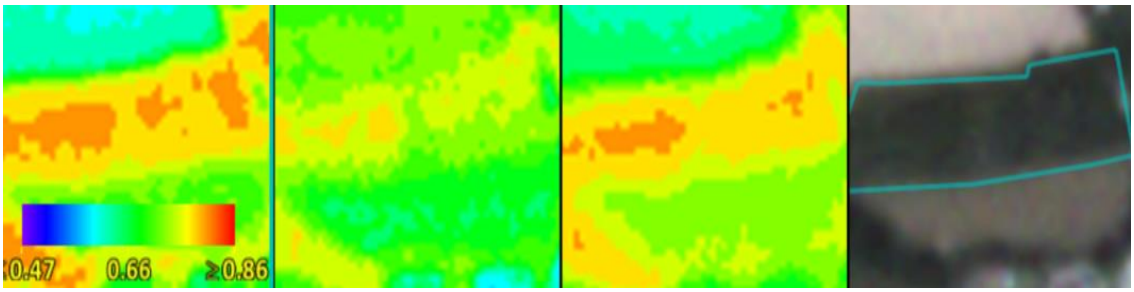

Fig.120 Comparison of Normalized Difference Vegetation Index (NDVI) index in the months of June, July and September for nuts

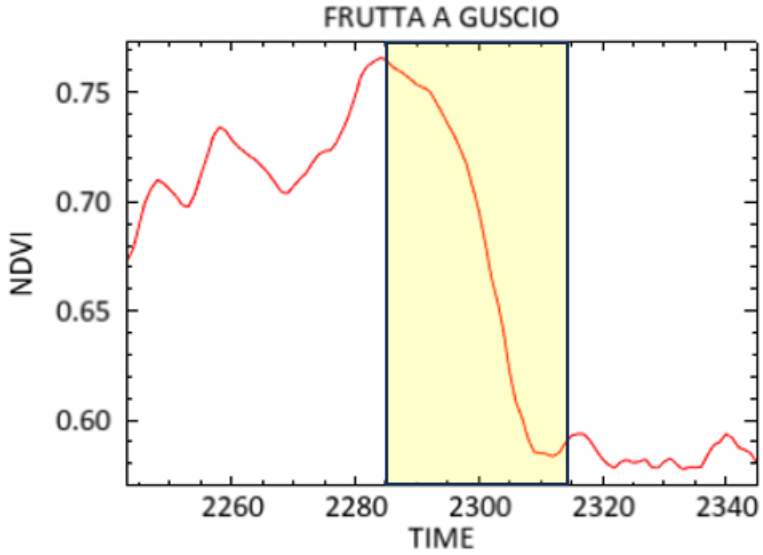

Fig.121 Normalized Difference Vegetation Index (NDVI) histogram in the months of June, July and September for nuts

- CHESTNUT TREES

Fig.122 shows the scale of variation of the NDVI index for the growth of the chestnut tree. It is clearly noted that the vegetation is more developed in the month of September and subsequently in the month of June. In the month of July, the NDVI index assumes lower values and the vegetation is less vigorous. **Fig.123** shows (through the NDVI histogram for the summer months of reference) the behavior of the crop from a graphic point of view. Following the trend of the spectral profile, initially there is a peak in the month of June (NDVI = 0.82), followed by a decrease in the curve in the month of July (NDVI = 0.77), until reaching the peak that assumes higher values in the month of September (NDVI = 0.85).

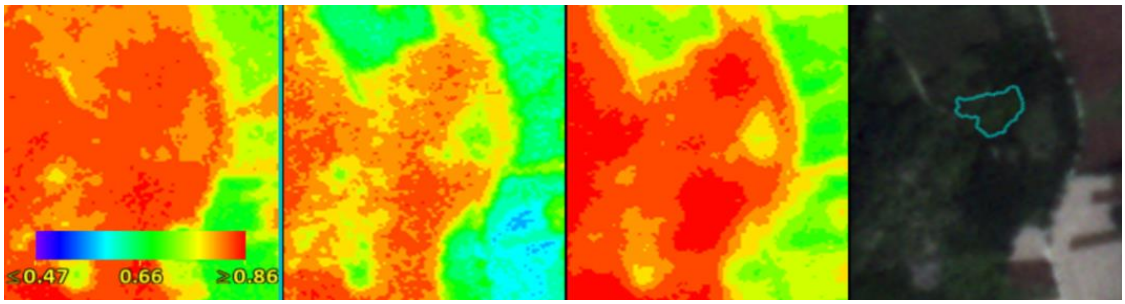

Fig.122 Comparison of the NDVI index in the months of June, July and September for chestnut

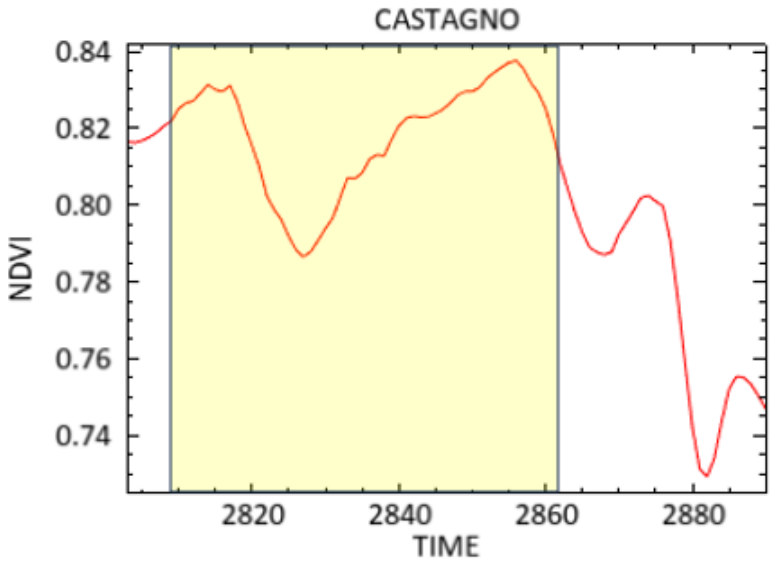

Fig.123 Normalized Difference Vegetation Index (NDVI) histogram in the months of June, July and September for chestnut

- OLIVE TREES

Fig.124 shows the scale of variation of the NDVI index for the growth of olive trees. It is clearly noted that the vegetation is more developed in the month of July and subsequently in the month of June. In the month of September, the NDVI index assumes lower values and the vegetation is less vigorous. **Fig.125** shows (through the NDVI histogram for the summer months of reference) the behavior of the crop from a graphic point of view. Following the trend of the spectral profile, initially there is a peak in the month of June (NDVI = 0.64) and almost attacked in the month of July (NDVI = 0.65), until reaching the minimum in the month of September (NDVI = 0.5).

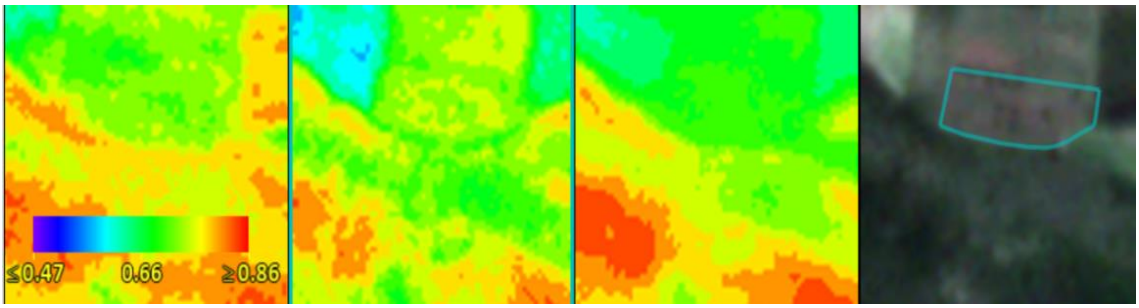

Fig.124 Comparison of the Normalized Difference Vegetation Index (NDVI) in the months of June, July and September for olive cultivation

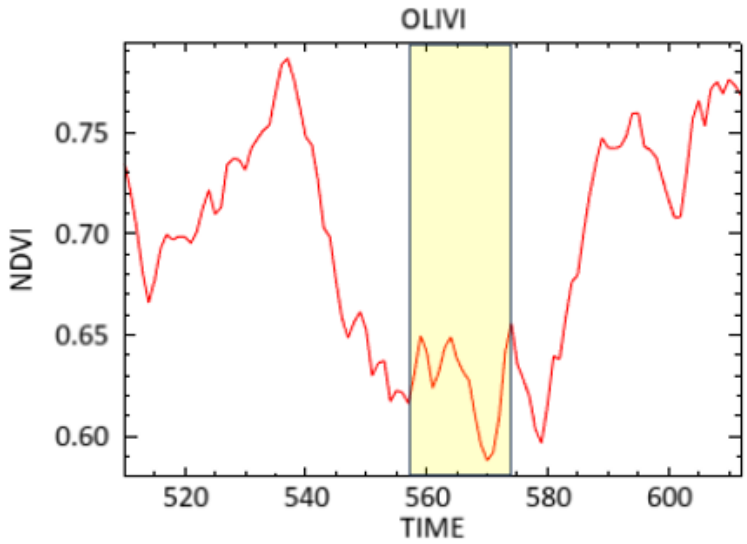

Fig.125 Normalized Difference Vegetation Index (NDVI) histogram in the months of June, July and September for olive cultivation

• ARABLE LAND

In **Fig.126** the NDVI vegetation index for the arable field taken as reference shows that the vegetation is more developed in the month of September, compared to June and July. From the spectral profile in **Fig.127** the growth of the spectral curve occurs from the month of June (NDVI = 0.52) to the month of September (NDVI = 0.63) in which flowering and maturation occurs. In accordance with what was said in the previous paragraphs, the vegetation of arable land depends on crop rotation, since, since a very large area was studied, it is not the same for the whole territory. In general, seeding takes place after harvesting, in this case in the spring season.

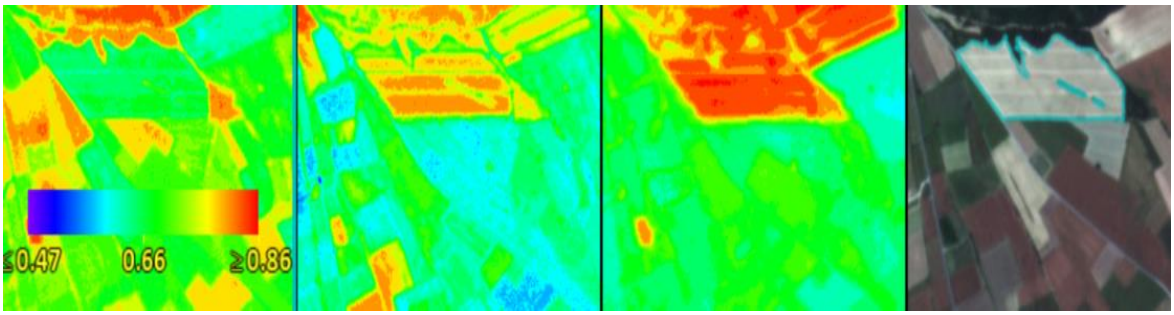

Fig.126 Comparison of the Normalized Difference Vegetation Index (NDVI) in the months of June, July and September for arable crops

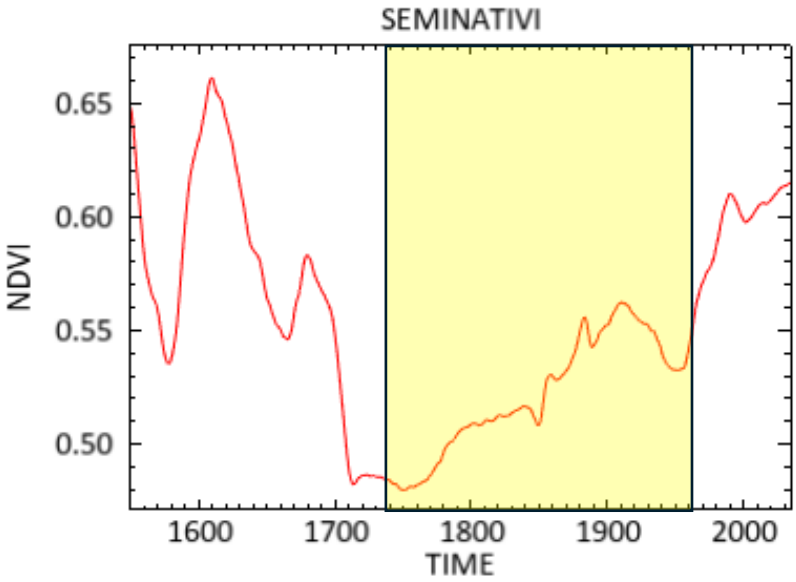

Fig.127 Normalized Difference Vegetation Index (NDVI) histogram in the months of June, July and September for arable crops

• HERBAL

In **Fig.128** the vegetation is more developed in the month of June, compared to July and September because the NDVI assumes higher values. From the spectral profile in **Fig.129** is possible to see a maximum in the month of June (NDVI=0.77), the curve decreases in the month of July (NDVI=0.63) reaching a minimum in the month of September (NDVI=0.10). The behavior is the same as the arable land with reseeding in September. For grasslands, haymaking takes place.

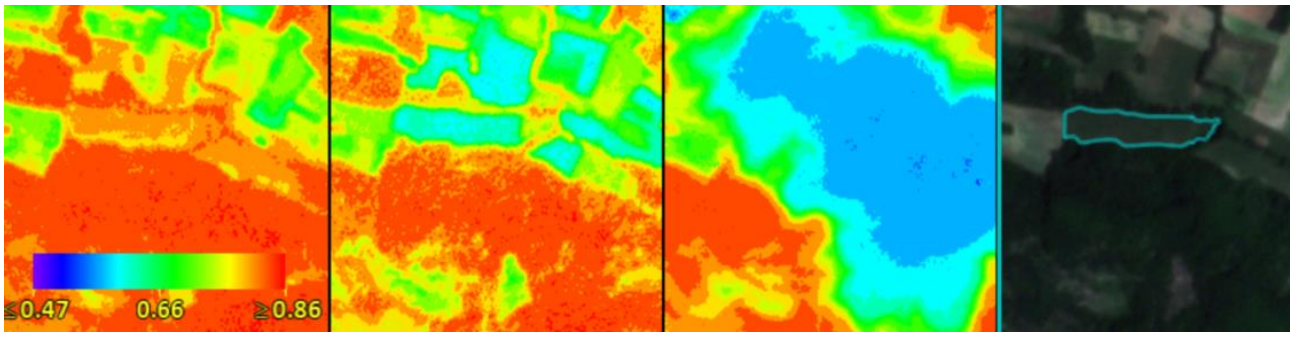

Fig.128 Comparison of Normalized Difference Vegetation Index (NDVI) in the months of June, July and September for grasslands

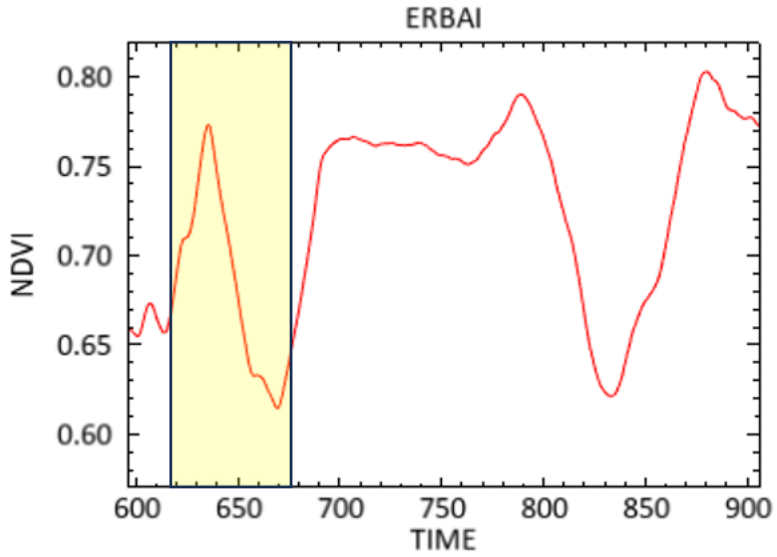

Fig.129 Normalized Difference Vegetation Index (NDVI) histogram in the months of June, July and September for grasslands

5.4 Monitored Crops and Related Agronomic Calendar

Table.9 shows the agronomic calendar of crops based on the data that were obtained from the previous graphs on the Normalized Difference Vegetation Index (NDVI) for the area taken as a reference of the city of Norcia in the Province of Perugia. The months of June, July and September of the summer season were taken as a reference and a total of 9 different types of crops were analyzed: Wood arboriculture, vines, chestnut trees, short-cycle tree crops, orchards, nuts, olive trees, grasslands and arable land. The latter are present in most of the cultivated area and also undergo a vegetative cycle of growth, crop maturation and harvest. From the analysis of the spectral profiles **(Fig.113, Fig.115, Fig.117, Fig.119, Fig.121, Fig.123, Fig.125, Fig,127, Fig.129)** of the crops it was possible to establish the interventions that saw the modification of the territory in those months, how the soil and the evolution of the vegetation changed over time, as well as the identification of a possible phenological cycle that reflects the actual behavior and the change of the crops in the field.

Table.9 Cultivation phases for the analyzed crops in the area of interest

	Interventions of Crops		
Crops	**GIUGNO**	**LUGLIO**	**SETTEMBRE**
Arboricoltura da legno	max vegetation	cut/use	growth
Vite	flowering	ripening	harvest
Castagno	flowering	cut/use	Max fruit ripening
Coltivazioni arboree a ciclo breve	ripening	cut	max vegetation
Erbai	max vegetation	mowing	mowing
Frutteti	flowering	growth	ripening/harvest
Seminativi	max vegetation	cut	reseeding
Frutta a guscio	flowering	cut/use	Ripening and harvest
Olivi	growth	max vegeta-tion	harvest

CHAPTER 6

6. Information extraction accuracy report

6.1 Classification approach

There are four classification approaches frequently used: (*https://gaview.org/drupal893/9-image-classification*)

1. Pixel-based image classification
- Unsupervised
- Supervised

2. Object-based image classification
- Unsupervised
- Supervised

The pixel-based approach clusters pixels using their spectral or temporal profile. The object-based image analysis (OBIA) creates polygonal objects by clustering neighboring pixels by looking at their statistical properties such as texture, size, shape, or directionality. Both approaches can be combined with either unsupervised or supervised approaches.

Supervised classification uses a different approach. First, statistical signatures are derived from a training dataset. And then, each pixel is compared with statistical signatures to find out the best-fit category. Eventually, the category of the best-fit signatures is assigned to the pixel **Fig.130**. Training samples can be collected from a field survey (*in situ* collection) or screen digitizing. Each polygonal area delineated by screen digitizing is called AOI (area of interest) or ROI (region of interest) in **Fig.131**.

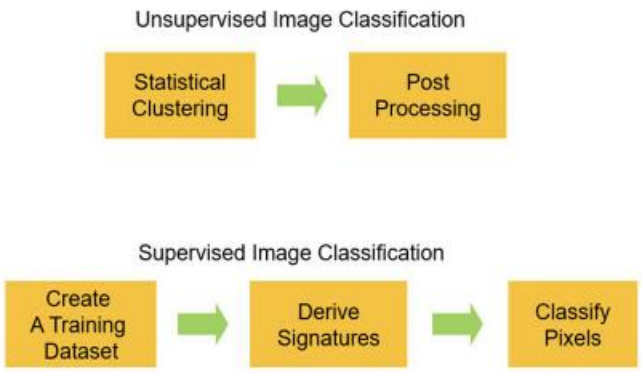

Fig.130 Classification procedures

6.2 MD classification and reality soil map comparing

The minimum distance method (MD) is a supervised image classification technique (*https://gaview.org/drupal893/9-image-classification*). In the minimum distance method, the distance between the mean of the signature dataset and the pixel value is calculated band-by-band. Then, the total distance is calculated. This total-distance calculation routine is repeated with all class signatures. The class that shows the minimum total distance is assigned to the pixel. This minimum distance method is very fast and simple in its concept. **Fig.133** shows the result of

minimum distance classification and how close it was possible to get to the ground reality **(Fig.90**) (land cover map produced by AGEA) by extracting Regions of Interest (ROI), **(Fig.131)** with the crops involved for the studied area through the ENVI software. In **Fig.134, Fig.135, Fig.136** are shown the comparisons between the ground reality and the ROIs extracted in the classification.

In **Fig.132** the characteristics of the ROIs are shown by comparing two values, the more they differ from the others, the greater the error produced in the classification. For example, taking the class of grasslands as a reference: the ROI that assumes the most divergent values is that of arable land.

Once an image is classified, the accuracy of the classification should be assessed. An error matrix is frequently used for checking errors. The error matrix is also known as a “contingency table,” or “confusion matrix.” Enough cases should be sampled to test classification errors. Results are shown in **Fig.132,** columns represent classification results, and rows represent reference data. The value of 55 pixels of Chestnut culture in the **Fig.137**, for example, means that 55 pixels in reality were classified to orchards culture, which means an error. From a user's perspective it is necessary to understand how well the original features are represented in the classification output. Producer's accuracy is calculated in association with reference data. However, from a user's perspective, what is important is how much the classification results are accurate. The user's accuracy is calculated in association with classification results. For example, in **Fig.137** the 61.15% of chestnut class is represented in the classification result, and only 4.52% of chestnut class is truly this class. The overall accuracy of the Minimum Distance (MD) classification is 46.23%.

Fig.138 shows the histogram of the classification of crops from the point of view of producer’s accuracy and user’s accuracy. For producer’s accuracy the crops present with the highest percentage are olive trees (68.82%), vines (63.47%) and orchards (64.03%). Instead, for user’s accuracy the crops present with the highest percentage are arable land (80.85%), grassland (39.89%) and pastures (59.16%).

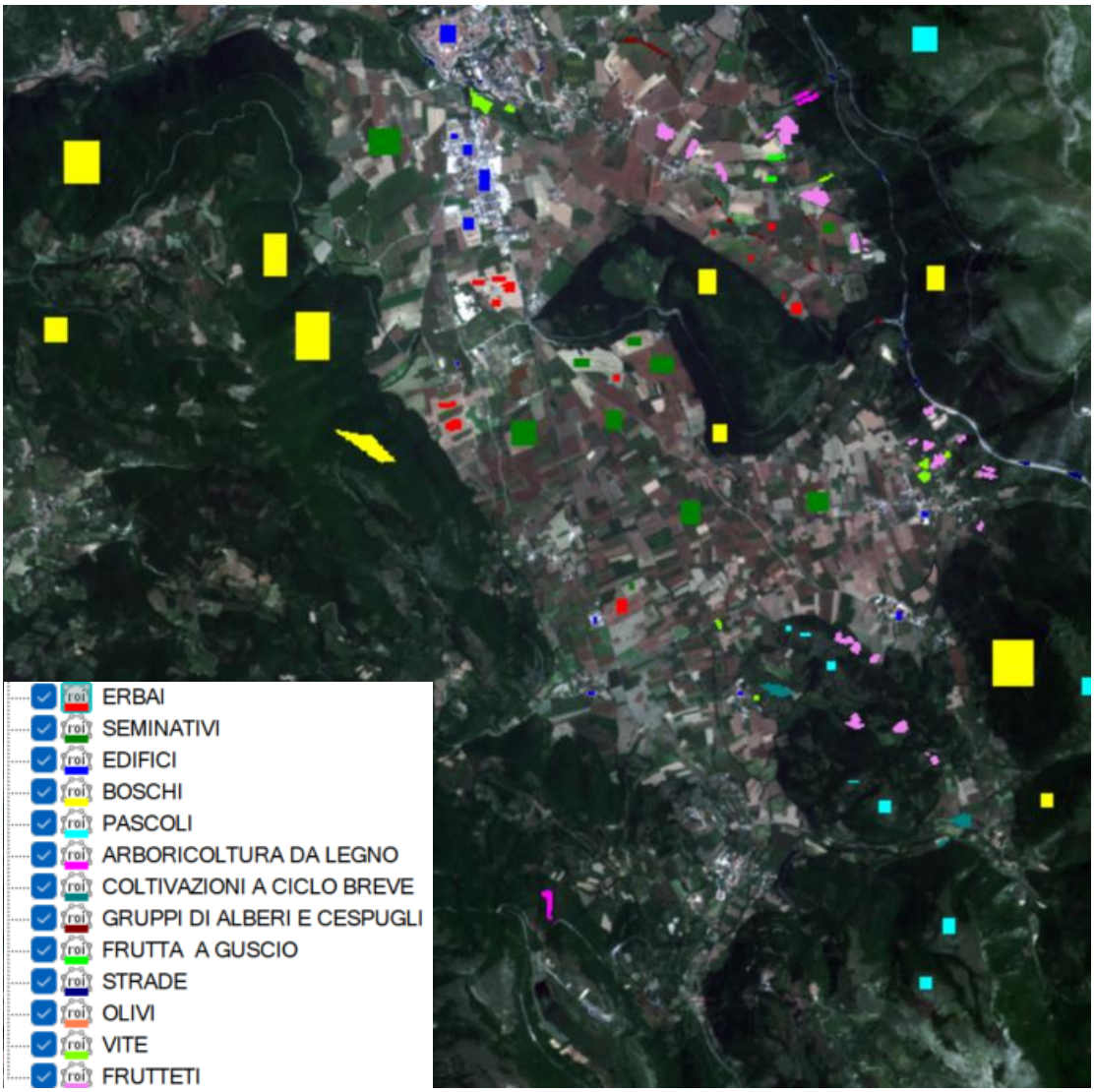

Fig.131 ROI choices for the classification map with Minimum Distance (MD) method

```
Input File: Giugno_21.dat
    ROI Name: (Jeffries-Matusita, Transformed Divergence)

ERBAI:
    SEMINATIVI: (1.70511036 1.99368031)
    EDIFICI: (1.95851161 2.00000000)
    BOSCHI: (2.00000000 2.00000000)
    PASCOLI: (1.99999713 2.00000000)
    ARBORICOLTURA DA LEGNO: (2.00000000 2.00000000)
    COLTIVAZIONI A CICLO BREVE: (1.99999913 2.00000000)
    GRUPPI DI ALBERI E CESPUGLI: (1.99999276 2.00000000)
    FRUTTA  A GUSCIO: (1.99999317 2.00000000)
    STRADE: (1.99999810 2.00000000)
    OLIVI: (1.99664291 1.99998961)
    VITE: (1.92309770 1.99961648)
    FRUTTETI: (1.99999885 2.00000000)
    CASTAGNO: (2.00000000 2.00000000)

SEMINATIVI:
    ERBAI: (1.70511036 1.99368031)
    EDIFICI: (1.78405743 1.95593883)
    BOSCHI: (1.96758659 2.00000000)
    PASCOLI: (1.63384852 1.99657204)
    ARBORICOLTURA DA LEGNO: (1.84550274 1.99957797)
    COLTIVAZIONI A CICLO BREVE: (1.74665143 1.98854831)
    GRUPPI DI ALBERI E CESPUGLI: (1.68933049 1.97482300)
    FRUTTA  A GUSCIO: (1.66058532 1.99631196)
    STRADE: (1.99839579 1.99983696)
    OLIVI: (1.20827229 1.76994444)
    VITE: (1.39627156 1.85779135)
    FRUTTETI: (1.69517124 1.99584741)
    CASTAGNO: (1.97517223 2.00000000)
```

```
EDIFICI:
    ERBAI: (1.95851161 2.00000000)
    SEMINATIVI: (1.78405743 1.95593883)
    BOSCHI: (1.99955521 2.00000000)
    PASCOLI: (1.98944570 1.99999205)
    ARBORICOLTURA DA LEGNO: (1.99616744 2.00000000)
    COLTIVAZIONI A CICLO BREVE: (1.99706879 1.99999998)
    GRUPPI DI ALBERI E CESPUGLI: (1.93859465 1.99946694)
    FRUTTA  A GUSCIO: (1.99249230 1.99999999)
    STRADE: (1.34779828 1.89565123)
    OLIVI: (1.96214923 1.99999999)
    VITE: (1.69231549 1.99195938)
    FRUTTETI: (1.98825408 2.00000000)
    CASTAGNO: (1.99993014 2.00000000)

BOSCHI:
    ERBAI: (2.00000000 2.00000000)
    SEMINATIVI: (1.96758659 2.00000000)
    EDIFICI: (1.99955521 2.00000000)
    PASCOLI: (1.91810784 1.99415628)
    ARBORICOLTURA DA LEGNO: (1.52480601 1.76251404)
    COLTIVAZIONI A CICLO BREVE: (1.52502645 1.91257189)
    GRUPPI DI ALBERI E CESPUGLI: (1.87430056 1.99927701)
    FRUTTA  A GUSCIO: (1.95021109 1.99867520)
    STRADE: (1.99999621 2.00000000)
    OLIVI: (1.99999878 2.00000000)
    VITE: (1.99453657 2.00000000)
    FRUTTETI: (1.91669064 1.98120077)
    CASTAGNO: (1.05719011 1.34125083)
```

Fig.132 ROI'S comparing

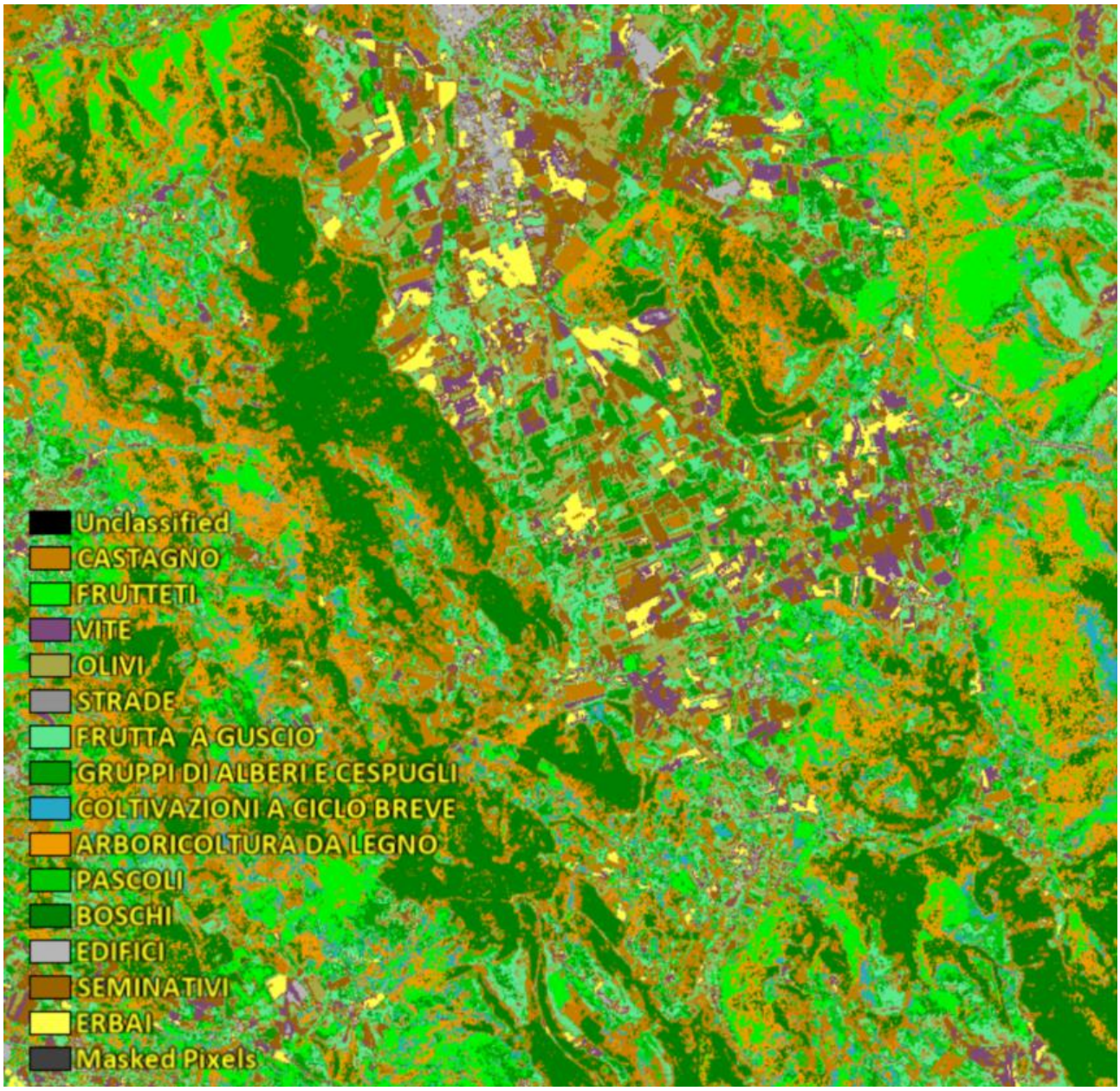

Fig.133 Minimum distance classification in June (Overall accuracy 46.23%)

Fig.134 Comparison of ground reality with classified image

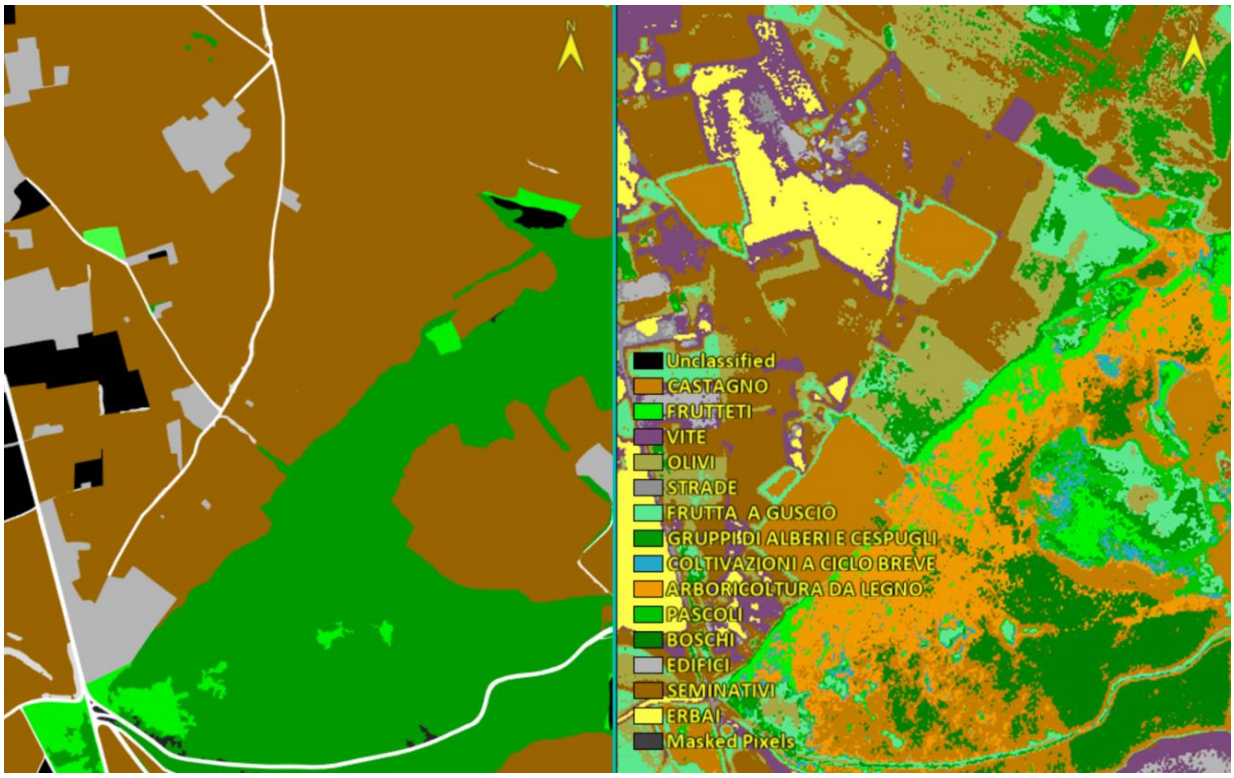

Fig.135 Comparison of ground reality with classified image

Fig.136 Comparison of ground reality with classified image

Confusion Matrix: C:\Users\seand\OneDrive\Desktop\TESI MAGISTRALE\ENVI GIUGNO\MDS-2

Overall Accuracy = (62386/134926) 46.2372%
Kappa Coefficient = 0.3395

	Ground Truth (Pixels)				
Class	CASTAGNO	FRUTTETI	VITE	OLIVI	STRADE
Unclassified	0	0	0	0	0
CASTAGNO	499	55	0	0	0
FRUTTETI	0	1766	1	0	0
VITE	0	0	980	0	59
OLIVI	0	64	16	384	19
STRADE	0	0	15	0	836
FRUTTA A GUS	0	80	144	8	1
GRUPPI DI ALB	0	246	40	7	3
COLTIVAZIONI	0	171	0	0	0
ARBORICOLTURA	138	32	0	0	0
PASCOLI	0	300	8	0	0
BOSCHI	179	0	0	0	0
EDIFICI	0	0	3	0	175
SEMINATIVI	0	44	185	159	174
ERBAI	0	0	152	0	31
Total	816	2758	1544	558	1298

Class	Commission (Percent)	Omission (Percent)	Commission (Pixels)	Omission (Pixels)
CASTAGNO	95.48	38.85	10553/11052	317/816
FRUTTETI	86.15	35.97	10983/12749	992/2758
VITE	80.21	36.53	3973/4953	564/1544
OLIVI	91.62	31.18	4200/4584	174/558
STRADE	62.48	35.59	1392/2228	462/1298
FRUTTA A GUS	90.87	58.83	3853/4240	553/940
GRUPPI DI ALB	94.54	78.82	5660/5987	1217/1544
COLTIVAZIONI	80.10	70.83	4363/5447	2632/3716
ARBORICOLTURA	98.00	80.85	19823/20228	1710/2115
PASCOLI	40.84	78.45	2306/5646	12157/15497
BOSCHI	1.42	45.46	575/40467	33254/73146
EDIFICI	5.50	43.62	242/4400	3217/7375
SEMINATIVI	19.15	69.27	1479/7725	14078/20324
ERBAI	60.11	36.81	3138/5220	1213/3295

Class	Prod. Acc. (Percent)	User Acc. (Percent)	Prod. Acc. (Pixels)	User Acc. (Pixels)
CASTAGNO	61.15	4.52	499/816	499/11052
FRUTTETI	64.03	13.85	1766/2758	1766/12749
VITE	63.47	19.79	980/1544	980/4953
OLIVI	68.82	8.38	384/558	384/4584
STRADE	64.41	37.52	836/1298	836/2228
FRUTTA A GUS	41.17	9.13	387/940	387/4240
GRUPPI DI ALB	21.18	5.46	327/1544	327/5987
COLTIVAZIONI	29.17	19.90	1084/3716	1084/5447
ARBORICOLTURA	19.15	2.00	405/2115	405/20228
PASCOLI	21.55	59.16	3340/15497	3340/5646
BOSCHI	54.54	98.58	39892/73146	39892/40467
EDIFICI	56.38	94.50	4158/7375	4158/4400
SEMINATIVI	30.73	80.85	6246/20324	6246/7725
ERBAI	63.19	39.89	2082/3295	2082/5220

Fig.137 Confusion matrix Minimum Distance classification (MD)

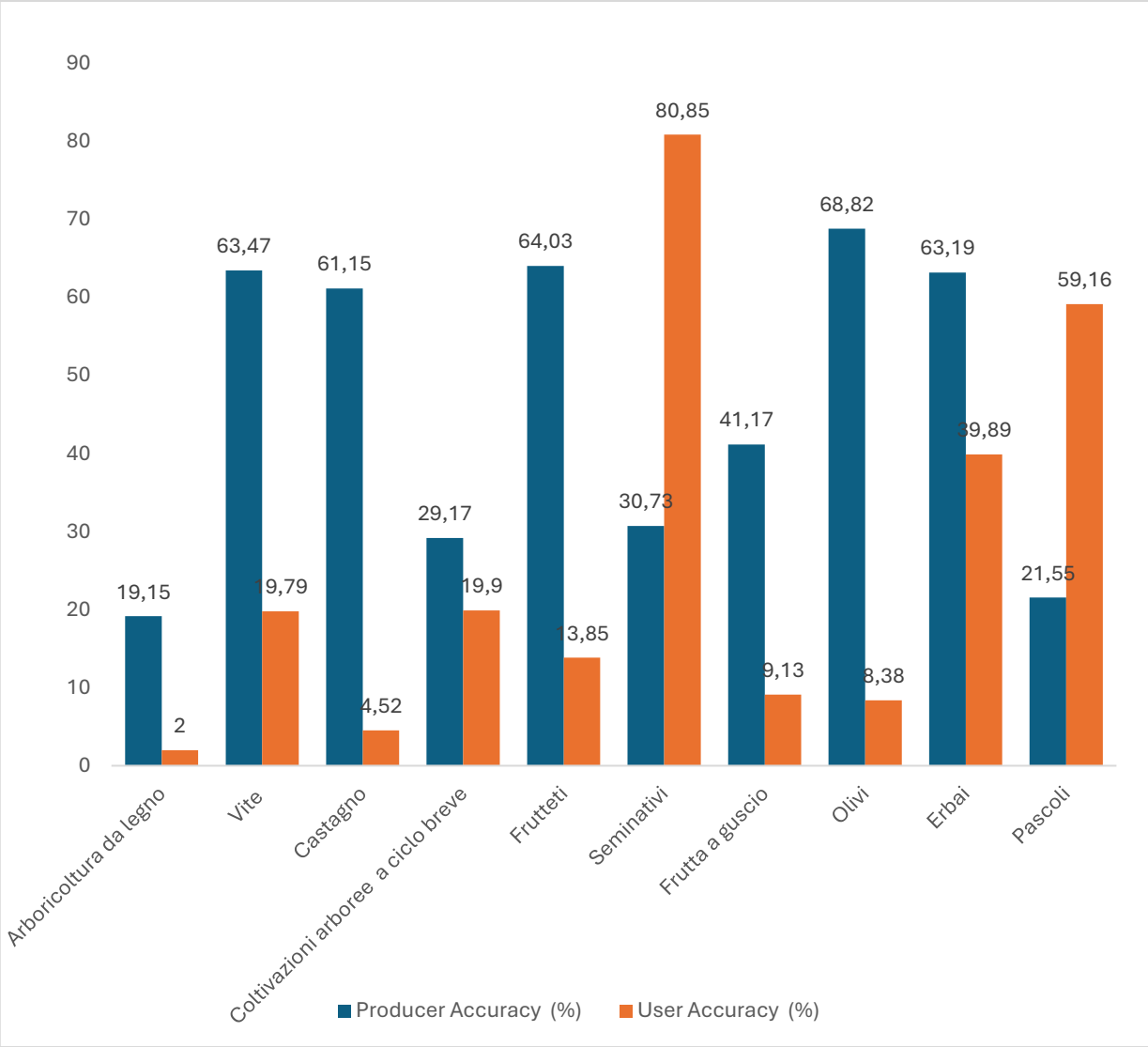

Fig.138 Producer and user Accuracy's crop classification (%) of the cultures in the interested area with Minimum Distance (MD) method

CHAPTER 7

7. Discussions

- In **Fig.90** from the map of the land covers, it was possible to identify the crops involved belonging to the study area and to identify their correct location. The map was created by (Agency for Agriculture Gants) AGEA and extracted a classification of the classes concerning the actual reality on the ground in an undefined period of time, in which it does not take into account the rotation of crops on an annual basis and their change based on the characteristics of the territory. Through the classification in **Fig.133** with the Minimum Distance (MD) algorithm it was possible to determine how the crops vary in the various months without the need to obtain information in the field and to collect further data, except for the satellite data of PlanetScope. The MD classification in **Fig.133** differs from that in **Fig.90** for about 50% of the results, but this depends on many factors: the accuracy with which the ROIs have been drawn, not intersecting pixels of other adjacent crops, the number and position of crops identified by the soil map in **Fig.90** to have a better reference of the crop type and the radiometric resolution of the Plantescope sensor for better focus of the crop target. For example, in **Fig.133** the chestnut or wood arboriculture classes are very present, even if in the soil map in **Fig.90** the classes are positioned in points that are difficult to allow recognition, as well as the presence of a low number of classes which affects the extraction of ROI. In fact, in **Fig.90,** the greater the number of species cataloged for that class, the greater the number of ROI that can be extracted more precisely, thus increasing the accuracy of the results.

- In **Fig.87, Fig.88** and **Fig.89** from the comparison between the false-color images and the images acquired in the visible band, the presence of meadows and green areas decreases from June to September and the mowing phase begins following the collection that took place in that month. The harvest is followed by mowing, for crops sown in the months of April-May and the reseeding of new crops, according to the crop rotation technique. From the false color images you can only have an idea of how the vegetation and the territory vary in the different months; a more detailed analysis should be carried out using the Normalized Difference Vegetation Index (NDVI) vegetation index and image classification to study crop behaviour in detail.

- The behaviour of the classes of trees and groves **in Fig.91** and of the mixed forests **in Fig.93** reflects that of the surrounding vegetation present in greater part: a decrease from June to September. From the histogram in **Fig.138,** the percentage of accuracy in which the data were classified thanks to the confusion matrix is about 55% and 98% for the producer's and user's accuracy respectively.

- The class of wood arboriculture, from the analysis of the spectral profiles in **Fig. 92,** can be seen to reflect very well in the NIR band in all months, in particular in the month of June. From the analysis of the NDVI vegetation index in **Fig.113**, in the month of July, in which temperatures increase and rainfall decreases, there is a decrease in vegetation and the

spectral response tends to decrease and then it grows slightly again in September. Through the analysis of the spectral profiles and the NDVI, an agronomic calendar of crops **(Table 9)** has been created, in which, in the month of July, the branches and trees are used and cut to be transported and transformed into products for industrial and manufacturing use. From the histogram in **Fig.138,** the percentage of accuracy in which the data were classified thanks to the confusion matrix is 19.2% and 2% for producer's and user's accuracy, respectively. The values just mentioned are not very high due to the difficulty of recognizing the ROI in the images and the number of species present in **Fig.90** (in the land cover map).

- For the cultivation of olive trees, from the NDVI vegetation index **(Fig.125),** it can be deduced that the maximum development of vegetation is in the months of June and July when flowering takes place. In September the olive harvest takes place **(Table.9).** This crop does not tolerate too much heat, too arid and intense, in fact the optimal temperature for its development is 25 degrees. From the histogram in **Fig.138,** the percentage of accuracy in which the data were classified thanks to the confusion matrix is 69% and 13.5% respectively for the producer's and user's accuracy although there is only one reference species in the soil map **(Fig.90).**

- In **Fig.95,** from the analysis of the spectral profiles for short-cycle crops, it can be seen that the vegetation reflects very well in the month of June when the ripening of the fruits takes place due to the increase in temperature in the summer months. In fact, from **Fig.119** through the analysis of the NDVI vegetation index it is clearly seen that in July, the vegetative profile reaches a relative minimum, since the complete flowering is now reached and the trees are cut down for industrial use, but in particular in September the vegetation is more developed **(Table.9)**. From the histogram in **Fig.138,** the percentage of accuracy in which the data were classified thanks to the confusion matrix is 29% and 20% for producer's and user's accuracy, respectively.

- In **Fig.101,** from the analysis of the spectral profiles for the vine crop, it can be seen that the vegetation reflects very well in September compared to the months of June and July. In the first summer months, with the increase in temperatures, the ripening of the fruit begins, in fact, from **Fig.117** through the analysis of the NDVI vegetation index, it is clearly seen that in September the vegetation is more developed, in these months the final ripening takes place and the plant prepares for the harvest of the fruits in September when the shoot turns black **(Table 9).** From the histogram in **Fig.138,** the percentage of accuracy in which the data were classified thanks to the confusion matrix is 64% and 19.8% respectively for producer's and user's accuracy.

- For the chestnut class, from the spectral profiles in **Fig.94,** it can be deduced that the greatest reflection occurs in the month of June in the NIR band. The spectral answer is the same as that in **Fig.91** for the trees and woodlands that make up most of the vegetation. From a more accurate analysis of the NDVI vegetation index **(Fig.122),** it can be seen that

the maximum vigor occurs in September when the fruit begins to ripen for harvesting in October, a second maximum occurs in June when flowering begins. It is possible to identify the phenological cycle for this class which is reported in **Table.9**. From the histogram in **Fig.138,** the percentage of accuracy in which the data have been classified thanks to the confusion matrix is about 61% and 5% respectively for producer's and user's accuracy; in the soil map **(Fig.90)** there is only one species for characterization in the classification of ROI and it blends in with the surrounding vegetation affecting the accuracy of the data.

- From the analysis of the spectral profiles for the class of orchards **Fig.97,** it can be seen that the vegetation reflects more in June and then July and September. The phenological behavior of the crop can be deduced from the NDVI index in **Fig.115** and mirrors that of the spectral profile. It can be seen from **Fig.36** that the cultivation of the orchards resides in particular towards the plain at the edge of the built-up area and the behavior of the vegetation, its growth and decrease, are in agreement with that of **Fig.89**. In general, there can be different species of fruit-bearing plants in which cultivation takes place at different times depending on the growth environment and therefore on the plant's ability to adapt. For most of the fruit crops considered for the study area, according to the crop calendar drawn up in **Table.9**, flowering takes place in June, ripening in July and September and finally harvesting in September and October. From the histogram in **Fig.138**, the percentage of accuracy in which the data were classified thanks to the confusion matrix is 64% and 14% respectively for producer's and user's accuracy.

- For grasslands, from the analysis of the spectral profiles in **Fig. 96,** it can be seen that the vegetation reflects in the NIR more in the month of June, followed by a decrease in the profile in July and September as mowing takes place; from **Fig.129** through the analysis of the NDVI vegetation index this behavior is confirmed with the main peak in June, this leads to the drawing up of the agronomic calendar of crops in **Table.9,** in which the phenological cycle of the cultivation of grasslands in the summer months of reference is described. For grasslands, from the histogram in **Fig.138**, the percentage of accuracy in which the data were classified thanks to the confusion matrix is 63.2% and 20% respectively for producer's and user's accuracy.

- **Fig.99** shows the spectral profile for the arable land class in the reference summer months: in June and September the vegetation reflects well in the NIR. In fact, in June the growth of vegetation in the fields takes place. Vegetation is followed by harvesting in July and reseeding in September with the beginning of the growth of new crops. In the crop calendar **(Table.9),** the complete phenological cycle is reported. This trend is shown in **Fig.127,** through the NDVI vegetation index, in this case the arable field starts from a harvest phase. From the histogram in **Fig.138,** the percentage of accuracy is 31% and 81% for producer's and user's accuracy, respectively. The data were classified in the percentage of accuracy thanks to the confusion matrix. Since the arable land class is the most present in the soil map in **Fig.90**, it is easy to extract ROI and reintercrop, nor does it follow an improvement in the accuracy of the result.

- The analysis of the NDVI vegetation index for nuts in **Fig.121,** shows that the maximum development of the vegetation is in June, while the profile decreases in the following months. For almonds in particular, the harvest takes place between July and September. The phenological cycle of this crop is represented in **Table.9** . In the case of hazelnuts, ripening is a bit late with harvesting in November. From the histogram in **Fig.138**, the percentage of accuracy in which the data were classified thanks to the confusion matrix is 41% and 19% respectively for producer's and user's accuracy.

- For the class of uncultivated land only 3 species were found in the soil map in **Fig.90** and the spectral signature in the three summer months is very similar: the vegetation in the NIR band reflects very well in all three months, in particular in June and July **(Fig.102).**

- The class of pastures from the analysis of the spectral signature in **Fig.98**, shows that the vegetation reflects in the NIR band in particular in the months of June and July, so they are more uncultivated, i.e., less cultivated than in September. From **Fig.106, Fig.108, Fig.110** it can be seen that the pastures increase in September, while the surrounding wooded vegetation decreases. From the histogram in **Fig.138,** the percentage of accuracy in which the data were classified thanks to the confusion matrix is 22% and 59% respectively for producer's and user's accuracy.

7.1. Comparison among works

In the work of *(Filippo Sarvia, Samuele De Petris, 2022),* the crops of interest (CoI) according to ARPEA (Piedmont Regional Agency for Agricultural Payments) were: soybeans, corn, wheat, rice and mead. The agronomic calendars were also taken into consideration to facilitate the recognition of the phenological cycle of the crops. Unlike *(Filippo Sarvia, Samuele De Petris, 2022*), the land cover map provided by AGEA (Agency for Agriculture Gants) was a useful tool for the purpose of recognizing the crops, to identify their position in the area of interest, while to determine the phenological cycles bibliographic research of the cultivation and the periods in which it is more prone were carried out. In *(Filippo Sarvia, Samuele De Petris, 2022),* particular attention is paid to the geometric resolution with which the fields were detected via the Sentinel-2 satellite, which is 10 m. Subsequently, the data were processed on Geographic Information System (GIS). In fact, for each area of fields that was taken into consideration, the spectral index (SI) was calculated taking into account the geometry and the size of the field to ensure that the spectral signature is different from the adjacent fields in which a mixing of pixels can occur, only 22% satisfied the shape and geometry requirements. The strongly anisotropic and fragmented fields are not significant for the contribution to the Common Agricultural Policy (CAP) and were excluded from the classification. In this work the PlanetScope satellite was used (geometric resolution of 3 m) and the data were processed on the ENVI software. The spectral index (SI) was not calculated for the studied area, as the fields were large enough and they were recognizable compared to those of *(Filippo Sarvia, Samuele De Petris, 2022)*, as regards the shape and geometry. The calibration of the images has the aim of improving the radiometric resolution through corrections; in both studies, the calibration uses the same “Top of the atmosphere” approach, and the Region of interest (ROI) separability assessment was performed according to Jeffries Matusita test. From the comparison between the ROIs, a greater similarity (and therefore a lower separation) was found for the lower values assumed in the NDVI (Normalize difference vegetation index) temporal profile, as they are related to crops with less active non-abundant vegetation or to sow areas. In

(Filippo Sarvia, Samuele De Petris, 2022) separability values lower than 0.9 were assumed. In the Minimum Distance (MD) classification in *(Filippo Sarvia, Samuele De Petris, 2022)* for the classes of corn, rice and grassland the producer's accuracy and the user's accuracy are both greater than 70%, soybeans and wheat have shown lower accuracy values. In fact, the separability was lower for these two classes, such as chestnut and woody arboriculture or grasslands and arable crops. Furthermore, the comparison shows that the lower the separability between the classes, the greater the similarity between the NDVI spectra of the phenological cycle that represent them. The work of (Filippo Sarvia, Samuele De Petris, 2022) has produced a greater accuracy of the results for the high number of collimated grounds GCPs and a richer database of data on the presence and position of crops, as well as from field surveys; the data are provided by the Geo-Spatial Aid Application (GSAA) website through the analyses of the suppliers in the field and by satellite.

7.2. Further developments

Some solutions are proposed that can represent a tool for crop recognition in the context of satellite images:

- The type of crop could be detected directly in the field thanks to the inspections with local farmers, able to communicate the time for sowing and harvesting, the changes that have been made during cultivation and crop rotation according to the seasons, as well as the date of the agronomic practices that have been carried out.

- An improvement in the spatial and radiometric resolution of the image acquired from PlanetScope satellites would guarantee a greater capacity for crop recognition and a more accurate classification.

- The Geo-Spatial Aid Application (GSAA) data reports the agricultural surfaces and the dimensions of the plots useful for calculating the spectral index (SI) and eliminating the fields that do not respect the appropriate shape and size suitable for satellite crop recognition. Anisotropic fields affect the spectral signature of the crops present.

- Use of Artificial Intelligence (AI) to improve classification by entering data such as: topography, field area, size, geometry and shape, spectral indices.

- Use of drones for image acquisition and more accurate mapping with a greater number of Ground Control Points (GCP) on the ground to be collimated.

- In order to update the database of data communicated by the supplier, it is necessary to check whether the Normalized Difference Vegetation Index (NDVI) analyses comply with the Common Agricultural Policy (CAP) guidelines with reference to a certain period of time.

CHAPTER 8

8. Conclusion

In this work, a possible application has been studied to catalogue the crops present in the field in accordance with the document for the classification of crops Title III of Reg. (EU) 1307/2013) of CAP 2020, without resorting to the continuous updating of farmers on the portal of the Common Agricultural Policy (CAP) which is sometimes unreliable. To compare the data of the network of suppliers that enter the crops present in the field into the network in real time, the PA uses the orthophotos that are acquired every three years. With this new method, through the temporal analysis of high-resolution images it is possible to have a database of the crops present in the field that is always updated, effectively solving the problem of "temporal latency", which is missing, of the constant updating by the suppliers. The spatial and radiometric resolution of Sentinel-2 is better than that of PlanetScope sensors, ensuring better data quality, but thanks to the new technology of multiple nanosatellites capable of acquiring a wider area with better temporal and geometric resolution, the PlanetScope system is more efficient with a less accurate but more up-to-date analysis, relevant to the real situation from the point of view of the analysis of agricultural crops through high-resolution satellite images. Knowing the agronomic calendars of the crops and comparing them with the profiles extracted through the Normalized Difference Vegetation Index (NDVI), a similarity of the periods in which the growth of the crop and its disappearance occurred was found. Understanding the trend of the NDVI profile over time has allowed us to better understand the phenological cycle of the crops, except for field surveys, and to identify the agricultural practices that are applied in the period of the three summer months of reference. Thanks to the extraction of the ROIs and the use of the Minimum Distance (MD) classification, it was possible to determine how much the deviation actually is compared to the real situation on the ground (land cover map provided by AGEA), but for the extracted crops the periods in which the vegetation is less active greatly influence the classification result.

CHAPTER 9

Bibliography

Prasad S. Thenkabail, Munir A. Hanjra, et. al., *A Holistic View of Global Croplands and Their Water Use for Ensuring Global Food Security in the 21st Century through Advanced Remote Sensing and Non-remote Sensing Approaches*, pp.211-261, 2010.

Filippo Sarvia, Samuele De Petris, *Possible roles of muti temporal optical remote sensing within the CAP framework: towards operational services for controls by paying agencies*, pp. 1-168, 2022.

Klaus Tempfli,Norman Kerle, Gerrit C. Huurneman and Lucas L. F. Janssen et.al, *principlesremotesensing,* pp.38-97, 2001.

Kurbanov, R.K., Zakharova, N.I., *Application of vegetation indexes to assess the condition of crops*. Agricultural machinery and technologies, pp.4-11, 2020.

Gascon, F., Cadau, E., Colin, O., Horesch, B., Isola, C., Fernandez, B.L,Martimort, P., *Copernicus Sentinel-2 mission: products, algorithms and Cal/Val, in: Earth Observing Systems* XIX, 2014.

Angelo Frascarelli, Tommaso Cesaretti , *L'agricoltura biologica in Umbria*, pp.1-4, 2019. cesarweb.com/wp-content/uploads/2020/12/AGRICOLTURA-BIO-IN-UMBRIA.pdf

Pierpaolo Brenta, Pier Giorgio Terzuolo, et.al, *Arboricoltura da legno*, pp.4-40, 2018. https://www.regione.piemonte.it/web/sites/default/files/media/documenti/2019-09/arboricoltura_da_legno_2018.pdf

Enrico Buresti Lattes, Paolo Mori, *Arboricoltura da legno*, schede per la produzione e progettazione delle piantagioni, pp.2-30, 2024. https://www.regione.fvg.it/rafvg/export/sites/default/RAFVG/economia-imprese/agricoltura-foreste/foreste/allegati/14112013_Schede_AdL_x2x.pdf

Mauro Gramaccia, Silvia Spedicato, Marco Caffarelli, Francesca Moretti, Ferdinando Desantis, Luciano Concezzi, *La Biodiversità d'interesse agrario della Regione Umbria*, pp.12-235, 2004. https://biodiversita.umbria.parco3a.org/wp-content/uploads/2020/05/3A_pomologica_interno.pdf

Ginacario Bounous, et.al, *Il castagno risorsa multifunzionale in Italia e nel mondo* , pp.1-29, 2017. https://static.tecnichenuove.it/edagricole/2020/03/5415-Il-castagno-II-Ed.-SFOGLIA.pdf

Barbara Mariotti, Tatiana Castellotti, Marco Conedera, Piermaria Corona, Maria Chiara Manetti, Raoul Romano, Andrea Tani, Alberto Maltoni, *Linee guida per la gestione selvicolturale dei castagneti da frutto* , pp.29-35, 2020. https://flore.unifi.it/retrieve/handle/2158/1160265/404583/Linee_Guida_castanicoltura_da_Frutto.pdf

Enrico Buresti Lattes, Paolo Mori*, Progettazione, Realizzazione e Gestione delle Piantagioni da legno policicliche di tipo Naturalistico,* pp-35-38 , 2016. portale.bonificaveronese.it/wp-content/uploads/2016/11/Manuale-InBioWood-Ottobre_2016.pdf

Giuseppe Frison, *Ciclo vegetativo e ciclo riproduttivo dei pioppi*, pp.3-36, 2021. http://www.giuseppefrison.it/wp-content/uploads/2021/05/Ciclo-vegetativo-e-ciclo-riproduttivo-dei-pioppi.pdf

Egidio Ciriciofolo, Andrea Onofri, *Gestione delle risorse foraggere*, pp.1-68 , 2003. (https://www.casaonofri.it/SistemiForaggeri/Presentations/Parte%20I%20-%20Le%20risorse%20foraggere.pdf).

Paolo Arice, Dino Biondi, et.al, *Frutti dimenticati e biodiversità recuperata*, Il germoplasma frutticolo e viticolo delle agricolture tradizionali italiane Casi studio: Umbria e Liguria, pp.8-74, 2020. https://www.isprambiente.gov.it/files2020/pubblicazioni/quaderni/quaderno-ispra-n-14-umbria-liguria-bassa-risoluzione.pdf

Moreno Moraldi, *Il nocciolo*, impianto e gestione delle coltivazioni da frutto, pp.7-70, 2021. https://www.umbriagricoltura.it/wp-content/uploads/2021/10/Libro_nocciolo.pdf

Alan Collison, Arin Jumpasut, Hannah Bourne, *ON-ORBIT RADIOMETRIC CALIBRATION OF THE PLANET SATELLITE FLEET*, DOVES AND SKYSAT, pp.3-38, 2022. https://assets.planet.com/docs/radiometric_calibration_white_paper.pdf

Sitography

- **STUDY AREA AND TYPES OF COLTURE**

Sportello dell'agricoltura, 2019, https://sportelloagricoltura.it/politica-agricola-comune/agea-ed-il-monitoraggio-agro-ambientale-degli-aiuti-in-agricoltura/

CAP 2023-2027, https://agriculture.ec.europa.eu/common-agricultural-policy/cap-overview/cap-2023-27_en

Norcia, 2024, https://it.wikipedia.org/wiki/Norcia

Landscapeunifi, 2014, https://www.landscapeunifi.it/2014/05/27/umbria

Fonterosa, 2023, https://www.fonterosa.eu/i-piani-di-castelluccio-di-norcia/

Centrometeo, 2024, http://www.centrometeo.com/articoli-reportage-approfondimenti/climatologia/5412-clima-umbria

Regione Umbria, 2021, https://www.regione.umbria.it/paesaggio-urbanistica/cartografia-geologica

Regione Umbria, 2021, https://www.regione.umbria.it/paesaggio-urbanistica/carte-pericolosita-sismica-locale-per-google-earth

Tenimenticiva, 2021, https://tenimenticiva.com/blog/fasi-fenologiche-della-vite/#:~:text=Le%20caratteristiche%20della%20pianta%2C%20la,la%20maturazione%2C%20il%20riposo%20invernale

Europlantsvivai, 2019, https://blog.europlantsvivai.com/coltivazione-olivo/#:~:text=Ciclo%20di%20coltivazione,%3A%208%20kg%2F10%20mq

Agrispoleto, 2004-2024, https://agrispoleto.wordpress.com/mais/

Cloud.idgis, 2013, https://cloud.ldpgis.it/sanvincenzo/sites/sanvincenzo/files/ps/RAC%20Schede%20uso%20del%20suolo_Pag29-44.pdf

Prunus_amygdalus, 2024, https://it.wikipedia.org/wiki/Prunus_amygdalus

Elaisian, 2024, https://www.elaisian.com/2022/09/22/la-raccolta-delle-mandorle/#:~:text=La%20raccolta%20avviene%20tra%20luglio,caduta%20delle%20mandorle%20a%20terra

- **PLANETSCOPE SYSTEM**

PlanetScope, 2024, PlanetScope-Earth Online esa.int

PlanetScope, 2024, https://developers.planet.com/docs/data/planetscope/

PlanetScope, 2024, https://developers.planet.com/docs/apis/data/sensors/

PlanetScope, 2024, https://www.planet.com/products/satellite-imagery-of-earth/

PlanetScope, 2023, https://assets.planet.com/docs/Planet_Combined_Imagery_Product_Specs_letter_screen.pdf

- **NDVI INDEX**

Humboldt, 2020, https://gsp.humboldt.edu/olm/Courses/GSP_216/online/lesson7/radiometric.html

NDVI, 2024, https://it.wikipedia.org/wiki/Normalized_Difference_Vegetation_Index

PlanetScope, 2024, https://assets.planet.com/marketing/PDF/Planet_Surface_Reflectance_Technical_White_Paper.pdf

- **MINIMUM DISTANCE (MD) CLASSIFICATION**

GeorgiaView & AmericaView University, 2020, https://gaview.org/drupal893/9-image-classification